

POSTER SESSION 1

Session held on 8 July 2016

doi:10.1093/cvr/cvw135

Cell growth, differentiation and stem cells - Heart

72

Understanding the metabolism of cardiac progenitor cells: a first step towards controlling their proliferation and differentiation?E. Andre; A. De Pauw; P. Porporato; C. Bouzin; N. Draoui; P. Sonveaux; J.-L. Balligand
Institute of Experimental and Clinical Research (IREC), Brussels, Belgium

Emerging evidence supports a mandatory metabolic shift from glycolysis to oxidative phosphorylation during stem cells differentiation. In this study, we investigate cardiac progenitor cells (CPC) metabolic adaptations to a hypoxic environment and the bioenergetic transition underlying cardiomyocyte differentiation process. We intend to identify key metabolic regulators which could be modulated to promote survival/proliferation/differentiation of CPC during the early steps of therapeutic interventions.

Under normoxia (21%O₂), glucose consumption and lactate release were significantly higher in Sca1+ CPC (isolated from adult mouse hearts by MACS separation) than in neonatal rat cardiac myocytes (NRCM) with a ratio of 2 moles of lactate released per mole of glucose supporting a high glycolytic metabolism. Glucose consumption and lactate release were increased in hypoxia (1%O₂), together with increased abundance of the monocarboxylic transporter MCT4 (lactate efflux mediator), of Glut-1 and of PFKFB3 (key regulator of glycolytic rate). BrdU incorporation in CPC was critically dependent on pyruvate, glucose and glutamine availability under normoxia and hypoxia. Oxygen consumption analysis indicated that CPC and NRCM display active mitochondrial ATP production. Notably, basal and maximal respiration were higher in NRCM compared to CPC. Consistently, mitochondrial populations were differentially active in both cell types, as reflected by a 40% decrease in tetramethylrhodamine methyl ester staining intensity (flow cytometry) in CPC compared to NRCM. Moreover, the expression of TOM20 (translocase of outer mitochondrial membrane) was also 50% lower in CPC compared to NRCM. This CPC phenotype dramatically changed upon differentiation (azacytidine/TGFβ/ascorbic acid), with a reduction by third of glucose consumption and lactate release compared to proliferative CPC, in parallel with increased expression of sarcomeric proteins (cardiac Tnl, alpha-sr-actinin).

In conclusion, despite active mitochondrial ATP production, undifferentiated CPC exhibit lower respiratory reserve than cardiac myocytes, which correlates with a less abundant mitochondrial network. However, they exhibit aerobic glycolysis and lactate production, which further increased under hypoxia together with (HIF-1α dependent) PFKFB3, Glut-1 and MCT4 to eliminate the excess of intracellular lactate. Such glycolytic activity, together with glutamine metabolism supports their proliferation but is dramatically downregulated upon differentiation. This may open the way for pharmacological modulation of the survival/differentiation of CPC for cell therapeutic repair through their mitochondrial fusion and biogenesis.

73

Expression of pw1/peg3 identifies a new cardiac adult stem cell population involved in post-myocardial infarction remodelingE. Yaniz-Galende¹; N. Mougenot¹; L. Formicola¹; S. Nadaud¹; F. Dierick¹; R.J. Hajjar²; G. Marazzi¹; D. Sassoon¹; J.-S. Hulot¹¹University Pierre & Marie Curie Paris VI, Institute of Cardiomatolism and Nutrition ICAN, Paris, France;²Mount Sinai School of Medicine, Cardiovascular Research Center, New York, United States of America

Rationale: There is growing evidence that myocardium responds to ischemic injury by recruiting cardiac adult stem cells (ASC) to the damaged tissue. Different types of cardiac ASC have been reported, but their exact nature and role in post-myocardial infarction (MI) cardiac repair remain unclear.

Purpose: PW1 gene (also called paternally expressed gene, Peg3) has recently been shown as a marker of stem cells in a wide array of adult tissues. Using a PW1-reporter mouse (PW1IRESnLacZ) we investigated PW1+ cells in normal hearts and in response to MI after permanent LAD ligation.

Methods and Results: Immunostaining experiments firstly showed PW1 expression in small elongated or roundish cells located in the epicardium and interstitium of normal hearts. Using C12FDG as a fluorescent substrate for β-galactosidase activity, PW1+ cells were isolated by fluorescence-activated cell sorting (FACS) from PW1IRESnLacZ mice hearts. PW1+ cells represent 3.4% ± 0.4% of the non-cardiomyocytes subset. In vitro, PW1+ cells were able to form colony-forming units-fibroblasts with multipotency for a range of mesodermal lineages (smooth muscle cells, endothelial cells,

fibroblasts, adipocytes, cartilage) but not cardiac myocytes. We further found that PW1+ cells are mainly CD45-, c-kit- and Sca1+, indicative of a mesenchymal-stem-cell (MSC)-like phenotype. In response to MI, the number of PW1+ cells increase and these cells were mainly located to the infarct and border zone. Using perdurance of β-gal expression, we were able to identify fibroblasts (as identified by FSP-1 expression) retaining β-gal expression, suggestive of a direct contribution of PW1+ cells to the fibrotic transformation post-MI. Whereas there is almost a mutual exclusion between PW1 and the popular cardiac stem cell marker c-kit in normal heart, there was a large increase in cells expressing both PW1 and c-kit markers in ischemic hearts. In vitro, c-kit+/PW1- cells can differentiate into cardiomyocytes. On the other hand, PW1+ cells (whatever the expression of ckit) were not able to differentiate into cardiomyocytes but rather into fibroblasts.

Conclusion: PW1+ identifies a new population of cardiac adult stem cells that resembles to MSC, represents an important proportion of adult stem cells in response to ischemia but lacks myogenic potential. PW1+ cells can rather differentiate into fibroblast-like cells, suggesting an involvement in post-MI fibrotic remodeling.

74

Long-term stimulation of iPS-derived cardiomyocytes using optogenetic techniques to promote phenotypic changes in E-C couplingC. Hamilton; VR. Zamora; FL. Burton; N. Macquaide; GL. Smith
University of Glasgow, Institute of cardiovascular and medical science, Glasgow, United Kingdom

Introduction: Induced pluripotent stem cell derived cardiomyocytes (iPSCMs) are emerging as a useful tool for high throughput cardiotoxicity assays. These cells have the benefit of being derived from human cells making them more clinically relevant and avoiding the use of animal cells.

One disadvantage in using these cells is that they display an immature phenotype both in terms of structure and function. In order to increase their maturity we use a light sensitive cation channel (channel rhodopsin-2 (ChR2)) to allow long term non-invasive pacing of these cells.

Purpose: Validate optogenetic stimulation as a mean of long-term stimulation of iPSCMs in culture and to examine the changes in phenotype associated with high frequency stimulation.

Methods: ChR2 was expressed in commercially available iPSCMs by means of an adeno-associated vector. The transfected cells were stimulated using 470nm light via epifluorescence optics of an inverted microscope or using graphite electrodes. Strength durations curves were plotted in order to compare optogenetic and electric field stimulation.

To test the effects of chronic stimulation, cells were paced at 2Hz or 3Hz for a period of 48 Hours or longer. Strength duration curves and video based contractility measurements were taken before and after pacing. Two stimulation protocols were employed: (i) single site, i.e. constantly pulsing light a defined 0.24mm² site or (ii) moving site, i.e. pacing a series of 6 sites around a central area.

Results: Transfected cells were fully responsive to optogenetic stimulation 5 days post transfection and continue to respond until at least 12 days post transfection.

Strength duration curves were similar when comparing optogenetic and solid state techniques. (Chronaxie time optogenetic = 1.53 ± 0.32ms, graphite = 2.17 ± 0.44 ms P = 0.24)

Chronic stimulation using light levels at 2x threshold at a single site caused cell death resulting in loss of pacing after 24-48 hours. This was overcome by employing a strategy of moving site stimulation. Using this approach cells could be paced at 2 and 3Hz, with a 50% duty cycle (100s on 100s off), for a period of 48 hours or longer. Stimulation over 48 hours caused no significant change in functional and structural parameters at 2 Hz. Using 3Hz, spontaneous rate of contraction was reduced after 48 hours (Interval time 422 ± 3ms to 703 ± 32ms P=0.0022).

Conclusions: ChR2 transfection and optogenetic stimulation is a viable method for pacing of iPSCMs including chronic high frequency stimulation. 48 hours of high frequency stimulation reduces the intrinsic rate of iPSCM contraction.

75

Benefits of electrical stimulation on differentiation and maturation of cardiomyocytes from human induced pluripotent stem cellsG. J. Dusting¹; D. Hernandez²; P. Sivakumaran³; R. Millard¹; RCB. Wong⁵; A. Pebay⁵; RK. Shepherd⁴; SY. Lim⁶¹University of Melbourne, OBrien Institute Department, StVincent's Institute and CERA and Dept Surgery, Melbourne, Australia; ²University of Melbourne, OBrien Institute Department, StVincent's Institute and Dept Medicine, Melbourne, Australia; ³University of Melbourne, University of Melbourne, OBrien Institute

Department, StVincent's Institute and Dept Medicine, Melbourne, Australia; ⁴University of Melbourne, Bionics Institute, Melbourne, Australia; ⁵University of Melbourne, CERA and Dept Surgery, Melbourne, Australia; ⁶University of Melbourne, O'Brien Institute Department, StVincent's Institute and Dept Surgery, Melbourne, Australia

Background: Regeneration of cardiac tissue raises the possibility of restoring cardiac function after myocardial infarction. In addition, the ability of human induced pluripotent stem cells (iPSCs) to differentiate into bona fide cardiomyocytes provides a platform for disease modelling, drug discovery and pharmacological safety testing of new drugs. One of the major limitations for the use of cardiomyocytes derived from iPSCs is that they resemble foetal cardiomyocytes and are immature. Given that the developing heart grows in an electric field, we considered that electrical stimulation (Est) might affect cardiogenesis of human iPSCs.

Purpose: To investigate whether Est promotes cardiac differentiation and maturation of cardiomyocytes derived from human iPSCs.

Methods: Cardiac differentiation of iPSCs was induced by the temporary addition of small molecules and growth factors in a feeder-free monolayer culture. A whole layer of beating cardiomyocytes was produced from day 14 after differentiation. Beating cells were enriched non-genetically by culturing them in a glucose-free medium supplemented with lactate (4mM) for 2 to 6 days. After enrichment, cardiomyocytes were stimulated electrically (alternating current, charge-balanced biphasic pulse, 1 ms pulse-width, 1 Hz frequency) at 200 mV/mm in custom-made plates for a further 7 days and longer. Control wells received no electrical pulses.

Results: Continuous Est at 200 mV/mm for 7 days significantly increased the percentage of cardiomyocytes with organized sarcomeres ($39 \pm 8\%$ vs. $23 \pm 11\%$, $p < 0.05$). Est also aligned more cardiomyocytes in parallel with the electric field ($10 \pm 1\%$ vs. $6 \pm 2\%$, $p < 0.05$) and decreased the circularity index (0.69 ± 0.02 vs. 0.74 ± 0.02 , $p < 0.05$) indicating that Est cells develop a more rod-like structure. Cardiac muscle specific mRNA expression tended to increase after Est compared to non-stimulated controls. The effects of longer stimulation periods are currently being evaluated. In addition, using a bionic approach, Est is now being applied locally to cardiomyocytes derived from iPSCs implanted in vivo in vascularised, rat tissue engineering chambers, for up to 4 weeks.

Conclusion: We previously showed that brief Est modestly enhanced cardiac differentiation of human iPSCs, and increased expression of cardiac-specific contractile muscle genes. We now show that longer term, continuous Est promotes further maturation of cardiomyocytes derived from human iPSCs. Mature cardiomyocytes recapitulate better the pathophysiological function of the human heart for more accurate disease modelling and drug testing, as well as providing a superior substrate for tissue engineering and neonatal or adult cardiac regeneration and repair.

76

Constitutive beta-adrenoceptor-mediated cAMP production controls spontaneous automaticity of human induced pluripotent stem cell-derived cardiomyocytes

N. Hellen¹; T. Owen¹; R.J. Jabbour¹; M. Kloc¹; T. Kodagoda¹; C. Denning²; S.E. Harding¹
¹Imperial College London, London, United Kingdom; ²Wolfson Centre for Stem Cells, Tissue Engineering and Modelling, Nottingham, United Kingdom

Background: Human induced pluripotent stem cell-derived cardiomyocytes (hiPSC-CM) show great potential for disease modelling, pharmaceutical testing and cardiac repair. In contrast to isolated adult ventricular cells, they form a spontaneously beating syncytium in vitro. In the heart beta adrenoceptors (β -ARs) play a key role in the control of heart function; endogenous catecholamine stimulation increases rate and force of contraction. Similar effects have been observed in hiPSC-CM, but the constitutive activity of these receptors and the contribution of downstream signalling pathways to spontaneous automaticity remain largely uncharacterised.

Purpose: The spontaneous contraction of hiPSC-CM has the potential to cause arrhythmia during transplantation, may act as a barrier to maturation and chamber specificity and could have implications for their use in drug screening. Precise understanding of the mechanisms controlling this attribute is crucial for future applications.

Methods: hiPSC-CM (Cellular Dynamics) were seeded at 0.18×10^6 cells per 0.38mm^2 to form a synchronous syncytium. Beating rates were determined using a Nikon Eclipse TE2000E microscope with Digital sight camera and NIS Elements3.2 software video tracking. Data is expressed as mean \pm SEM; statistical significance determined by Student's t-test.

Results: Using inverse agonists to reduce constitutive activity of unstimulated β_1 -ARs (CGP 20712A; $10\mu\text{M}$; 20 minutes) or β_2 -ARs (ICI 118551; $10\mu\text{M}$; 20 minutes) resulted in a $50.6 \pm 3.0\%$ ($p < 0.0001$; $n=5$) or $83.7 \pm 8.9\%$ ($p < 0.0002$; $n=5$) reduction in basal beating rate respectively. Inhibition of the downstream cAMP effector, PKA, resulted in complete cessation ($p < 0.0001$; $n=6$) or a $97 \pm 3.3\%$ ($p < 0.002$; $n=5$) decrease in spontaneous beating with H-89 dihydrochloride ($5\mu\text{M}$; 30 minutes) or the protein kinase inhibitor, PKI 14-22 amide ($5\mu\text{M}$; 30 minutes) respectively. Hyperpolarization-activated cyclic nucleotide-gated (HCN; If generating) channel blockade with ivabradine ($20\mu\text{M}$; 60 minutes) decreased beating rate by $78.2 \pm 4.2\%$ ($p < 0.001$; $n=5$) and sarcoplasmic reticulum calcium ATPase (SERCA) inhibition with thapsigargin ($10\mu\text{M}$; 60 minutes) resulted in an $89.3 \pm 3.4\%$ decrease ($p < 0.001$; $n=6$).

Conclusion: β -ARs have high constitutive activity in hiPSC-CM, with β_2 -ARs having a larger contribution to the spontaneous automaticity. The downstream second messenger, cAMP, plays a prominent role in the control of spontaneous beating of hiPSC-CM with intracellular calcium cycling by SERCA playing a significant role and If having a smaller contribution.

77

Formation and stability of T-tubules in cardiomyocytes

CE. Poulet; S. Ramos; C. Terracciano; J. Gorelik
 Imperial College London, National Heart and Lung Institute, London, United Kingdom

The T-tubular network in adult cardiomyocytes supports the propagation of the electric signal deep in the cells and enables a fast and efficient excitation-contraction coupling due to its connections with the sarcoplasmic reticulum. Neonatal cardiomyocytes lack such tubular system as the formation of T-tubules (TTs) occurs during post-natal development, the specifics of which are still poorly understood. Cardiomyocytes derived from embryonic- or induced pluripotent stem cells are also devoid

of TTs, a feature that is likely to be responsible for the poor excitation-contraction coupling observed in those cells.

We wish to understand what controls TT formation and stability in cardiomyocytes in order to reproduce the development of a functional tubular network in immature cells. We are especially interested in two proteins: BIN1, member of the BAR-domain family that induces membrane tubulation, and JPH2, which connects TTs to the sarcoplasmic reticulum.

In order to investigate the components of TT stability, we kept adult rat ventricular myocytes in culture for up to 1 week. Membrane staining with Di-8-ANEPPs showed that TTs were already significantly remodelled after 2 days of culture as shown by measurement of density (day 0: $50.7 \pm 4.0\%$, $n = 10$; day 2: $34.3 \pm 2.8\%$, $n=5$; $p < 0.001$) and regularity (day 0: $17.2 \pm 0.34 \text{ AU} \times 10^6$, $n = 10$; day 2: $5.85 \pm 0.68 \text{ AU} \times 10^6$, $n=10$; $p < 0.001$) which kept decreasing in the following days until TT structures were completely lost. Using scanning ion conductance microscopy, we found, in contrast, that clear TT openings were still present at the cell surface after 2 days of culture, and significantly disrupted only after 4 days (z-groove index day 0: $0.65 \pm 0.05 \text{ AU}$, $n = 6$; day 2: $0.61 \pm 0.07 \text{ AU}$; $n = 6$; n.s.; day 4: $0.29 \pm 0.03 \text{ AU}$, $n=6$; $p < 0.001$). TT remodelling was accompanied by alterations in JPH2 distribution: while at day 0 JPH2 staining appeared as small dots regularly distributed along TTs, after 2 days many areas in the cells showed a significantly reduced number of JPH2 elements as a consequence of its clusterization inside the cells and relocalization to the membrane. On the mRNA level, JPH2 was strongly downregulated after only 24h while BIN1 expression slightly increased during the first 3 days of culture. Interestingly, overexpressing JPH2 in cultured cardiomyocytes prevented the extensive loss of TTs (density at day 4, control: $8.8 \pm 1.7\%$, $n=5$; $n=4$; at day 4, JPH2-overexp: $40.4 \pm 4.5\%$, $n=5$; $p < 0.01$).

We now wish to investigate the effect of JPH2 overexpression on the expression and localization of other TT proteins, including caveolin3 and L-type calcium channels, and identify JPH2 binding partners in TTs. In parallel, BIN1 and JPH2 will be overexpressed in neonatal rat ventricular myocytes and cardiomyocytes derived from induced pluripotent stem cells to promote the formation of TT structures. The presence of TT openings at sites of BIN1 expression will be investigated using scanning surface confocal microscopy.

78

Identification of miRNAs promoting human cardiomyocyte proliferation by regulating Hippo pathway

M. Diez Cunado¹; K. Wei¹; P. Bushway¹; P. Ruiz-Lozano²; M. Mercola²
¹Sanford Burnham Prebys Medical Discovery Institute, La Jolla, United States of America; ²Stanford University, Palo Alto, United States of America

Adult mammalian cardiomyocytes (CMs) have exited from the cell cycle and lost most of their proliferative capacity, consequently, the ability of the adult myocardium to repair itself following injury is very restricted. A recent study¹ revealed a number of synthetic miRNAs could promote neonatal rat ventricular cardiomyocyte proliferation upon transfection, but the targets of the miRNAs remained elusive. We screened a whole genome collection of synthetic human miRNAs and we identified 96 capable of promoting DNA synthesis and also cytokinesis in human induced Pluripotent Stem Cell-derived CMs (hiPSC-CMs). 62 of these miRNAs increase the translocation of YAP into the nucleus, and their ability to promote cardiomyocyte division is blocked by silencing of YAP, indicating that more than 60% of the proliferation-promoting miRNAs act through repression of Hippo signal transduction. Interestingly, after screening the anti-miRs we identified 16 microRNAs that are normally involved in maintaining replication of human iPSC-CMs and target Hippo. Therefore, this study revealed that the Hippo pathway is a remarkably common target of miRNAs that stimulate iPSC-CM replication, and also suggest that the Hippo pathway and CM proliferation is tightly controlled by endogenous miRNAs.

1- Eulalio et al., doi 10.1038/nature11739

79

A direct comparison of foetal to adult epicardial cell activation reveals distinct differences relevant for the post-injury response

AM. Smits; AT. Moerkamp; AMD. Vegh; E. Dronkers; K. Lodder; T. Van Herwaarden; MJ. Goumans
 Leiden University Medical Center, Department of Molecular and Cellular Biology, Leiden, Netherlands

Background: During cardiac development, the epicardium actively contributes to the formation and differentiation of many cellular components of the myocardium. In the adult the epicardium is a quiescent layer enveloping the heart. However, upon injury the epicardium is reactivated, resulting in partial recapitulation of the developmental response including epicardial to mesenchymal transition (EpMT), re-expression of Wilms' Tumor-1 (WT1), proliferation, and migration of epicardial-derived cells (EPDCs). Given their function during embryonic development, EPDCs represent an appealing source for endogenous cardiovascular repair. Unfortunately, adult epicardial cells appear to be less efficient in their contribution to cardiac homeostasis and repair than their embryonic counterparts. Therefore, we aim to identify the differences in foetal and adult epicardial activation and EpMT, to ultimately optimise the adult post-injury response.

Methods: A novel isolation procedure allows the isolation of human foetal and adult EPDCs from cardiac specimens obtained after informed consent. EPDCs were cultured in an epithelial-like morphology in the presence of Alk5 kinase inhibitor (A5ki). EpMT was induced with 1 ng/ml TGFbeta for at least 5 days. Immunofluorescent staining, qPCR and RT2-PCR arrays for human EMT genes were performed to characterise and to compare the process of activation and EpMT in foetal and adult EPDCs.

Results: Both foetal and adult EPDCs can be expanded for several passages under strict culture conditions. TGFbeta stimulation results in EPDCs undergoing EpMT, leading to a morphological change from cobblestone cells into a mesenchymal phenotype. This change is accompanied by a downregulation of WT1 and E-cadherin, and an upregulation of mesenchymal genes including α -SMA, and F-actin. Importantly, removal of the Alk5ki in foetal EPDCs instantly causes a spontaneous EpMT, while adult cells remain epicardial-like. This indicates that foetal EPDCs are in a more advanced activation state, which may reflect their role during development. Additional data from PCR arrays and subsequent cluster analyses corroborate this. Furthermore, these arrays point towards several genes that are differentially expressed in foetal compared to adult cells including the TGFbeta receptors Endoglin and

Alk1. Interestingly, inhibition of Endoglin in foetal cells prevents spontaneous EpMT from occurring. Overexpression experiments will be performed to reprogram adult cells to a foetal responsiveness. **Conclusion:** Besides many similarities, foetal and adult EPDCs show distinct differences that may be used to enhance the epicardial post-injury response.

80

Role of neuropilins in zebrafish heart regeneration

V. Lowe; C. Pellet-Many; I. Zachary
University College London, Division of Medicine, Cardiovascular Biology and Medicine, London, United Kingdom

Background: In contrast to humans, zebrafish are able to fully regenerate their hearts after injury. Transforming growth factor β and platelet-derived growth factor play key roles in zebrafish cardiac regeneration and are able to trigger intracellular responses via receptor complexes including neuropilins (NRP). NRP1 and NRP2 are co-receptors for VEGFs, and other cytokines that play essential roles in developmental angiogenesis and diverse pathophysiological processes, but little is known of their role following myocardial infarction.

Hypothesis: We hypothesised that neuropilins play a role in zebrafish heart regeneration and examined this in the zebrafish cryoinjury model of myocardial infarction and regeneration.

Results: Quantitative PCR shows that *nrp1a*, *nrp1b* and *nrp2a* are significantly upregulated 1 and 3 days post-cryoinjury (dpci), whereas *nrp2b* does not change. In situ hybridisation and immunofluorescent staining indicates that *nrp1a* and NRP1 expression are localised to the epicardium proximal to the injury and epicardial NRP1 expression was demonstrated in epicardial cells in vitro. In contrast, NRP2 is expressed by leucocytes during the initial inflammatory phase after injury and by cardiomyocytes migrating into the injured zone.

Conclusions: Neuropilin isoforms are differentially expressed following cryoinjury; NRP1 contributes to the epicardial response, whereas NRP2 may be required for inflammation and cardiomyocyte replacement.

81

Highly efficient immunomagnetic purification of cardiomyocytes derived from human pluripotent stem cells

D. Eckardt; K. Noack; A. Bosio
Miltenyi Biotec GmbH, Research & Development, Bergisch Gladbach, Germany

Pure cardiomyocytes derived from human pluripotent stem cells (hPSCs) are of high interest for heart disease modeling, drug safety studies and development of cellular therapies. Although several protocols for cardiac differentiation of hPSCs have been developed, major limitations are high variability in differentiation efficacy e.g. due to clone-to-clone or experiment-to-experiment variations and heterogeneity of generated cardiomyocyte populations. For that reason we have developed several tools to improve the complete workflow starting with CM differentiation, monolayer dissociation, immunomagnetic purification of CMs and downstream analysis using flow cytometry.

hPSCs were maintained under xeno-free conditions in StemMACS iPS-Brew XF medium to keep pluripotency for more than >20 passages and enable for efficient cardiac differentiation. We chose a monolayer differentiation protocol based on the timely regulated activation and inhibition of Wnt signaling by small molecules. In order to identify antibodies suitable for CM enrichment or depletion of non-myocytes, we performed a surface marker screen with more than 400 antibodies between days 10-20 of differentiation. Besides identification of new surface markers, our screen confirmed expression of known markers like Sirpa (CD172a) and VCAM-1 (CD106). Interestingly, our data indicate that these markers either label CMs and non-myocytes or only subpopulations of CMs. Based on these data we developed a novel magnetic cell separation procedure consistently delivering CM purities of up to 98%, independent of the differentiation protocol, the hPSC line used or time point and efficacy of differentiation. Magnetically enriched CMs showed a typical morphology and sarcomeric structure. Moreover, they initiated contractions after replating and could be stably maintained in culture. Interestingly, enriched CMs could also be cryopreserved in StemMACS CryoBrew medium. In order to address potential CM subtype heterogeneity in hPSC-CM cultures, we additionally developed recombinant antibodies against general CM markers such as α -Actinin, Myosin Heavy Chain or cardiac Troponin T as well as subtype-specific antibodies against MLC2a and MLC2v distinguishing between atrial and ventricular CMs, respectively.

Taken together, we have developed novel tools supporting the workflow for efficient generation, magnetic purification and flow cytometry or immunofluorescence-based characterization of hPSC-derived cardiomyocytes.

82

Cardiac progenitor cells possess a molecular circadian clock and display large 24-hour oscillations in proliferation and stress tolerance

B. Du Pre¹; DAM. Feyen²; E.J. Demkes³; P.J. Dierickx³; PA. Doevendans²; MA. Vos⁴; AAB. Van Veen⁴; LW. Van Laake²

¹University Medical Center Utrecht, Cardiology and Medical Physiology, Utrecht, Netherlands; ²University Medical Center Utrecht, Cardiology, Utrecht, Netherlands; ³Hubrecht Institute, Utrecht, Netherlands; ⁴University Medical Center Utrecht, Medical Physiology, Utrecht, Netherlands

Background: Circadian (24-hour) rhythms are biorhythms present in the heart. These rhythms are regulated by molecular clocks and play an important role in cardiovascular physiology and disease. So far however, it is unknown whether circadian rhythms also exist in cardiac progenitor cells (CPCs), a population of adult stem cells resident in the heart and of interest for its potential in cell-based cardiac regeneration therapy and pharmacological research.

Purpose: The aim of the current study was to discover: (1) if a molecular circadian clock is present in CPCs and, (2) if CPC functions display 24-hour rhythmicity?

Methods: Human foetal CPCs were isolated and cultured in vitro. To investigate the presence of a functional molecular clock, 24-hour oscillations in core clock components Bmal1 and Cry1 were analysed using PCR, WB, immunohistochemistry, and a luminescent reporter system. Levels of proliferation, migration, stress tolerance, and paracrine factor release were measured during a 48-hour

period. To analyse involvement of the circadian clock, experiments were done with and without clock synchronisation.

Results: Expression of clock components displayed oscillations with a 24-hour period both at the transcriptional and protein level, confirming that CPCs contain a molecular circadian clock ($p < 0.05$ for all). Proliferation and stress tolerance showed a 24-hour rhythm with large difference between peak and trough (21% and 25% for proliferation and stress tolerance respectively, $p < 0.01$). CPC migration and paracrine factor release on the other hand, were not subject to circadian oscillations.

Conclusions: 24-hour rhythms play an important role in CPCs: CPCs contain a circadian molecular clock and CPC functions such as proliferation and stress tolerance display significant 24-hour oscillations. Taking circadian rhythms into account may improve reproducibility and outcome of research and therapies using CPCs.

83

Influence of sirolimus and everolimus on bone marrow-derived mesenchymal stem cell biology

R. Sanz Ruiz¹; ME. Fernandez Santos¹; S. Suarez Sancho¹; L. Fuentes Arroyo¹; V. Plasencia Martin¹; P. Velasco Sevillano¹; A. Casado Plasencia¹; AM. Climent¹; M. Guillem²; F. Atienza Fernandez¹; F. Fernandez-Aviles¹
¹University General Hospital Gregorio Marañon, Department of Cardiology, Madrid, Spain; ²ITACA, Universitat Politecnica de Valencia, Valencia, Spain

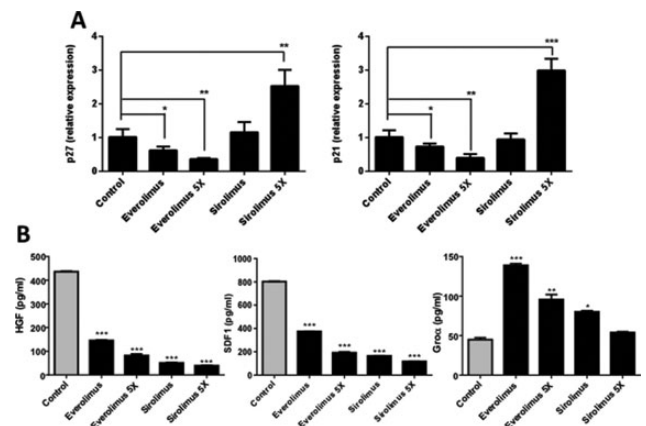
Introduction: Most stem cell trials have used the intracoronary route for cell infusion, after stent implantation. No data are available on the effect of antiproliferative drugs that are released from drug-eluting stents (DES) on bone marrow-derived stem cells.

Purpose: To analyze the effect of sirolimus (S) and everolimus (E) on mesenchymal stem cell (MSC) biology.

Methods: Human bone marrow-derived MSC were cultured. S and E were added mimicking their pharmacokinetics as when released from 40-mm DES (total doses: 300mg for S and 240mg for E). A 5-fold higher dose was also administered. Cell characterization studies included: viability (7-AAD), cell cycle-related gene expression (p21, p27) and flow cytometry (CD106, CD71, CD184, VEGF). Functional assessments included: migration (wound-healing test, FBS/SDF-induced chemotaxis), differentiation-related gene expression (ETV1, FOXO1, GATA 6, PRDM16, Hmga2, SOX11) and secreted protein levels (48-protein immunoassay).

Results: Viability was not modified. Levels of cell-cycle inhibitors were raised only with doses of Sx5 (fig.A). Surface markers showed no differences. Wound-healing was normal for E-exposed MSC (100% confluence at 48h), but was reduced to 72% for S and to 50% for Ex5/Sx5. Invasion assays showed no changes in chemotaxis, except for Ex5 (73% cells/field for FBS and 38% for SDF, both $p < 0.01$ vs controls). Five transcription factors were upregulated with E. PRDM16, Hmga2 and SOX11 were downregulated with S. MSC showed higher secretion of IL8, GRO α and IP10, and lower secretion of HGF, SDF-1 and VEGF (fig.B).

Conclusion: Doses of S and E which are usually released by DES do not affect MSC viability, proliferation, surface marker expression or migration. 5-fold higher doses would be needed to affect them. However, MSC differentiation and secretion could be altered by DES. The clinical impact of these findings warrants further investigations.



Cell-cycle genes and secretome after S/E

84

Endoglin is important for epicardial behaviour following cardiac injury

A T. Moerkamp; CKE. Dingenouts; K. Lodder; BPT. Kruihof; T. Van Herwaarden; AMD. Vegg; MJ. Goumans; AM. Smits
Leiden University Medical Center, Molecular Cell Biology, Leiden, Netherlands

Background/Introduction: The epicardium plays an active role during development of the myocardium. In the adult heart the epicardium is dormant, but can be reactivated upon cardiac injury. This results in upregulation of a developmental gene program, like expression of Wilms' Tumour 1 (WT-1), proliferation and thickening of the epicardial layer. More importantly, as observed in cardiac development, epicardial-derived cells (EPDCs) undergo epithelial to mesenchymal transition (EMT) and migrate into the underlying diseased myocardium where they contribute to the endogenous repair mechanism. As such, the occurrence of EMT in EPDCs is crucial for a 'healthy' epicardial post-injury response. The TGF- β signalling pathway plays a key role in this process. Interestingly, we previously observed that mice heterozygous for the TGF- β co-receptor Endoglin display reduced cardiac function post-myocardial infarction (MI) suggesting that Endoglin is important in the cardiac response to injury.

Purpose: Given the fundamental role of EPDCs following cardiac injury, the aim is to investigate the role of Endoglin in the epicardial post-MI response.

Methods: MI was induced in wildtype (wt) and Endoglin heterozygous (eng^{+/-}) mice by ligation of the left anterior descending coronary artery. Hearts were collected at 4 and 14 days post-MI. Epicardial thickening was measured, and immunostainings for WT-1, Ki-67, CXCR4 and MAC3 were performed. In vitro studies were conducted on EPDCs isolated from human cardiac tissue. EMT was induced by TGF-beta stimulation and interference of Endoglin-mediated signalling was done via virus transduction and a neutralizing antibody.

Results: Immunostainings on human heart tissue confirmed that Endoglin is present in the epicardial region. At day 4 post-MI, epicardial thickening in eng^{+/-} is less pronounced than in wt hearts. In contrast, at 14 days post-MI the eng^{+/-} hearts display a significantly thicker epicardial layer compared to wt (wt 15.12 ± 1.99 μm vs. eng^{+/-} 27.85 ± 4.63 μm, P=0,018). At day 14, we did not observe a difference in the percentage of immune cells within the epicardial region. Furthermore, preliminary data suggest that there is no difference in the number of WT-1 positive cells. This suggests that dysregulation of Endoglin results in either a defect in EMT or it affects proliferation/migration of epicardial cells. Preliminary in vitro data point towards the former and suggest that interfering with Endoglin-mediated signalling changes the EMT response of human EPDCs.

Conclusion: Our data show that dysregulation of Endoglin levels leads to a defect in the epicardial post-injury response and suggest an important role of this TGFβ co-receptor in epicardial behaviour.

Cell death and apoptosis - Heart

87

Ultrastructural alterations reflecting Ca²⁺ handling and cell-to-cell coupling disorders precede occurrence of severe arrhythmias in intact animal heart

N. Tribulova¹; V. Knezl²; B. Szefflova Bacova¹; T. Egan Benova¹; C. Vicenczova¹; E. Goncalvesova³; J. Slezak¹

¹Slovak Academy of Sciences, Institute for Heart Research, Bratislava, Slovak Republic; ²Slovak Academy of Sciences, Institute of Experimental Pharmacology & Toxicology, Bratislava, Slovak Republic; ³The National Institute of Cardiovascular Diseases, Bratislava, Slovak Republic

Objectives: Myocardial abnormalities in calcium handling as well as defects in mechanical and electrical couplings facilitate occurrence of malignant arrhythmias in diseased heart. Using electron microscopy examination we aimed to explore whether such disorders promote development of severe arrhythmias in structurally intact heart.

Methods: Three types of acute interventions were performed that are known to be accompanied by disturbances in intracellular free Ca²⁺ and intercellular coupling. K⁺-deficient perfusion of isolated rat and guinea pig hearts that promote occurrence of ventricular fibrillation (VF); burst atrial pacing of aged isolated perfused guinea pig heart for induction of atrial fibrillation (AF); local intramyocardial noradrenaline (NA) infusion administered to open chest pig heart that induce ventricular tachycardia (VT). Tissue samples for electron microscopic examination were taken prior and during acute interventions as well as during occurrence of malignant arrhythmias.

Results: All acute intervention resulted in similar subcellular alterations: injury of mitochondria of various degree, non-uniform sarcomere shortening most likely reflecting cytosolic Ca²⁺ oscillations; disturbances in Ca²⁺ wave propagation and Ca²⁺ overload. Moreover, impairment of cardiac cell-to-cell mechanical and electrical coupling was recognized according to presence of dissociated adhesive junctions and occurrence of relaxed cardiomyocyte connected with contracted once. These mostly reversible alterations were heterogeneously distributed throughout myocardium and preceded occurrence of VT, VF or AF. Deterioration and occurrence of irreversibly injured cardiomyocytes were found early during occurrence of malignant arrhythmias. Pronounced intracellular Ca²⁺ overload led to both defects in intercellular coupling and disruption of myofibrils, hence promoting myocardial dysfunction.

Conclusions: Results suggest a novel paradigm linking high Ca²⁺-related arrhythmogenesis with contractility disorders while both may contribute to persistence of malignant arrhythmias and acute heart failure.

88

Urocortin-1 promotes cardioprotection through ERK1/2 and EPAC pathways: role in apoptosis and necrosis

T. Smani; E. Calderon-Sanchez; I. Diaz; A. Ordonez

Instituto de Biomedicina de Sevilla, Fisiopatología Cardiovascular, Sevilla, Spain

Background: Urocortin-1 (Ucn-1) is an endogenous peptide that protects hearts from ischemia and reperfusion (I/R) injuries. However, Ucn-1 role apoptosis and in the transcription of specific genes related to survival signaling pathway has not been fully addressed.

Purpose: The aim of this study was to determine signaling pathways implicated in the improvement of cardiomyocytes survival induced by Ucn-1.

Methods and Results: We used a preconditioning protocol applying Ucn-1 before ischemia and at the onset of reperfusion in adult cardiac myocytes isolated from wistar rats hearts. We observed that the administration of Ucn-1 enhanced cell viability using trypan blue experiments, and decreased significantly lactate dehydrogenase (LDH) release in cardiomyocytes subjected to I/R. Experiments using Annexin V-FITC/PI staining indicated that Ucn-1 promoted cell survival and decreased cell necrosis. We found that Ucn-1 shifted cell death from necrosis to apoptosis and activated caspases 9 and 3/7. These effects were inhibited by selective inhibitors of Epac2 (exchange protein directly activated by cAMP) and ERK 1/2 (extracellular signal-regulated kinases 1/2). Mini-array, RT-qPCR and protein analyses showed that Ucn-1 upregulated the expression of anti-apoptotic genes CD40lg and Xiap but it enhanced the expression of BAD, a pro-apoptotic gene. Ucn-1 effects on genes regulation involved also Epac2 and ERK1/2 activation.

Conclusion: Our data demonstrates that Ucn-1 efficiently protects hearts from I/R injuries by increasing the cell survival and stimulating the overexpression of apoptotic genes, CD40lg, Xiap and BAD, involving Epac2 and ERK1/2 activation.

89

Expression p38 MAPK and Cas-3 in myocardium LV of rats with experimental heart failure at melatonin and enalapril introduction

Y V. Liskova¹; S P. Salikova²

¹Orenburg State Medical Academy, Orenburg, Russian Federation; ²Kirov Military Medical Academy, Saint Petersburg, Russian Federation

Purpose: To determine an expression pattern p38 MAPK and Cas-3 in the myocardium left ventricle (mLV) rats with experimental heart failure (EHF) at melatonin and enalapril introduction.

Methods: The study was conducted on 35 adult outbred female rats, 30 animals EHF was caused by s.c. injection of a 1% mezon solution (0.1ml) followed by an intensive swimming regimen for 14 day (d). 5 - in the control group, 6 - derived from the experiment on 14d EHF. 24 animals after modeling EHF were divided into 3 groups, each within 14d daily intraperitoneally administered drug: group 1 (n=8) melatonin (M) 2 mg/kg (Sigma-Aldrich), group 2 (n=8) enalaprilat (E) 0.5 mg/kg, group 3 (n=8) 0.1 ml physiological saline (1:9) (FS). mLV studied light microscopic, immunocytochemical (p38α MAPK and CAS-3 protein expression) methods. Assessment of localization and intensity of the immune response p38α MAPK (p38) was performed semiquantitatively +/+ + + in randomly selected fields of view under mikrovizorom mVizo-101: (-) no immunopositive cardiomyocytes (PCM), (+) light 1-4 PCM; (++) moderate, more than 5 PCM, (+++) high immunoreactivity, almost all CM immunopositive. To identify cells with signs of apoptosis was determined apoptotic index as the number of stained cells divided by the 1000 cells in randomly selected fields of view.

Results: In the control group of myocardial sites predominated mild to moderate immunoreactivity p38 (+/+ +). Areas with high immunoreactive p38 (+++) prevailed in the myocardium on 14d EHF. A significant reduction in the intensity of expression p38 (+) observed in 1 group (EHF+M), a moderate decrease in p38 (++) in 2 group (EHF+E) and in 3 group (EHF+FS). Analysis of expression of Cas-positive cardiomyocytes (Cas+CM) groups showed increase of the amount of CM with the phenomena of apoptosis 10 ± 0.4% for 14d EHF and in 3 group EHF+FS - 9 ± 1.2%, in 2 group (EHF+E) Cas+CM were 6 ± 0.4% and in group 1 (EHF+M) Cas+CM - 3 ± 0.1%; control 1 ± 0.1% (p<0.05). We found that under the action of melatonin in rats- female with EHF was a significant regression of pathological changes in the mLV, less common sites with interstitial edema, hemodynamic compromise, which was accompanied by a decrease in the amount of CM with the phenomena apoptosis and significantly reduced expression p38 MAPK, compared with enalapril group.

Conclusions: Our study demonstrated cardioprotective effects melatonin in rats- female significantly superior over enalapril, indicating the presence of angiotensin-independent mechanisms of myocardial remodeling and CM death in heart failure.

Transcriptional control and RNA species - Heart

92

Accumulation of beta-amyloid 1-40 in HF patients: the role of lncRNA BACE1-AS

S. Greco¹; G. Zaccagnini¹; C. Voellenkle¹; I. Sadeghi¹; B. Maimone¹; S. Castelvecchio¹; C. Gaetano²; L. Menicanti¹; F. Martelli¹

¹Ircs Policlinico San Donato, san donato milanese, Italy; ²JW Goethe University, Frankfurt am Main, Germany

Background: The long noncoding RNA BACE1-AS is transcribed from the opposite strand of the β-secretase (BACE1) gene, coding for a protease producing the β-amyloid (Aβ) peptides. Moreover, BACE1-AS modulates BACE1 expression. Additionally, heart failure (HF) and Alzheimer's disease (AD) share several non-genetic effectors and risk factors. Indeed, data from literature show that amyloid-like peptides accumulate also in cardiomyocytes and are associated with cardiovascular disorders.

Purpose: In keeping with these findings, this study aims to evaluate if the BACE1-AS/BACE1 axis is dysregulated in heart failure (HF).

Methods: BACE1 and BACE1-AS RNA expression was measured in left ventricle (LV) biopsies from 18 patients affected by non-end stage dilated ischemic cardiomyopathy and 17 matched controls by qPCR. The tissual and cellular localization of BACE1-AS RNA was evaluated by in situ hybridization (ISH) assay. Levels of Aβ 1-40 and 1-42 peptide were measured in plasma from HF patients and healthy individuals by immunoenzymatic assay. In vitro modulation of BACE1-AS expression was performed in human aortic endothelial cells and in mouse cardiomyocytes. BACE1 and Aβ 1-40 protein expression was assessed by immunohistochemistry (IHC) and immunofluorescence (IF) in heart biopsies and cells, respectively. The toxicity of Aβ peptides was evaluated in both HAOEC and in mouse cardiomyocytes.

Results: We found that: 1) BACE1-AS and BACE1 transcripts were both up-regulated in LV biopsies derived from HF patients; 2) ISH showed that BACE1-AS RNA was expressed in the nucleus of cardiomyocytes, endothelial and fibroblast heart cells; 3) in vitro up- or down-modulation of BACE1-AS levels induced the concordant regulation of BACE1 RNA, and both BACE1 and Aβ 1-40 protein levels; 4) Aβ 1-40 protein expression levels were significantly increased in HF patients in both plasma and LV tissue; 5) the number of cells decreased after Aβ peptides administration in both endothelial cells and cardiomyocytes and 6) transcriptomic analysis of endothelial cells, where BACE1-AS expression was blocked, indicated changes of relevant pathways for cardiovascular ischemic diseases.

Conclusions: Given the neurotoxic role of β-amyloids in AD, dysregulation of the BACE1/BACE1-AS axis might be a relevant component of HF pathogenesis, further involving noncoding RNAs in the complex scenario of proteotoxicity in cardiac dysfunction.

93

Role of miR-182 in zebrafish and mouse models of Holt-Oram syndrome

E. Guzzolino¹; C. Hatcher²; R. D'aurizio³; M. Groth⁴; M. Baumgart⁴; A. Mercatanti¹; F. Russo³; L. Mariani¹; C. Magliaro⁵; L. Pitto¹

¹Institute of Clinical Physiology, CNR, Pisa, Italy; ²Philadelphia College of Osteopathic Medicine, Department of Bio-Medical Sciences, Philadelphia, United States of America; ³Institute of Informatics and Telematics CNR, Pisa, Italy; ⁴Fritz Lipmann Institute for Age Research, Jena, Germany; ⁵University of Pisa, Research Center "E. Piaggio", Pisa, Italy

Background/Introduction: Tbx5 is a key gene involved in heart/limb development. Tbx5 mutations cause Holt-Oram syndrome (HOS) in humans, which is characterized by upper limb malformations and congenital heart defects (CHDs) with an incidence of 1:100000 births.

Purpose: The transcription factor Tbx5 regulates hundreds of genes including miRNAs, important negative post-transcriptional regulators. To understand parts of this complex network of molecular regulation, we looked for Tbx5-modulated microRNAs with a functional role in heart development.

Method: We performed a miRNA-profiling on RNA extracted from E11.5–E12.0 hearts isolated from WT and HOS mice. Via a bioinformatic approach we selected differentially expressed miRNAs putatively targeting evolutionary conserved genes related to heart development. Selected miRNAs were functionally tested with experiments of misexpression and in situ hybridization both in vivo in zebrafish, and in vitro in culture of mouse cardiac HL1 cells.

Results: We focused on miR-182, which was recently identified as a potential prognostic marker in cardiac heart failure and is overexpressed in patients with coronary artery disease. miR-182 was found to be up-regulated in HOS mouse hearts. In line with this data, its overexpression in zebrafish embryos resulted in dose-dependent cardiac defects. Furthermore, downregulation of miR-182 by morpholino microinjection partially rescues HOS phenotype in zebrafish embryos depleted by Tbx5. In situ hybridization experiments revealed that the miR-182 overexpression was able to affect proliferation and migration of myocardial cells during the first stages of zebrafish development and in vitro assays in HL1 cells confirmed these results.

Conclusions: Our approach further supports the importance of microRNA regulation in HOS pathology and demonstrates that miR-182 is a phylogenetically conserved Tbx5 effector able to affect cardiac development.

94

Mir-27 distinctly regulates muscle-enriched transcription factors and growth factors in cardiac and skeletal muscle cells

D. Franco; E. Lozano-Velasco; A. Jodar-García; J. Galiano-Torres; I. Lopez-Navarrete; A. Aranega
University of Jaen, Department of Experimental Biology, Jaen, Spain

microRNAs are non-coding RNA that exert post-transcriptional regulatory mechanisms by either blocking transcript translation or promoting mRNA degradation. Over the last decade, novel insights have been gained on the functional role of distinct microRNAs in cardiovascular development and disease. We have previously reported a discrete number of microRNAs that are differentially expressed during cardiogenesis. In particular, we demonstrated that miR-27, which is overtly expressed in the developing heart, targets Mef2c muscle-enriched transcription factor. More recently, a role for miR-27 regulating Pax3 has been reported in skeletal muscle. In this study we sought to get further insights into the regulatory mechanisms exerted by miR-27 in cardiac and skeletal muscle cells. We assayed whether distinct muscle-enriched transcription factors and growth factors predicted to be targeted by miR-27 are deregulated after miR-27 overexpression in three distinct cell types, i.e. Sol8 skeletal myoblast, HL-1 cardiomyocytes and 3T3 fibroblasts, respectively. qPCR analyses demonstrated that miR-27 overexpression deregulated Runx1 and Mef2c expression in both cardiac and skeletal muscle cells, in line with previous reports. In contrast, Mstn, Myocd, Mdf1, which are also predicted to be targeted by miR-27, display different deregulated patterns in cardiac as compared to skeletal muscle cells, while Mef2d displayed no significant differences. Similarly, miR-27 over-expression lead to no significant differences for Tgfb1, Tgfb3 and Bmpr1a, while Egfr1 and Fgf1 showed different deregulated patterns in cardiac vs skeletal muscle cells. Overall these results demonstrate that miR-27 can selectively up-regulate and down-regulate a discrete number of target mRNAs in a cell-type specific manner. A mechanistic working hypothesis as how this is exerted will be presented.

95

AF risk factors impair PITX2 expression leading to Wnt-microRNA-ion channel remodeling

E. Lozano-Velasco¹; R. Wagensteen²; A. Quesada²; A. Aranega¹; D. Franco¹
¹University of Jaen, Department of Experimental Biology, Jaen, Spain; ²University of Jaen, Department of Health Sciences, Jaen, Spain

Atrial fibrillation (AF) is the most frequent arrhythmogenic defect in the human population, with an estimate incidence ranging from 2-10%. Genetic defects have been recently described underlying AF, with the homeobox transcription factor PITX2 as a major cornerstone. We have previously described that PITX2 expression is impaired in AF patients. Furthermore, distinct studies demonstrate that Pitx2 insufficiency leads to complex gene regulatory network remodeling, i.e. Wnt>microRNAs, leading to ion channel impairment and thus to arrhythmogenic events. Whereas large body of evidences has been provided in recent years on PITX2 downstream signaling pathways, scarce information is available on upstream pathways influencing PITX2. Multiple risk factors are associated to the onset of AF, such as e.g. hypertension (HTA), hyperthyroidism (HTD), obesity and redox homeostasis impairment. In this study we have analysed whether HTA and/or HTD impact on PITX2 and its downstream signaling pathways. Using rat models for HTA and HTD we have observed that both cardiovascular risk factors lead to severe Pitx2 downregulation. Interestingly HTD, but not HTA, leads to up-regulation of Wnt signaling as well as deregulation of multiple microRNAs and ion channels as previously described in Pitx2 insufficiency. In addition, redox signaling is impaired as consequence of HTD but not HTA, in line with similar findings in atrial-specific Pitx2 deficient model. Furthermore in vitro cell culture analyses using gain- and loss-of-function strategies demonstrate that Pitx2, Zfhx3 and Wnt signaling influence redox homeostasis in cardiomyocytes. Thus, redox homeostasis seems to play a pivotal role in this setting, providing complex regulatory feedback loop. Overall these data demonstrate that HTA and HTD can impair Pitx2>>Wnt signaling providing thus a molecular mechanistic model as how these cardiovascular risk factors lead to AF.

Cytokines and cellular inflammation - Heart

98

Post-infarct survival depends on the interplay of monocytes, neutrophils and interferon gamma in a mouse model of myocardial infarction

M. Knorr¹; S. Finger²; S. Karbach¹; S. Kossmann¹; T. Muenzel¹; P. Wenzel¹
¹University Medical Center, Department of Medicine 2, Mainz, Germany; ²University Medical Center of Mainz, Center of thrombolysis and hemostasis, Mainz, Germany

Background: Myelomonocytic cells participating in the initial injury as well as in the later healing mechanisms of myocardial infarction (MI). Still, the specific interplay of inflammatory myeloid cells and primary mediators remains to be further determined.

Cardiovascular Research Supplements

Objective: The aim of this study was to investigate the cardio protective or in part adverse role of lysosome M positive (LysM+) and granulocyte-receptor 1 positive (Gr-1+) immune cells on cardiac injury and healing in a murine model of MI.

Methods and Results: MI was induced in 8 to 12 week-old male mice (C57BL/6 background) by permanent ligation of the left anterior descending coronary artery (LAD). Compared to LysMCre controls, LysM+ cell depleted LysM^ΔDTR transgenic mice (depletion 3d prior MI by diphtheria toxin application, 25 ng/g body weight) displayed a reduced influx of CD45.2+/CD3-/CD11b+/-Gr-1high neutrophils into infarcted myocardium 1d post MI (measured by flow cytometric analysis). Additionally, cardiac mRNA expression levels of inflammatory cytokines interferon gamma (INFγ) and tumor necrosis factor alpha (TNFα) were decreased 7d post MI. Mortality after MI was significantly increased in LysM-depleted mice within 28d post MI. To more specifically estimate the role of neutrophils, we depleted C57BL/6 mice with a monoclonal anti-Gr-1 antibody and found increased mortality early after MI as well as a decrease in INFγ mRNA expression. MCP-1 (CCL2) and CCR2 mRNA were decreased 3d after MI according to reduced amount of CD11b+/Ly6G/Ly6Chigh inflammatory monocytes in the infarcted myocardium of neutropenic mice. LAD ligated INFγ-/- mice and TNFα-/- mice displayed a significantly decreased post-infarct survival, worsening of left ventricular function and an impaired inflammatory cell infiltration compared to C57BL/6 controls.

Conclusion: We provide evidence that monocytes, neutrophils and INFγ play a crucial role in post-infarct survival and cardiac remodeling. Our data suggest that neutrophils are needed for monocyte chemotaxis. We argue that strategies to oppose the adverse cardiac remodeling processes must consider a potentially beneficial effect of early neutrophil influx into infarcted myocardium.

99

Inflammatory cd11b/c cells play a protective role in compensated cardiac hypertrophy by promoting an orai3-related pro-survival signal

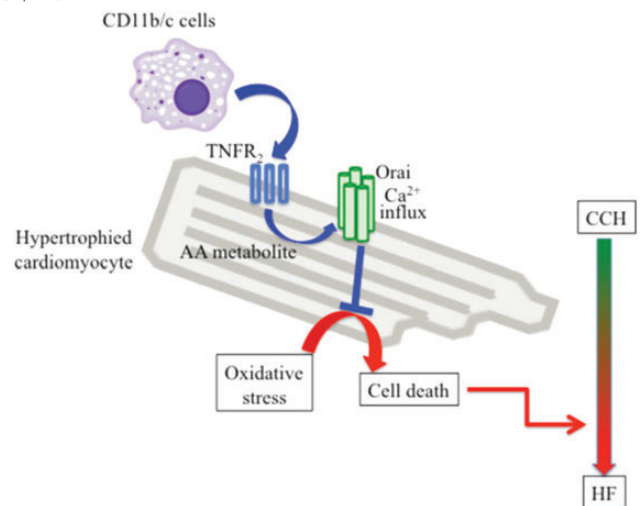
C. Pavoiné; M. Keck; N. Mougnot; S. Favier; A. Fuand; F. Atassi; C. Barbier; AM. Lompre; JS. Hultot
University Pierre & Marie Curie Paris VI, INSERM UMR_S 1166 ICAN, Paris, France

Background: Inflammation and cardiac macrophages play a crucial role in the process of cardiac remodeling towards heart failure (HF), with conflicting results as to whether they are beneficial or detrimental.

Purpose: We aimed to evaluate the protective role of inflammation and cd11b/c cells in compensated cardiac hypertrophy (CCH)

Methods and Results: Intraperitoneal injection of the anti-inflammatory drug with anti-macrophage actions, semapimod, to mice displaying CCH (12 days with chronic isoproterenol infusion) precipitates evolution to HF, as attested by echocardiography analysis. Incubation of adult hypertrophied cardiomyocytes with TNFα or conditioned medium (cmed) from cardiac CD11b/c cells activated either in vivo (isolated from rats displaying CCH), or in vitro (isolated from normal rats and in vitro treated with LPS) increases resistance to oxidative stress. Preincubation of CD11b/c cells with semapimod prior LPS application neutralizes the protective impact of cmed. Mechanistically, pro-survival impact of TNFα or CD11b/c cmed are TNFR2-dependent. Ca2+ imaging studies, using pharmacological or molecular (intracardiac injection of siRNA) approaches, show that TNFα or CD11b/c cmed enhance arachidonic acid (AA)-activated Orai3-driven Ca2+ influx in hypertrophied cardiomyocytes, in a semapimod- and TNFR2-dependent manner. In hypertrophied cardiomyocytes, pharmacological inhibition of Orai3 (YM58483) blunts the beneficial impact of TNFα and CD11b/c cmed on resistance to oxidative stress.

Conclusion: In CCH, cardiac inflammatory CD11b/c cells limit the evolution to HF and increase resistance of adult hypertrophied cardiomyocytes to oxidative stress by activating a TNFR2-dependent Orai3-driven Ca2+ influx.



protective inflammation in CCH

100

Anti-inflammatory effects of endothelin receptor blockade in the atrial tissue of spontaneously hypertensive rats

A. Bukowska¹; Y. Nikonova²; F. Pluteanu²; J. Kockskaemper²; RK. Chilukoti³; C. Wolke³; U. Lendeckel³; A. Gardemann¹; A. Goette⁴
¹Otto-von-Guericke University of Magdeburg, Institute of Clinical Chemistry and Pathobiochemistry, Magdeburg, Germany; ²Philipps University of Marburg, Institute of Pharmacology and Clinical Pharmacy, Marburg, Germany; ³University Medicine of Greifswald, Institute of Medical Biochemistry and Molecular Biology, Greifswald, Germany; ⁴St. Vincenz-Krankenhaus, Paderborn, Germany

Introduction: Detailed characterisation of atrial remodelling in the spontaneously hypertensive rat (SHR) has revealed that atrial remodelling involves early and prominent augmentation of endothelin

(ET) signalling which is associated with increased inflammation, fibrosis, and altered Ca²⁺ signalling. Based on our results, we postulated that atrial ET receptors constitute a novel therapeutic target in hypertension-mediated left atrial remodelling and tested whether an endothelin receptor antagonist (ERA), macitentan, could reduce atrial remodelling in hypertensive rats.

Methods: Male SHR at the age of 7-9 months were randomly assigned to the following experimental groups: SHR control (n=23), SHR treated with ERA (macitentan 30 mg/kg/d, n=18), and SHR treated with alpha-adrenergic antagonist (α -blocker, doxazosin, 30 mg/kg/d, n=18). After 2 months of treatment we performed comprehensive molecular analysis on genes and proteins involved in endocardial inflammation and dysfunction. To study the molecular changes in response to pacing, atrial slices were subjected to electrical field stimulation at 5 Hz (vs. 0.6 Hz) up to 20 h (in vitro model of atrial fibrillation).

Results: RT-qPCR analysis revealed that hypertension in SHR was characterised by increased expression of cytokines: IL6, IL8, adhesion molecules, the prothrombotic molecule PAI-1, and a marker of endocardial dysfunction, TNF α . The inflammatory state was accompanied by activated MAP kinases: ERK, p38, and the activated transcription factor NF- κ B p65. ERA administration lowered VCAM-1 mRNA expression, whereas α -blocker had no effect. Interestingly, both treatments reduced ICAM-1 at the transcriptional and protein level predominantly in left atria [LA]. Similarly, expression of IL-8 mRNA was down-regulated in LA (SHR-ERA: 0.52 ± 0.06 ; P<0.01, SHR- α -blocker: 0.57 ± 0.05 ; P<0.05, vs SHR control: 1.0 ± 0.24). Whereas the treatment with ERA blunted the activation of NF- κ Bp65 and MAP kinases, the treatment with α -blocker showed no effects on NF- κ Bp65. Moreover, treatment with ERA prevented the high frequency-induced stimulation of pro-inflammatory genes.

Conclusion: The blockade of endothelin receptors decreases inflammation via reduction of MAP-kinases activation, NF- κ B, and downregulation of adhesion molecules and cytokines in hypertensive atria.

101

Mesenchymal stromal cells reduce NLRP3 inflammasome activity in Coxsackievirus B3-induced myocarditis

S. Van Linthout¹; K. Miteva¹; K. Pappritz¹; I. Mueller¹; M. El-Shafeey¹; J. Ringe¹; C. Tschoepe²
¹Berlin-Brandenburg Center for Regenerative Therapies, Berlin, Germany; ²Charité - Universitätsmedizin Berlin, Campus Virchow-Klinikum (CVK) Kardiologie, Berlin, Germany

Purpose: Recent evidence indicates the relevance of the inflammasome Nod-like receptor protein 3 (NLRP3) in the pathogenesis of Coxsackievirus B3 (CVB3)-induced myocarditis. The NLRP3 inflammasome comprises NLRP3, the adaptor protein ASC, and caspase 1, and is responsible for the processing of pro-IL-1 β to IL-1 β . Mesenchymal stromal cells (MSC) have immunomodulatory and cardioprotective properties. We previously have demonstrated that intravenous MSC application in CVB3-induced myocarditis reduces myocardial inflammation and improves left ventricular (LV) function. The aim of the present study was to evaluate the effect of MSC on CVB3-induced NLRP3 inflammasome activity.

Methods: C57BL/6 mice were intravenously injected with one million MSCs one day post CVB3 infection and sacrificed at day 7. LV were collected for molecular biology and the spleen for flow cytometry analysis of F4/80, CD49b and CD11b cells expressing ASC and the active caspase 1 form p10. MSC were co-cultured with HL-1 at a ratio 1:10. Four hours post CVB3-infection at a m.o.i. 5, cells were collected for ASC, caspase 1, pro-IL-1 β , and IL-1 β flow cytometry. To distinct HL-1 cells from MSC, HL-1 were prelabelled with DiO or DiI.

Results: LV NLRP3 mRNA expression was 8.8-fold (p<0.005) increased in CVB3-infected versus control mice and paralleled by a 6.5-fold (p<0.005), 1.7-fold (p=0.22), and 14.0-fold (p<0.001) induction of LV caspase 1, IL-1 β and IL-18 mRNA expression, respectively. MSC application in CVB3-infected mice reduced the LV expression of NLRP3, caspase 1, IL-1 β , and IL-18 by 10.6-fold (p<0.005), 4.2-fold (p<0.005), 3.8-fold (p<0.05) and 8.2-fold (p<0.005), respectively. An MSC-mediated decrease in NLRP3 inflammasome activity could be observed systemically. This is evidenced by a 1.8-fold (p<0.01), 1.7-fold (p<0.01), and 1.7-fold (p<0.05) decrease of the CVB3-induced ASC expressing splenic F4/80, CD49b and CD11b cells, respectively. Furthermore, a 1.8-fold (p<0.001), 1.7-fold (p<0.0005), and 1.4-fold (p<0.05) decrease of further downstream p10 expressing splenic F4/80, CD49b and CD11b cells, respectively, was observed. Co-culture of MSC with CVB3-infected HL-1 cardiomyocytes decreased the CVB3-induced % of ASC+ cells by 1.9-fold (p<0.0005). This was associated with a downstream 1.3-fold (p<0.001) reduction of caspase 1 activity in HL-1 cells, which was on its turn reflected by a decrease in processing of pro-IL-1 β to IL-1 β as shown by a 1.9-fold (p<0.0001) decline in % of IL-1 β + cells in the absence of a drop in pro-IL-1 β expressing cells.

Conclusion: MSC reduce NLRP3 inflammasome activity in CVB3 myocarditis mice.

102

Mesenchymal stromal cells modulate monocytes trafficking in Coxsackievirus B3-induced myocarditis

K. Miteva¹; K. Pappritz¹; M. El-Shafeey¹; J. Ringe¹; C. Tschoepe²; S. Van Linthout¹
¹Berlin-Brandenburg Center for Regenerative Therapies, Cardiovascular biology, Berlin, Germany; ²Charité - Campus Virchow-Klinikum (CVK), Cardiology, Berlin, Germany

Purpose: Cardiac monocytes infiltration is a major trigger of inflammatory cardiomyopathy. Mesenchymal stromal cells (MSC) have immunomodulatory and cardioprotective properties. We have shown that MSC application in Coxsackievirus B3 (CVB3)-induced myocarditis reduces myocardial inflammation, fibrosis and improves left ventricular (LV) function. The aim of the present study was to evaluate the effect of MSC on CVB3-induced cardiac monocytes trafficking.

Methods: C57BL/6 mice were intravenously injected with one million MSCs one day post CVB3 infection and sacrificed at day 7. LyC6highCD115+CD11b+CCR2highCX3CR1low, LyC6middleCD115+CD11b+CCR2highCX3CR1low, and LyC6lowCD115+CD11b+CCR2lowCX3CR1high monocytes were analysed in the blood and heart via flow cytometry. LV mRNA expression was determined via real-time PCR.

Results: MSC application reduced the % of pro-inflammatory LyC6highCD115+CD11b+CCR2highCX3CR1low and LyC6middleCD115+CD11b+CCR2highCX3CR1low monocytes by 5.4-fold (p<0.0001) and 2.6-fold (p<0.001) in the blood and by 2.4-fold and 1.9-fold

(p<0.0001) in the heart compared to CVB3 mice, respectively. CVB3+MSC mice exhibited 2.4-fold (p<0.01) and 2.5-fold (p<0.05) higher % of anti-inflammatory monocytes LyC6lowCD115+CD11b+CCR2lowCX3CR1high in the blood and heart versus CVB3 mice, respectively. MSC application reduced LV mRNA expression of the chemokines MCP-1, MCP-3 and CCL5, attracting pro-inflammatory monocytes, into the heart by 51.4-fold, 225-fold, and 71.8-fold, respectively (p<0.001 vs CVB3 mice), while induced a 3.4-fold (p<0.001) increase in LV mRNA expression of SDF-1 α , attracting cardiac-reparative monocytes. In parallel, CVB3+MSC mice exhibited a 5.1-fold (p<0.001) and 11.7-fold (p<0.001) diminished expression of the adhesion molecules ICAM-1 and VCAM-1 compared to CVB3 mice, respectively. MSC treatment also downregulated the LV mRNA expression of the pro-inflammatory cytokines IL-6, TNF- α , IL-1 β and TGF- β by 86.8-fold (p<0.01), 30.4-fold (p<0.0001), 3.8-fold (p<0.05) and 5.6-fold (p<0.01), respectively, compared to CVB3 mice, and induced 2.2-fold (p<0.05) higher LV eNOS mRNA expression. CVB3+MSC mice manifested 3.2-fold (p<0.0001) and 2.6-fold (p<0.001) lower MCP-1 and MCP-3 serum levels, in comparison to CVB3 mice, respectively.

Conclusion: MSC application in CVB3 myocarditis mice modulates the chemokine pattern and induces a shift in the cardiac infiltrating monocytes from a pro-inflammatory to an anti-inflammatory subset.

103

The impact of regulatory T lymphocytes on long-term mortality in patients with chronic heart failure

P. Sulzgruber; L. Koller; B. Richter; S. Blum; M. Koprak; M. Huelsmann; R. Pacher; G. Goliash; J. Wojta; A. Niessner
 Medical University of Vienna, Cardiology, Vienna, Austria

Background: Chronic heart failure (CHF) constitutes a global health issue representing a prevalent clinical syndrome. While pro-inflammatory cytokines proved to have a pivotal role in the development and progression of CHF, less attention has been paid to the cellular immunity. Regulatory T lymphocytes (Tregs) have an important role in the induction and maintenance of immune homeostasis. However recent evidence suggests a deregulation in Treg function causing abnormal immune responses leading to progression of pathology in inflammatory disease. Therefore we aimed to investigate the impact of Tregs on the outcome of patients presenting with CHF.

Methods: We prospectively enrolled 112 patients with CHF defined by New York Heart Association (NYHA) functional class > II and left ventricular ejection fraction (LVEF) <40%. Cells from fresh heparinized blood were stained and analyzed using BD FACS Canto II flow cytometry. Cox regression hazard analysis was used to assess the influence of Tregs on survival. The multivariate model was adjusted for age, gender, type of CHF, LVEF and Nt-proBNP.

Results: After a mean follow-up time of 4.5 years 32 (28.6%) patients died due to cardiovascular causes. Comparing survivors to non-survivors we found a significantly higher count of Tregs in surviving individuals (p<0.001). Interestingly we were able to show a lower total lymphocyte count (p=0.004) as well as a significantly lower fraction of CD4+ cells (p=0.042) among survivors. More specifically, there was a significantly higher fraction of cytotoxic T cells characterized by the loss of CD28 within CD4 T cells (p=0.032) detectable in deceased individuals. Moreover Tregs were significantly associated with cardiovascular survival in the entire study cohort with a crude HR per one standard deviation (1-SD) of 0.49 (95% CI 0.33-0.72; p<0.001). Even after adjustment for potential cofounders Tregs remained independently associated with long-term survival with an adjusted HR per 1-SD of 0.59 (95% CI 0.36-0.98; p=0.043).

Conclusion: Our results might indicate a potential influence of Tregs in the pathogenesis and progression of CHF, fostering the implication of cellular immunity in CHF pathophysiology and proving Tregs as a predictor for long-term survival among CHF-patients.

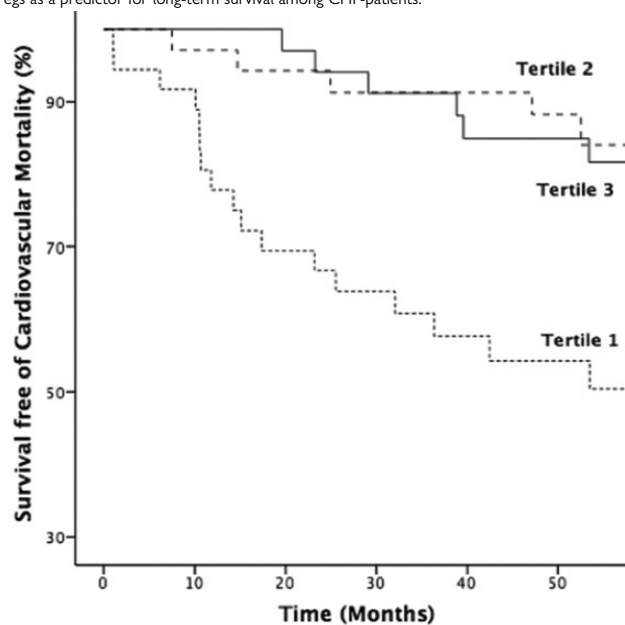


Figure 1: Survival Curves of Cardiovascular Mortality. Kaplan-Meier plots showing cardiovascular mortality stratified by tertiles of Treg fraction among CD4+ cells (Tertile 1: low; Tertile 2: mid; Tertile 3: high). Tertiles were compared using log-rank test (p<0.001).

104

Temporal dynamics of dendritic cells after ST-elevation myocardial infarction relate with improvement of myocardial function

S. C. Latet¹; P. L. Van Herck²; M. J. Claeys²; S. E. Haine²; G. D. Lenders²; H. P. Miljoen²; V. F. Segers²; T. R. Vandendriessche²; V. Y. Hoymans¹; C. J. Vrints¹

¹University of Antwerp, Translational Pathophysiological Research, Cardiovascular Diseases, Antwerp, Belgium;

²University of Antwerp Hospital (Edegem), Department of Cardiology, Antwerp, Belgium

Background: The healing response after acute myocardial infarction (MI) consists of several distinct but overlapping phases. In the inflammatory phase (from onset to 2 days post-MI) neutrophils and phagocytic monocytes are recruited from the bloodstream into the myocardium to clear dead cells and matrix debris. In the subsequent proliferative phase (from 2 days to 2 weeks post-MI) reparative monocytes, dendritic cells and lymphocytes are mobilized to resolve the inflammatory reaction.

Purpose: To measure serial changes in circulating dendritic cell (DC) subsets after STEMI and to determine whether there is a relationship between temporal changes in DC and left ventricular (LV) remodelling post-MI.

Methods: Peripheral blood samples were obtained from 17 patients at the acute inflammatory (admission), transition (day 2) and proliferative phases (day 5). Circulating myeloid (mDC: CD45+CD14-CD19-BDCA1+) and plasmacytoid (pDC: CD45+CD14-CD19-BDCA2+) DC were quantified with flow cytometry. Peak troponin was used to estimate infarct size. LV ejection fraction (LVEF), end-diastolic (EDV) and end-systolic (ESV) volumes were measured by 3D-echocardiography at post-MI day 1 and at 6 months.

Results: STEMI induces a differential response of DC subsets. There were time-dependent changes in circulating mDC, but not pDC, post-STEMI compared with control subjects (stable angina pectoris; n=11; figure 1). The mDC count at day 5 correlated with troponin peak value ($\rho=-0.682$, $p=0.004$). There was a significant inverse correlation between mDC early after MI (days 2 and 5) and the change in LVEF at 6 months ($\rho=-0.574$, $p=0.016$; $\rho=-0.709$, $p=0.002$; figure 1). DC counts showed no correlation with Δ EDV or Δ ESV.

Conclusion: Our findings point towards an association between mDC and improvement of ventricular function after STEMI.

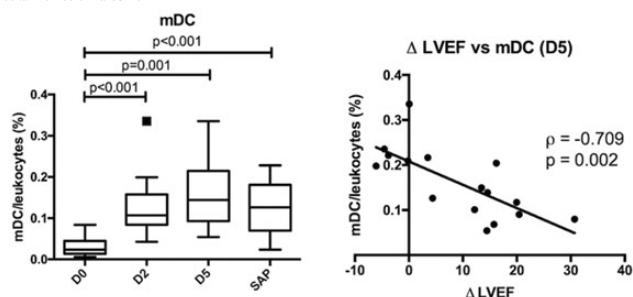


Figure 1: Temporal dynamics of myeloid dendritic cells and their correlation with the change in LVEF after 6 months.

Growth factors and neurohormones - Heart

107

Preconditioning of hypertrophied heart: miR-1 and IGF-1 crosstalk

A. Portnychenko; T. Lapikova-Bryhinska; V. Gurianova; H. Portnychenko; M. Vasylenko; Y. Zapara; V. Portnychenko

Bogomoletz Institute of Physiology, NAS of Ukraine; ICAMER, NAS of Ukraine, Kyiv, Ukraine

Purpose: Insulin like growth factor IGF-1 mediates heart hypertrophy, as well as promotes cell survival by reduction of apoptosis and oxidative stress, limitation of inflammatory response and endothelial dysfunction. However, cardioprotective mechanisms in the hypertrophied myocardium is not fully elucidated. In particular, microRNA miR-1 may take a part as negative regulator for IGF-1 expression. The aim was to determine whether IGF-1 maintains its cardioprotective properties in the hypertrophied heart.

Methods: In male Wistar rats or SHR aged 6 months, hypertrophy of left heart ventricle was induced by isoproterenol (5 mg/kg, 7 days). The next day, delayed cardioprotection was induced by preconditioning with whole body hypoxia séance (10% O₂, 3 h). In 24 h, hearts were isolated with urethane narcosis and subjected to ischemia/reperfusion in a Langendorff mode, infarct size was detected with TTC staining. Dynamic changes in mRNA, microRNA and protein expression in left ventricles were examined using reverse transcription with real-time PCR, and Western blotting.

Results: In control SHR, the expression of IGF-1 mRNA and protein was lower by 34% and 42%, respectively, but miR-1 expression with significantly elevated compared to Wistar. During isoproterenol treatment, the IGF-1 mRNA decreased by 25% in Wistar and by 36% in SHR on 3rd day, then the values recovered. The dynamics of protein expression in Wistar was in accordance to mRNA level, but in SHR the indicators remained consistently low. The expression of miR-1 showed opposite fluctuations according to the level of IGF-1 expression in all cases. Wortmannin, inhibitor of PI3K, abolished delayed cardioprotection in hypertrophied myocardium, as well as in control hearts in view of infarct size and cardiac function recovery in posts ischemic reperfusion. Blocker of IGF-1 receptor picropodophyllin influenced similarly, but more pronounced in Wistar.

Conclusions: Short-time left ventricular hypertrophy in Wistar rats is regulated by transient miR-1-mediated limitation of IGF-1-dependent prohypertrophic signalling, but IGF-1-receptor/PI3K-mediated cardioprotective response is maintained. However, prolonged left ventricular remodeling in SHR is characterized with IGF-1 mRNA and protein suppression due to intensified miR-1 inhibitory action, and with limited cardioprotection. Thus, left ventricular remodeling is accompanied with miR-

1 and IGF-1 crosstalk to regulate cell hypertrophy vs cardioprotection. But miR-1-mediated suppression of hypertrophic growth of myocardium may be the increasing risk factor for infarction damage.

108

Modulation of catecholamine secretion from human adrenal chromaffin cells by manipulation of G protein-coupled receptor kinase-2 activity

A. Cannavo¹; D. Liccardo¹; A. Lyemperopoulos²; M. Santangelo³; D. Leosco⁴; W.J. Koch¹; N. Ferrara⁴; G. Rengo⁵

¹Temple University School of Medicine, Center for Translational Medicine, Philadelphia, United States of America;

²Nova Southeastern University, Pharmacology, Fort Lauderdale, United States of America;

³Federico II University Hospital, Naples, Italy;

⁴Federico II University of Naples, Naples, Italy;

⁵Scientific Institute of Telesse Terme, Telesse Terme, Italy

Background: Adrenal G protein-coupled receptor kinase-2 (GRK2) up-regulation represents a crucial mechanism in heart failure-related sympathetic nervous system hyperactivity. In fact, increased GRK2 levels causes desensitization of the sympatho-inhibitory alpha 2-adrenergic receptors (a2ARs) thus leading to enhanced catecholamine (CA) secretion from the chromaffin cells of the adrenal medulla. Purpose: In the present study, we sought to investigate whether manipulation of adrenal GRK2 levels/activity regulates CA secretion in isolated primary human chromaffin cells.

Methods: Chromaffin cells isolated from human adrenal glands were cultured and infected in vitro with adenovirus (Ad) encoding for full length bovine GRK2 for overexpression or Green Fluorescent Protein (GFP), as control. After 24 hours, we performed in vitro CA secretion assays using nicotine to activate nicotinic cholinergic receptors (the pharmacological stimulus for CA secretion from these cells) and the a2AR-selective full agonist UK14304 to activate these negative feedback receptors. Results: Nicotine induced a similar Epinephrine and Norepinephrine secretion from the chromaffin cells of both experimental groups. As expected, in Ad-GFP-treated chromaffin cells, UK14304 almost completely abolished CA secretion in response to nicotine, but this effect of UK14304 disappeared in human chromaffin cells-treated with Ad-GRK2. Moreover, to mimic a condition of elevated adrenergic tone, we exposed human chromaffin cells to isoproterenol stimulation. Importantly, human chromaffin cells exposed to isoproterenol showed a 2.5-fold increase in GRK2 protein expression compared to non-treated cells and UK14307 failed to inhibit CA release in these cells, indicating GRK2-dependent a2AR dysfunction (desensitization). Finally, when cells stimulated with isoproterenol were pre-infected with bARKct (a potent GRK2 inhibitor), isoproterenol-induced a2AR dysfunction was prevented; in fact, UK14307 retrieved its ability to inhibit CA release from these cells.

Conclusion: These data clearly demonstrate that adrenal GRK2 expression is an important physiological regulator of CA secretion in humans and suggest that its inhibition might be a useful therapeutic strategy in diseases that are precipitated or confounded by sympathetic overactivity, such as chronic heart failure, pheochromocytoma and hypertension.

Conclusion: These data clearly demonstrate that adrenal GRK2 expression is an important physiological regulator of CA secretion in humans and suggest that its inhibition might be a useful therapeutic strategy in diseases that are precipitated or confounded by sympathetic overactivity, such as chronic heart failure, pheochromocytoma and hypertension.

109

Evaluation of cyclic adenosin-3,5- monophosphate and neurohormones in patients with chronic heart failure

U. Kamilova¹; T. Alieva²; Z. Rasulova¹; D. Masharipova¹

¹Republican specialized scientific-practical Medical Center Therapy and Medical Rehabilitation, Tashkent, Uzbekistan;

²Tashkent medical academy, Tashkent, Uzbekistan

Purpose: To study contents of 3',5'-cyclic adenosine monophosphate(cAMP) and neurohormones parameters in patients with chronic heart failure (CHF).

Methods: This study includes 92 patients, males at the age from 40 to 60 years with CHF, mean age in the study group was 53,3 ± 4,9 years. All patients were divided into 2 groups in relation to functional class (FC) of CHF according to New York classification of cardiologists (NYHA): group 1 included 48 patients with CHF FC II and group 2 consisted of 44 patients with CHF FC III. Control group comprised 20 healthy volunteers, mean age was 56,3 ± 1,65 years. cAMP studied by radioimmunoassay method. Neurohumoral status of the patients studied by plasma concentrations of brain natriuretic peptide (BNP) and aldosterone (AL), which were determined in plasma.

Results: The contents of cAMP of CHF FC II was increased in patients by 147,5% ($p<0,05$) in comparison with parameters of control group. The same high parameters of the cAMP were found in CHF FC III, it was increased in patients by 220,2% ($P<0,05$) in comparison with parameters in control group. In the patients with CHF FC II there was noted increase in contents BNP by 181,8% ($P<0,001$), and in patients with FC III by 319,5% ($P<0,001$) in comparison with control group. Consequently, the level BNP was higher 2,8 times in FC II and 4,1 times in FC III in comparison with values in control group. There was also observed reliable increase in contents of aldosterone in the both groups of patients: in patients with CHF FC II aldosterone level increased by 36,8% ($P<0,001$) in comparison with control group. In group of patients with FC III increase in AL contents accounted for 66,7% ($P<0,001$). The level of AL increase 1,3 times in FC II and 1,6 times in FC III of CHF.

Conclusion: Thus, in patients with CHF there was found increased levels of BNP and AL well as the contents of cAMP, and in the patients with FC II the moderate high levels of neurohormones prevailed, but in FC III the high levels of BNP and AL were noted. Increase in cAMP level in blood reflects increase in dysfunction of the left ventricle and functional class.

Nitric oxide and reactive oxygen species - Heart

112

Hydrogen sulfide donor inhibits oxidative and nitrosative stress, cardiohemodynamics disturbances and restores cNOS coupling in old rats

V.F. Sagach; N. A. Dorofeyeva; KO. Drachuk

Bogomoletz Institute of Physiology, Circulation, Kiev, Ukraine

In view of the fact that aging increases the risk of cardiovascular diseases, the objective of the study was to examine the effect of exogenous hydrogen sulfide donor, sodium hydrosulfide (NaHS), on free

radical generation and cNOS uncoupling in the myocardium and cardiohemodynamics in old rats. To evaluate the systolic and diastolic function of the heart in experiments *in vivo*, we used pressure-volume (PV) conductance catheter system (Millar Instruments, USA). Markers of oxidative and nitrosative stress determined by biochemical methods. The cNOS coupling index calculated as relation — cNOS/*O₂-. It has been revealed that a combined oxidative and nitrosative stress develops in the heart of old rats, leading to cNOS uncoupling, which correlates with a decrease in diastolic function, as evidenced by a decrease in the maximum rate of left ventricle pressure decline (dp/dt_{max}) by 33%, an increase end-diastolic pressure in 4.5 times, and an increase in the time constant of left ventricular relaxation (Tau) by 44%. Hydrogen sulfide suppresses oxidative stress in heart (*O₂- generation decreases in 7.4 times, hydrogen peroxide - 3.3 times, reactive hydroxyl radical (*OH) reduces in 4.3 times). It has been found that NaHS inhibits nitrosative stress: cNOS activity increases in 2.8 times; NO₂- pools, as a marker of both constitutive synthesis of NO and oxygenation increases in 3.8 times, iNOS activity reduces in 4 times. The cNOS coupling index after sodium hydrosulfide increases in 8 times, that indicate restores cNOS coupling and promotes to improvement diastolic function in old rats. It was shown that dp / dt_{max} increased by 20% (P<0.05), Tau decreased by 13% (P<0.05). In conclusion, hydrogen sulfide inhibits oxidative and nitrosative stress, restores cNOS coupling and increases constitutive de novo synthesis of nitric oxide and improves diastolic heart function in old rats.

113

Role and mechanisms of action of aldehydes produced by monoamine oxidase A in cardiomyocyte death and heart failure

Y. Santin; P. Sicard; Y. Yuce; M. Dutaur; C. Vindis; A. Parini; J. Mialet-Perez
Institute of Cardiovascular and Metabolic Diseases, Toulouse, France

The accumulation of aldehydes (R-CHO) in the heart induces a "carbonyl stress" that contributes to the development of heart failure (HF). However, these R-CHO sources are not clearly identified. Monoamine oxidase A (MAO-A), a mitochondrial enzyme responsible for the degradation of catecholamines and serotonin, produces R-CHO and hydrogen peroxide (H₂O₂) during its enzymatic reaction. Moreover, several studies indicate that the increase of its activity is associated with a HF phenotype.

We believe that MAO-A could be a major source of R-CHO in the heart, through a direct production or via H₂O₂, which would contribute to the deleterious cardiac effects.

Neonatal Rat Ventricular Myocytes (NRVMs) were transfected with a MAO-A adenovirus and treated with tyramine, a substrate of the enzyme. We observed that the activation of MAO-A resulted in a R-CHO accumulation, an inhibition of the activity of the Aldehyde Dehydrogenase (ALDH) 2, mitochondrial enzyme responsible for the metabolism of aldehydes, and the death of NRVMs. The inhibition of R-CHO with a carbonyl scavenger, Hydralazine, and the allosteric activation of ALDH2 by Alda-1, protect NRVMs death induced by MAO-A. Our study also shows a mitochondrial alteration by the R-CHO produced by MAO-A, indicated by an energy depletion and a loss of mitochondrial membrane potential. However, the molecular targets of these R-CHO in the organelle are still to be determined. *In vivo*, we observed a cardiac accumulation of carbonyl stress in mice with cardiomyocyte-specific MAO-A overexpression. These mice exhibit a cardiac dysfunction at the age of 5 months, which is preserved by increasing the detoxification of R-CHO thanks to the intravenous injection of AAV9-cTnT-ALDH2.

Our work shows for the first time the deleterious involvement of R-CHO in cardiac damage produced by MAO-A.

114

Exercise training has contrasting effects in myocardial infarction and pressure-overload due to different endothelial nitric oxide synthase regulation

Y. Octavia; ED. Van Deel; M. De Boer; MC. De Waard; DJ. Duncker
Erasmus Medical Center, Division of Experimental Cardiology, Department of Cardiology, Thoraxcenter, Rotterdam, Netherlands

Background: The beneficial effects of exercise training (EX) on cardiac pathology are well recognized. Previously, we found that effects of EX on cardiac dysfunction critically depend on the underlying etiology.

Aims: To test whether the contrasting effects of exercise on cardiac dysfunction are due to divergent effects on the balance between nitric oxide (NO) and superoxide (O₂-), as a result of different responses of endothelial NO synthase (eNOS).

Methods: Mice were subjected to sham surgery, myocardial infarction (MI) or transverse aortic constriction (TAC), and subsequently exposed to 8 weeks of voluntary wheel running or sedentary housing. Left ventricular (LV) function was assessed by echocardiography and hemodynamic measurements; fibrosis by Picro-sirius Red staining; peroxynitrite (ONOO-) and O₂- production by luminol- and lucigenin-chemiluminescence, with or without L-NAME (NOS inhibitor); uncoupling, activity and S-glutathionylation of eNOS by immunoblotting and coimmunoprecipitation; cardiac NO by the Griess reaction.

Results: EX ameliorated LV dysfunction and fibrosis in MI but not TAC (Table). Strikingly, O₂- generation was blunted by EX in MI, but exacerbated by EX in TAC, which was largely NOS-dependent. Accordingly, uncoupling and S-glutathionylation of eNOS were corrected by EX in MI but aggravated in TAC mice. In parallel, ONOO- levels was attenuated by EX in MI but aggravated by EX in TAC. Cardiac NO levels were reduced in MI and TAC and normalized by EX in MI.

Conclusion: The contrasting effects of EX in MI vs TAC can be explained by the highly divergent effects of EX on eNOS regulation, resulting in blunted vs aggravated oxidative stress by EX in MI vs TAC.

SED vs EX after SH, MI, and TAC

	SHSED	SHEX	MISED	MIEX	TACSED	TACEX
Fractional shortening (%)	37 ± 2	39 ± 1	8 ± 1*	12 ± 1*§	18 ± 2*	16 ± 1*
LV dp/dt _{max} (mmHg/s)	8215 ± 574	8209 ± 447	4865 ± 198*	6089 ± 254*§	6486 ± 346*	5569 ± 329*
LV end diastolic pressure (mmHg)	4.2 ± 0.7	4.2 ± 0.4	9.8 ± 0.9*	8.0 ± 0.9*	13.9 ± 1.5*	18.4 ± 1.6*§
Collagen content (%)	1.3 ± 0.1	1.9 ± 0.3	6.9 ± 0.7*	3.0 ± 0.7*§	11.4 ± 2.2*	16.7 ± 2.7*§
Total O ₂ - (RLU/sec/mg)	18 ± 1	24 ± 3	41 ± 2*	29 ± 1*§	45 ± 3*	65 ± 3*§
NOS-dependent O ₂ - (RLU/sec/mg)	4 ± 1	4 ± 2	22 ± 1*	15 ± 2*§	20 ± 2*	43 ± 4*§
eNOS monomer/dimer ratio (AU)	1.0 ± 0.1	1.0 ± 0.2	2.1 ± 0.1*	1.5 ± 0.1*§	3.0 ± 0.4*	4.7 ± 0.7*§
eNOS S-glutathionylation (AU)	1.0 ± 0.1	1.0 ± 0.1	1.4 ± 0.1*	1.1 ± 0.1§	1.5 ± 0.1*	2.9 ± 0.3*§
Peroxyntirite (RLU/sec/mg)	0.08 ± 0.01	0.09 ± 0.03	0.22 ± 0.05*	0.12 ± 0.02§	0.27 ± 0.05*	0.64 ± 0.01*§
Cardiac NO (µM/mg protein)	12.4 ± 0.1	14.7 ± 1.2	8.0 ± 0.7*	10.8 ± 1.0§	6.2 ± 0.4*	7.4 ± 0.8*

Data are mean ± SEM. RLU: relative light unit. n = 6 - 20 per group. *p < 0.05 vs corr. SH; §p < 0.05 vs corr. SED

115

S-Nitroso Human Serum Albumin dose-dependently leads to vasodilation and alters reactive hyperaemia in coronary arteries of an isolated mouse heart model

PM. Haller¹; F. Nagel¹; M. Inci¹; D. Santer¹; S. Hallstroem²; BK. Podesser³
¹Ludwig Boltzmann Cluster for Cardiovascular Research, Vienna, Austria; ²Medical University of Graz, Department for Physiological Chemistry, Graz, Austria; ³Medical University of Vienna, Department for Biomedical Research, Vienna, Austria

Background: S-NO-HSA has proven its positive effects in ischemia/reperfusion models to preserve endothelial and cardiac function. This study intends to investigate the vasodilatory potency on coronary arteries. Additionally, the effects of S-NO-HSA are investigated after a short period of ischemia that provokes reactive hyperaemia, a phenomenon that could be modulated using S-NO-HSA.

Materials and Methods: Hearts of male OF-1 mice are crystalloid perfused in a Langendorff-heart. After an adapting-period of 15' and measuring of baseline values administration (drug or control) lasts for 10', followed by 20' of haemodynamic measurements. S-NO-HSA is tested during solely Langendorff perfusion (0,5µmol/kg/h, n=10; 5µmol/kg/h, n=3) to evaluate the extent of vasodilation. In the second part, after 5 minutes of drug administration, hearts undergo a 2 minutes period of global ischemia to provoke reactive hyperaemia (RH). Either S-NO-HSA (0,5µmol/kg/h+RH, n=10; 5µmol/kg/h+RH, n=7) or human serum albumin (control: n=5 and n=5) are administrated. Coronary flow (CF) and heart rate (HR) are monitored under constant afterload. Tissue samples for evaluation of high-energy phosphates are taken in the end. Data are presented as mean ± SEM compared to baseline (recovery in %).

Results: HR remained stable in all groups and showed no significant changes between groups. 5µmol/kg/h S-NO-HSA treatment increased CF recovery compared to 0,5µmol/kg/h S-NO-HSA (144,71% vs. 85,86%, p=0,011). Upon reperfusion, there is a trend of reducing RH with 0,5µmol/kg/h S-NO-HSA compared to control (25,94% vs. 74,04%, p=0,076). No significant changes were observed with 5µmol/kg/h S-NO-HSA in RH compared to control. HEP showed no significant changes between groups.

Conclusion: S-NO-HSA is able to dilate coronary arteries dose-dependently and is likely to decrease the extent of reactive hyperaemia provoked with 2' global cardiac ischemia.

116

Modulating endothelial nitric oxide synthase with folic acid attenuates doxorubicin-induced cardiomyopathy

Y. Octavia¹; G. Kararigas²; M. De Boer³; R. Kietadison³; M. Swinnen⁴; H. Duimel⁵; F. Verheyen⁵; I. Chirif²; MM. Brandt²; C. Cheng³; S. Janssens¹; AL. Moens¹; DJ. Duncker³
¹Maastricht University, CARIM, Department of Cardiology, Maastricht, Netherlands; ²Charite University Hospital, Institute of Gender in Medicine and Center for Cardiovascular Research, Berlin, Germany; ³Erasmus Medical Center, Division of Experimental Cardiology, Department of Cardiology, Thoraxcenter, Rotterdam, Netherlands; ⁴KU Leuven, Department of Cardiovascular sciences, Leuven, Belgium; ⁵Maastricht University Medical Centre (MUMC), Electron Microscopy Unit, Department of Molecular Cell Biology, Maastricht, Netherlands

Background: Endothelial nitric oxide synthase (eNOS) has a pivotal role in the pathogenesis of doxorubicin (DOXO)-induced cardiomyopathy

Hypothesis: Folic acid (FA), as an eNOS modulator, attenuates DOXO-induced cardiomyopathy and mortality.

Methods: Male C57BL/6 mice (n=265) received DOXO (1x 20 mg/kg, ip) or saline (sham). FA (10 mg/d po) or placebo was administered from 7d before DOXO administration until the end of the experiment (10d). Left ventricular (LV) function was measured by echocardiography; fibrosis and apoptosis by Picro-sirius Red and TUNEL staining, respectively; eNOS uncoupling, activity, and S-glutathionylation by co-immunoprecipitation and immunoblotting; superoxide (O₂-) production by lucigenin chemiluminescence, with or without L-NAME (NOS inhibitor); cardiac NO by Griess reaction. Mitochondrial oxygen consumption measurements and electron microscopy were performed at day 6. To test if the protection of FA is eNOS-dependent, we knocked-down eNOS in human

microvascular endothelial cells (HMVEC).

Results: DOXO produced 70% mortality ($P < 0.01$ vs sh), while mice receiving DOXO and FA (DOXOFA) had significantly lower mortality (45%; $P < 0.01$). FA ameliorated DOXO-induced LV dysfunction, fibrosis, and apoptosis (Table). Uncoupling, activity and glutathionylation of eNOS were restored in DOXOFA, and subsequently lead to a reduction in O_2^- generation, which mainly NOS-dependent, and an increase in cardiac NO. FA attenuated mitochondrial dysfunction and morphological changes ($P < 0.05$). The protection effects of FA were abolished in eNOS knocked-down HMVEC ($P < 0.05$).

Conclusion: FA as eNOS modulator might be a new and immediate therapeutic approach to reduce DOXO-induced cardiomyopathy.

Effects of folic acid after doxorubicin	Sham	ShamFA	DOXO	DOXOFA
Stroke volume/tibia length (μ l/cm)	36.1 \pm 1.4	34.4 \pm 2.1	24.2 \pm 4.6*	36.0 \pm 3.2§
Collagen content (%)	1.3 \pm 0.2	1.6 \pm 0.2	9.4 \pm 1.9*	5.2 \pm 0.6*§
Apoptosis (%)	0.16 \pm 0.03	0.15 \pm 0.04	1.10 \pm 0.16*	0.56 \pm 0.09*§
eNOS uncoupling (AU)	1.00 \pm 0.04	0.89 \pm 0.04	1.68 \pm 0.14*	1.34 \pm 0.10*§
eNOS activity (AU)	1.00 \pm 0.03	1.24 \pm 0.08	0.63 \pm 0.06*	1.04 \pm 0.05*§
eNOS S-glutathionylation (AU)	1.00 \pm 0.09	1.00 \pm 0.06	1.93 \pm 0.26*	1.27 \pm 0.14*§
Superoxide generation (RLU/sec/mg)	188 \pm 14	206 \pm 8	683 \pm 79*	401 \pm 27*§
Δ L-NAME (RLU/sec/mg)	23.5 \pm 7.2	8.2 \pm 3.6	415.8 \pm 71.1*	207.4 \pm 32.5*§
Cardiac NO (AU)	11.0 \pm 1.0	14.0 \pm 0.7	5.0 \pm 0.8*	8.9 \pm 1.1*§

Data are mean \pm SEM. RLU, relative light unit. n = 4-10 per group. * $p < 0.05$ vs corr. sham; § $p < 0.05$ vs corr. DOXO

119

Effects of long-term very high intensity exercise on aortic structure and function in an animal model

C. Rubies¹; M. Batlle¹; AP. Dantas¹; M. Sanz²; M. Sitges²; L. Mont²; E. Guasch²

¹Institute of Biomedical Research August Pi Sunyer (IDIBAPS), Barcelona, Spain; ²Hospital Clinic de Barcelona, Cardiology department, Barcelona, Spain

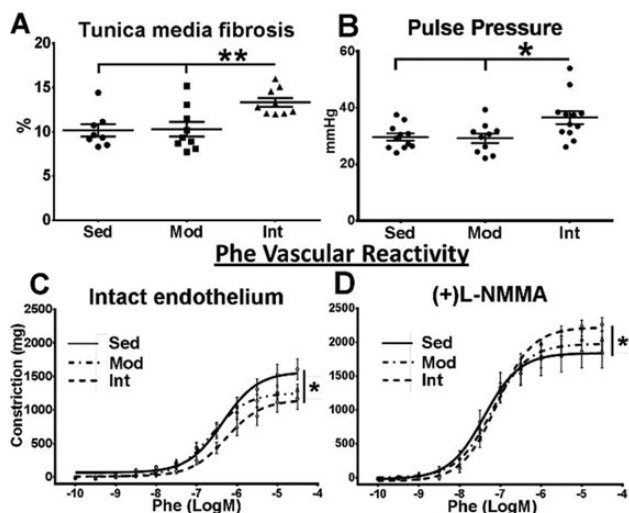
Background: Regular moderate physical activity is an efficient therapeutic strategy to reduce cardiovascular risk factors. However, recent data show increased cardiovascular disease burden and mortality in the most trained individuals.

Purpose: To assess vascular remodeling after high intensity training.

Methods: Wistar rats underwent very high (INT, 60min 60cm/s, n=20) or moderate intensity (MOD, 45min 35cm/s, n=20) treadmill training for 16 weeks. Sedentary rats (SED, n=20) served as controls. Morphometric analysis and fibrosis quantification were performed in paraffin-embedded and OCT-fixed aortic sections. In vivo ascending aorta functional remodeling was assessed in a hemodynamic study and transthoracic echocardiography. Ex vivo vascular reactivity to carbachol (Cch), phenylephrine (Phe) and potassium chloride (KCl) was studied in intact-endothelium aortic rings; NO signaling was blocked with nitric oxide synthase inhibitor L-NMMA. Protein levels were quantified with Western Blot and oxidative stress with dihydroethidium (DHE).

Results: INT exercise promoted an increase of tunica media fibrosis (Fig A) and elastic lamina discontinuities compared to MOD and SED groups. A higher pulse pressure in the hemodynamic study and a decreased ascending aorta pulsatility (echocardiography) further supported a stiffer aorta after INT training. Conversely, MOD exercise resulted in increased aorta pulsatility and improved endothelial function (increased Cch-mediated vasodilatation and reduced Phe vasoconstriction). INT exercise did not result in further benefits (Fig B), but showed a marked increase of endothelial-independent Phe response (Fig C) and intact endothelium KCl response. ACE protein levels and oxidative stress (DHE) were increased in the aorta of INT rats.

Conclusions: While moderate exercise improves endothelial function and aorta compliance, very high intensity exercise increases wall stiffness and induces tunica media hyperactivity. Oxidative stress and renin-angiotensin system likely mediate these effects. Our findings provide important insights into increased atherosclerotic burden in very high trained individuals.



120

Electron paramagnetic resonance spectroscopy quantification of nitrosylated hemoglobin (HbNO) as an index of vascular nitric oxide bioavailability in vivo

F. Dei Zotti; I. Lobysheva; C. Beauloye; J-L. Balligand

Institute of Experimental and Clinical Research (IREC), Brussels, Belgium

Reduced bioavailability of signaling molecule nitric oxide is a major feature of endothelial dysfunction in cardiovascular and metabolic diseases, but for its short half-life its quantification in circulating blood is still a challenge. In erythrocytes NO can react with hemoglobin forming iron-nitrosyl complexes (5-coordinate- α -HbNO) quantifiable by EPR spectroscopy in mouse, rat and human venous blood ex vivo. The paramagnetic complex concentration is ~ 425 nM in rodents and ~ 92 nM in human venous blood. We hypothesized that HbNO reflects bioavailability of vascular NO and endothelial function in vivo. NO could be supplied from vascular or intraerythrocytic NOS. We tested NOS activity in human, eNOS(+/+) and (-/-) mice RBCs measuring nitrite/nitrate production and HbNO formation after addition of NOS and arginase inhibitors. Both signals increased with arginase inhibition and were abrogated upon NOS inhibition in human and eNOS(+/+) mice, but insensitive in eNOS(-/-) RBCs. However, HbNO signal from freshly drawn venous RBCs was minimally sensitive to NOS inhibitors ex vivo suggesting a minor contribution of erythrocytic NOS to HbNO complex compared with vascular endothelial NOS or other NO sources. HbNO signal, upon exogenous NO donor exposure, is influenced by O_2 , temperature and pH. The stability of HbNO was significantly higher after 30min in hypoxic condition (17 \pm 0.4% degradation vs 49 \pm 0.2% at room air), at 20°C (16 \pm 0.3% degradation vs 30 \pm 0.1% at 37°C) and under acidic pH (32 \pm 1.1% vs 62 \pm 0.7% at physiological pH). HbNO was significantly preserved by RBCs incubation with catalase (2 μ M HbNO/L vs 0.5 μ M HbNO/L in untreated controls) whereas superoxide dismutase had minimal effect. Conversely, catalase inhibition highly increased ROS formation. This suggested that HbNO formation is sensitive to oxidative degradation, possibly by H₂O₂. HbNO level also varies dynamically with release of bioavailable NO in systemic circulation i.e. after in vivo administration of isosorbide dinitrate (40% increase compared to control). Finally, we compared circulating HbNO levels in venous RBCs from healthy volunteers or patients with cardiovascular diseases and found decreased HbNO in patients (0.141 \pm 11 μ M/L vs 0.22 \pm 12 μ M/L in volunteers; N=38 and 48). HbNO was significantly correlated with endothelial function (ENDO-PAT) and (inversely) correlated with major cardiovascular risk factors. We conclude that HbNO reflects exposure of RBCs to NO in vivo and is sensitive to oxidative degradation by H₂O₂. HbNO could be developed as a biomarker of NO bioavailability and/or oxidative stress ex vivo.

121

Deletion of repressor activator protein 1 impairs acetylcholine-induced relaxation due to production of reactive oxygen species

KHK. Wong; PM. Vanhoutte; EHC. Tang

The University of Hong Kong, Pharmacology and Pharmacy, Hong Kong, Hong Kong SAR People's Republic of China

Introduction: Repressor activator protein 1 (Rap1) is a telomeric protein which resides within the shelterin complex docked at chromosomal ends. Besides regulating chromosome integrity, it also takes part in metabolic regulation and body-weight homeostasis. Its role, if any, in vascular responsiveness is unknown.

Purpose: The present study investigated if Rap1 deletion affects vascular responsiveness in mice.

Methods: Rap1 knockout and wild-type littermates on a C57BL/6N background [aged between 12-16 weeks and fed standard chow] were used. Thoracic aortae were harvested and rings (with or without endothelium) were suspended in wire myographs to determine contractions and relaxations (during contractions to 10-6 mol/L phenylephrine). Contractions were expressed as percentage to the reference response obtained with 60mmol/L potassium solution at the beginning of the experiment, while relaxations were expressed as percentage of the contraction to phenylephrine.

Results: Relaxations to acetylcholine in aortic rings with endothelium were abolished by NG-nitro-L-arginine methyl ester (L-NAME; 10-4 M; nitric oxide synthase inhibitor) and diminished significantly in Rap1 knockout compared to wild type preparations. Relaxations to other endothelium-dependent vasodilators [insulin, UK14304 (α_2 adrenergic agonist), A23187 (calcium ionophore)] were not significantly different between aortae of Rap1 knockout compared to wild type mice. Likewise, relaxations to exogenous nitric oxide donors were similar in aortae without endothelium of both groups. In Rap1 knockout aortae, treatment with reactive oxygen species scavengers could significantly restore acetylcholine-induced relaxations.

Conclusion: Deletion of Rap1 results in impaired acetylcholine-induced endothelium-dependent relaxations. This impairment can be attributed to the increased production of reactive oxygen species reducing the bioavailability of nitric oxide, without changes in the responsiveness of vascular smooth muscle to the endothelium-derived mediator.

Extracellular matrix and fibrosis - Heart

124

MicroRNA-19b is associated with myocardial collagen cross-linking in patients with severe aortic stenosis. Potential usefulness as a circulating biomarker

A. Gonzalez Miqueo¹; J. Beaumont¹; B. Lopez¹; S. Ravassa¹; N. Hermida²; F. Valencia³; J.J. Gomez-Doblas³; G. San Jose¹; E. De Teresa³; J. Diez¹

¹CIMA, University of Navarra, Program of Cardiovascular Diseases, Pamplona, Spain; ²Universite Catholique de Louvain, Institute of Experimental and Clinical Research, Brussels, Belgium; ³University Hospital Virgen de la Victoria, Division of Cardiology, Malaga, Spain

Background: Myocardial fibrosis, a major hallmark of myocardial remodelling in patients with aortic valve stenosis (AS), is involved in the development of their clinical manifestations. It is the result of variable alterations not just in the quantity (i.e. collagen deposition) but also in the quality (e.g. degree of collagen cross-linking or CCL) of collagen. Different myocardial microRNAs have been shown to

play a role in this process. However, their impact on CCL has not been analysed in depth. On the other hand, the usefulness of circulating microRNAs to identify qualitative alterations of the extracellular matrix (i.e. CCL) has not been investigated.

Purpose: This study was designed to analyze the association of circulating levels of fibrosis-related microRNAs with their cardiac expression and with myocardial CCL in patients with severe AS, as well as to explore their potential involvement in CCL.

Methods: Peripheral blood and endomyocardial biopsies were obtained from 28 AS patients. Nineteen and ten subjects were used as controls for blood and myocardial determinations, respectively. Collagen volume fraction (CVF), the degree of CCL, and the expression of lysyl oxidase (LOX), the main enzyme involved in CCL, were analyzed in myocardial biopsies. MicroRNA expression was quantified in myocardial and blood samples. In vitro studies were performed in human adult fibroblasts.

Results: AS patients showed increased ($P < 0.001$) myocardial CVF, CCL and LOX expression, compared with control subjects. Out of the 8 microRNAs analysed, miR-122, miR-133a and miR-19b were decreased ($P < 0.01$) both in the serum and the myocardium of AS patients compared with controls. No associations were found between circulating and myocardial levels of miR-122 and miR-133a. Interestingly, a direct correlation ($r = 0.375$, $P < 0.01$) was found between serum and myocardial miR-19b expression in AS patients, suggesting a cardiac origin of its circulating levels.

Myocardial miR-19b was inversely correlated with LOX protein ($r = -0.594$, $P < 0.05$), and consequently with CCL ($r = -0.449$; $P < 0.05$) in AS patients. Of note, myocardial miR-19b was associated with increased left ventricular stiffness ($r = -0.379$; $P < 0.05$) and with the presence of heart failure (O.R.: 0.005, $P < 0.05$) in these patients. In human fibroblasts miR-19b inhibition increased ($P < 0.05$) the expression of LOX protein, suggesting that miR-19b might regulate LOX and subsequently CCL. Importantly, serum levels of miR-19b were also inversely associated with LOX ($r = -0.452$, $P < 0.05$) and CCL ($r = -0.410$; $P < 0.05$), suggesting that this microRNA could be useful as a non invasive biomarker of CCL.

Conclusions: Our results suggest that miR-19b may be involved in myocardial CCL through the regulation of LOX. Moreover, serum miR-19b is associated with myocardial CCL in AS patients. Thus, this microRNA could be a novel biomarker of the quality of myocardial fibrosis in these patients.

125

A new ex vivo model to study cardiac fibrosis

BPT. Kruithof¹; AF. Van De Merbel¹; M. Kruithof-De Julio²; M.J. Goumans¹

¹Leiden University Medical Center, Department of Molecular Cell Biology, Leiden, Netherlands; ²University of Bern, Department of Urology, Bern, Switzerland

Background/Introduction: Fibrosis is a phenomenon observed in several cardiac diseases that lead to heart failure. As no effective treatment exists, there is an urgent need to obtain new insights in this process in order to develop better therapeutics that will aid in its prognosis and treatment. In vivo mouse models (aortic banding, coronary artery ligation) have offered great insights in the definition and characterization of fibrosis. However, controlled manipulation of single or specific combination of potential effectors cannot be achieved. Therefore a controlled and inducible ex vivo system that will allow us to study the excessive deposition of extracellular matrix by heart myofibroblasts is required.

Purpose: The goal of our study is to develop an ex vivo culture system in which cardiac fibrosis can be induced and regulated in the adult mouse heart.

Methods: Mouse hearts are isolated and placed in the perfusion chamber of our, recently developed, ex vivo flow system. The medium is pumped from a reservoir into the perfusion chamber, where it will enter the heart via a blunt needle that is inserted into the aorta. Thereby, the medium is directed through the coronary circulation, and exits the heart via the right atrium. Medium from the perfusion chamber is directed back to the reservoir creating a closed circuit system. Culture is performed under specific flow conditions at 37 degrees Celsius. After culture, the hearts are processed for histopathological analysis. Myofibroblast accumulation and collagen production are measured as indicators of the fibrotic load.

Results: Under specific culture conditions, cardiac fibrosis can be induced throughout the ventricular myocardium within a week, as shown by the high number of collagen-expressing myofibroblasts (alpha smooth muscle actin-positive cells). After 2 weeks, the extracellular matrix accumulation is evident by the high collagen deposition which is observed in the interstitium, perivascular, epicardial and endocardial regions of the heart. Interestingly, decreasing the flow speed, reduces the fibrotic extent, indicating the involvement of mechanical regulation. As a proof of principal we have modulated the known profibrotic TGFbeta growth factor pathway and observed, by selective inhibition of its receptor, a strong reduction of the fibrotic load.

Conclusions: The ex vivo flow system allows induction of cardiac fibrosis ex vivo in intact adult mouse hearts. In this powerful tool mechanical or biochemical stimuli can be altered, individually or in combination, in order to model the different stages of cardiac fibrosis. Moreover, the use of genetically modified mice hearts will give the opportunity to understand the cellular and molecular mechanisms underlying fibroblast expansion and function, revealing new therapeutic targets, paving the road towards the treatment of cardiac fibrosis.

126

Heterogeneity of fibrosis and fibroblast differentiation in the left ventricle after myocardial infarction

C. Kadur Nagaraju¹; P. Claus²; E. Dries¹; A. Angelo Singh¹; K. Vermeulen¹; H.L. Roderick¹; K.R. Sipido¹; R.B. Driesen¹

¹KU Leuven, Division of Experimental Cardiology, Department of Cardiovascular Sciences, KU Leuven, Leuven, Belgium; ²KU Leuven, Division of Imaging and Cardiovascular Dynamics, Department of Cardiovascular Sciences, Leuven, Belgium

Background: After myocardial infarction (MI) remodeling of the non-infarcted tissue contributes to reduced cardiac function; fibroblast (Fb) differentiation and interstitial fibrosis are part of this remodeling process.

Purpose: We investigated the Fb differentiation and properties in different regions of the heart after MI.

Methods: A copper coated stent was implanted in the left anterior descending coronary artery (LAD, young adult pigs) leading to high grade stenosis and MI (10% of left ventricular mass). After

6 weeks after MI, biopsies were collected from the MI scar, the myocardium adjacent (Mladjacent) and remote to MI (Mlremote) and from corresponding regions in SHAM (N=6 SHAM, N=10 MI). Fb were isolated and cultured in DME medium with 10% fetal bovine serum for 4 days to determine Fb phenotypes and proliferation capacity. Immuno-staining and 3-D collagen contraction was used to evaluate Fb differentiation. Fibrosis and collagen subtypes were studied in sirius red stained paraffin sections and imaged using polarized light. Tissue lysates were used to measure TGF- β 1 and lysyl oxidase (Lox) concentration and lox enzyme activity, markers for collagen cross-linking.

Results: Fb from all regions of MI demonstrated differentiation towards myofibroblasts (MyoFb) as shown by the high number of cells with F-actin stress fibers and increase in cell size. The MyoFb induced contraction of 3-D collagen matrices: this was highest for scar > Mladjacent > Mlremote. Despite differentiation, proliferation capacity was maintained for MyoFb from all the regions. Interstitial fibrosis was increased by 3-fold in Mladjacent but not in Mlremote. A 7-fold increase of collagen type I was noted within the interstitial area of the Mladjacent. Arteriole perivascular fibrosis was increased solely in the Mladjacent (5-fold increase of collagen type I). Protein levels of TGF- β 1 were elevated in Mladjacent and Mlremote whereas Lox protein expression and enzyme activity were only upregulated in Mladjacent by 1.4-fold and 1.5-fold respectively.

Conclusion: Differentiation to MyoFb occurs in all regions of the heart after MI with little cellular phenotype difference in vitro. In vivo, MyoFb in Mladjacent contributes to interstitial fibrosis via collagen cross-linking and this is less so for Mlremote. This in vivo difference may be due to increase in lysyl oxidase activity present only in Mladjacent.

127

Effect of carbohydrate metabolism degree compensation to the level of galectin-3 changes in hypertensive patients with chronic heart failure and type 2 diabetes mellitus

Y. Shaposhnikova; I. Ilchenko; L. Bobronnikova
Kharkiv National Medical University, Kharkiv, Ukraine

The goal of the study was to evaluate galectin-3 (Gal-3) level changes of depending on condition of compensation of carbohydrate metabolism in patients with chronic heart failure (CHF), diabetes mellitus 2 type (DM-2) and arterial hypertension (AH).

Materials and Methods: The study involved 65 patients (age 58.2 ± 3.6 years, 30 of them women) with CHF II functional class according to NYHA classification, mild to moderate AH (1-2 grade) and DM-2. All patients were divided into 3 groups depending on the degree of compensation of DM-2 (according to the level of glycosylated hemoglobin (HbA1c)): group 1 included 18 patients with HbA1c < 7%; group 2 - 26 patients with HbA1c 7-9%; group 3 - 21 patients with HbA1c > 9%. Serum Gal-3 concentration was measured by enzyme immunoassay analyzer using mono- or polyclonal antibodies to the analytes in accordance with the manual of the kit reagents (kits «Human Galectin-3 Platinum ELISA», Cat BMS 279/2, production "Bender MedSystems, GmbH»). General clinical, standart laboratory examination and Gal-3 level was dynamically measured at the baseline, after 1 and 3 months, also was studied the relationship between the concentration of Gal-3 and carbohydrate metabolism degree compensation.

Results: Initially, concentration of Gal-3 was greatest in patients of group 3 and exceed the value Gal-3 of the 1st and 2nd groups (respectively 1, 2 and 3 groups: 29.64 ± 0.52 ng / ml; 33.79 ± 0.48 ng / ml; 36.94 ± 0.86 ng / ml). The difference between the Gal-3 values at the 1st and 3rd groups was significant ($p < 0.05$). Repeated measurements at 1 and 3 months remained elevated levels of Gal-3 in the patients with insufficient glycemic control; significant difference of Gal-3 levels was observed between the 1st and 3rd groups. The concentration of Gal-3, respectively amounted: after 1 month in patients 1, 2 and 3 groups 24.18 ± 0.32 ng / ml; 27.28 ± 0.38 ng / ml; 32.48 ± 0.41 ng / ml; after 3 months concentration of Gal-3 respectively: 22.32 ± 0.38 ng / ml; 26.32 ± 0.25 ng / ml; 30.64 ± 0.52 ng / ml ($p < 0.05$).

Conclusions: Persistent increasing Gal-3 values in the patients with CHF, AH and DM-2 may be associated with increasing of glycosylation processes developing in poor glycemic control state. Hyperglycemia contributes to the accumulation of glycation products in the extracellular matrix, causes structural changes in tissues that contribute to reduced susceptibility to catabolism and induces fibrosis. Increasing Gal-3 may be considered as a marker of irreversible structural changes in myocardial tissues and important predictor of CHF progression and cardiovascular disease complications development.

128

Statin paradox in association with calcification of bicuspid aortic valve interstitial cells

P. Songia; V. Myasoedova; F. Alamanni; E. Tremoli; P. Poggio
Cardiology Center Monzino IRCCS, Milan, Italy

Background: Bicuspid aortic valve (BAV) is the most common cardiac congenital anomaly dominated by valve dysfunction, such as calcific aortic valve disease (CAVD) and aortic valve insufficiency (AVI). CAVD is an active multi-factorial process involving morphological changes and calcification of valve interstitial cells (VIC). Aortic valve calcification process appears to be similar between BAV and tricuspid aortic valve (TAV) patients. However, BAV patients experience an accelerated progression. It is likely that the abnormal BAV morphology in combination with altered hemodynamics raise the onset and progression of tissue degeneration.

Purpose: Previous studies have been shown that statin treatments did not halt nor revert CAVD; however, it has been hypothesised that the therapy was initiated to late. Here we investigated the role of pravastatin on VICs derive from BAV and TAV patients.

Methods: Human VICs were isolated from freshly resected bicuspid (n = 7) and tricuspid (n = 5) aortic valves. We implemented a classical in vitro calcification assay based on the addition of two different concentration of inorganic phosphate (Pi, 2 mM and 5 mM). After seven days of treatments, we dissolved the calcium, deposited on the cell surface, with hydrochloric acid and measured the amount of calcium with a colorimetric assay.

Results: In our analyses as expected, we observed a significant calcium deposition on VICs derived from BAV and TAV, after seven days in calcifying media. Interestingly, BAV cells deposited larger amount of calcium crystals when compared to TAV cells in vitro. BAV cells treated with 2 mM Pi deposited 188.1 ± 24.2 ng/ug (calcium / total proteins) vs. 129.8 ± 16.5 ng/ug of TAV cells ($p = 0.04$).

After seven days of 5 mM Pi, BAV cells deposited 312.4 ± 11.9 ng/un vs. 97.1 ± 16.7 of TAV cells ($p < 0.001$). Pravastatin pre-treatments prevented calcium formation only with low Pi concentrations in both, BAV and TAV VICs ($p < 0.001$). Surprisingly, at high Pi concentrations, pravastatin did not show any effect on VICs from TAV, while increased significantly the calcium deposits on BAV VICs (312.4 ± 11.9 ng/ug vs. 392.9 ± 10.5 ng/ug; $p = 0.002$).

Conclusions: Our study show for the first time that VICs derived from BAV patients calcifies more than TAV, *in vitro*. In addition, our results support the idea of the statin paradox on valve interstitial cells and in particular the detrimental effects of pravastatin on cells derived from bicuspid stenotic valves exposed to high Pi concentrations.

129

Cardiac function remains impaired despite reversible cardiac fibrosis after healed experimental viral myocarditis

D. Lindner¹; PM. Becher¹; F. Gotzheim¹; K. Klingel²; S. Blankenberg¹; D. Westermann¹
¹University Heart Center Hamburg, Department of General and Interventional Cardiology, Hamburg, Germany; ²Eberhard-Karls-University Tübingen, Institute for Pathology, Department of Molecular Pathology, Tübingen, Germany

Background: Infection with coxsackievirus B3 induces myocarditis. We aimed to compare the acute and chronic phases of viral myocarditis to identify the immediate effects of cardiac inflammation as well as the long-term effects after resolved inflammation on cardiac fibrosis and consequently on cardiac function.

Material and Methods: We infected C57BL/6j mice with coxsackievirus B3 and determined the hemodynamic LV-function 7 as well as 28 days after infection. Subsequently, we analyzed viral burden and viral replication in the cardiac tissue as well as the expression of cytokines and matrix proteins. Furthermore, cardiac fibroblasts were infected with virus to investigate if the viral infection alone induces pro-fibrotic signaling.

Results: Severe cardiac inflammation was determined and cardiac fibrosis was predominantly colocalized with inflammation during the acute phase of myocarditis. Declined cardiac inflammation but no significantly improved hemodynamic function was observed 28 days after infection. Interestingly, cardiac fibrosis declined to basal levels as well.

Both, cardiac inflammation and fibrosis were reversible, whereas the hemodynamic function remains impaired after healed viral myocarditis in B6 mice.

Conclusion: During the acute phase of myocarditis, observed cardiac fibrosis was consistently colocalized with the foci of inflammation. CVB3 infection of cardiac fibroblasts does not induce pro-fibrotic signaling but pro-inflammatory chemokine expression inducing cardiac inflammation. Furthermore, the copy number quantification revealed that cardiac fibroblasts are even more susceptible for viral infection compared to cardiomyocytes. Moreover, 28 days after CVB3 infection cardiac inflammation as well as cardiac fibrosis were resolved without regaining the hemodynamic function.

Ion channels, ion exchangers and cellular electrophysiology - Heart

132

Identifying a novel role for PMCA1 (Atp2b1) in heart rhythm instability

C. Wilson; M. Zi; E. Cartwright
 University of Manchester, Institute of Cardiovascular Sciences, Manchester, United Kingdom

Background/Introduction: Arrhythmias continue to be a leading cause of death and disability across the world, and genetics are one of the mechanisms that are known to increase susceptibility. By identifying new genetic influences and further understanding of the pathways involved in heart rhythm control we can begin to tackle some of the main challenges facing treatment development, including the identification of at risk patients.

Purpose: Here we aim to identify a new role for a gene linked to several features of heart failure Atp2b1 (Plasma membrane calcium ATPase 1, PMCA1). Along with its role in hypertension, we believe PMCA1 may also influence heart rhythm stability and consequently the development of arrhythmias.

Methods: Cardiac electrical properties of cardiomyocyte-specific knockout mice (PMCA1CKO) were assessed. Heart rhythm stability was determined using *in vivo* electrocardiography and arrhythmia susceptibility was identified using programmed electrical stimulation. Related cardiac ion channel expression was assessed using qRT-PCR and immunohistochemistry. Further structural and functional characteristics associated with heart failure were investigated by echocardiography and appropriate histological analysis.

Results: PMCA1CKO mice displayed abnormal heart rhythms related to cardiac repolarisation dysfunction, evident by prolonged QT and JT intervals ($p < 0.01$) when compared to littermate controls. These animals also presented with increased susceptibility to arrhythmic events including ventricular tachycardia ($p < 0.05$). Relating to cardiac electrical activity, PMCA1CKO ventricular tissue also showed evidence of cardiac channel remodelling with reduced expression of Kv4.2 ($p < 0.05$). These changes occurred in the absence of detectable structural heart disease, with the function and structure of PMCA1CKO hearts being comparable to controls.

Conclusion: Our findings suggest a novel role for PMCA1 in heart rhythm stability, specifically cardiac repolarisation, distinct from other cardiac disease. Furthermore, alterations in expression of Atp2b1 could influence an individual's susceptibility to developing arrhythmias.

133

Mutations of the caveolin-3 gene as a predisposing factor for cardiac arrhythmias

P. Benzioni; G. Campostrini; M. Bonzanni; R. Milanesi; A. Bucchi; M. Baruscotti; D. DiFrancesco; A. Barbuti
 University of Milan, Bioscience, Milan, Italy

Caveolinopathies are genetic disorders due to mutations of the caveolin-3 gene (CAV3). Caveolin-3 plays a key role in caveolae formation and thus in the maintenance of plasma membrane integrity, and interacts with several signaling proteins and with ion channels (HCN, NaV1.5, CaV1.2, KV1.5, Kir2.1). To date, 30 CAV3 mutations have been identified in patients with either skeletal muscle or cardiac diseases even though the pathogenic mechanisms are not completely understood.

We investigated the CAV3 variants Δ TFT, T78K and T78M, previously associated with limb-girdle muscular dystrophy, long QT syndrome and hypertrophic cardiomyopathy. Recent genetic studies have identified the T78M SNP also in the healthy population suggesting that its pathogenicity should be considered with caution. On the contrary Δ TFT and T78K variants prevent membrane expression of CAV3 and caveolae formation due to retention in the Golgi.

Here, we evaluated the functional effects of wild type (WT), T78M, T78K and Δ TFT CAV3 on the properties of human Kv1.5, Kir2.1 and HCN4 channels expressed in caveolin-free mouse embryonic fibroblasts (mef-KO) and on the action potential profile of neonatal rat cardiomyocytes (rCMs).

Confocal analysis of mef-KO revealed that the membrane distribution of the T78M CAV3 is uniform compared to the spot-like distribution of the WT CAV3 while the T78K and Δ TFT CAV3 accumulated in cytoplasmic organelles.

Electrophysiological analysis of neonatal rCMs revealed that the T78M CAV3 induced a positive shift (+ 7.1 mV) of HCN4 activation curve and a negative shift of both activation (-6.4 mV) and inactivation curves (-6 mV) of Kv1.5, but did not affect Kir2.1 currents. Methyl- β -cyclodextrin (M β CD)-dependent caveolae disruption did not affect channels co-expressed with CAV3 T78M but, as expected, affected channels co-expressed with CAV3 WT. Expression of CAV3 T78M in spontaneously beating neonatal rCMs induced an arrhythmic phenotype, similar to that caused by M β CD treatment, while expression of CAV3 WT had no effects. No HCN4 current could be recorded from mef-KO expressing either the T78K or the Δ TFT variants. The condition of heterozygosity has also been evaluated, knowing that these mutations have a dominant negative effect on WT CAV3. Preliminary analysis reveals a retention of CAV3 WT in the Golgi network in the presence of Δ TFT and T78K CAV3. This data show that the CAV3 mutations cause alteration in ion channels properties/distribution and in membrane excitability that can potentially generate a pro-arrhythmic substrate.

Electrophysiological analysis of neonatal rCMs revealed that the T78M CAV3 induced a positive shift (+ 7.1 mV) of HCN4 activation curve and a negative shift of both activation (-6.4 mV) and inactivation curves (-6 mV) of Kv1.5, but did not affect Kir2.1 currents. Methyl- β -cyclodextrin (M β CD)-dependent caveolae disruption did not affect channels co-expressed with CAV3 T78M but, as expected, affected channels co-expressed with CAV3 WT. Expression of CAV3 T78M in spontaneously beating neonatal rCMs induced an arrhythmic phenotype, similar to that caused by M β CD treatment, while expression of CAV3 WT had no effects. No HCN4 current could be recorded from mef-KO expressing either the T78K or the Δ TFT variants. The condition of heterozygosity has also been evaluated, knowing that these mutations have a dominant negative effect on WT CAV3. Preliminary analysis reveals a retention of CAV3 WT in the Golgi network in the presence of Δ TFT and T78K CAV3. This data show that the CAV3 mutations cause alteration in ion channels properties/distribution and in membrane excitability that can potentially generate a pro-arrhythmic substrate.

134

The human sinoatrial node action potential: time for a computational model

A. Fabbri¹; M. Fantini¹; R. Wilders²; S. Severi¹
¹University of Bologna, DEI - Department of Electrical, Electronic and Information Engineering "Guglielmo Marconi", Bologna, Italy; ²Academic Medical Center of Amsterdam, Amsterdam, Netherlands

Introduction: Sinoatrial node (SAN) cells are responsible for heart rhythm in physiological conditions. They are self-oscillating, so they are able to generate an action potential (AP) without external stimuli. The large amount of experiments carried out on SAN cells isolated from small mammals (e.g. rabbits) has allowed to identify and characterize the currents underlying the pacemaking and to formulate comprehensive computational AP models.

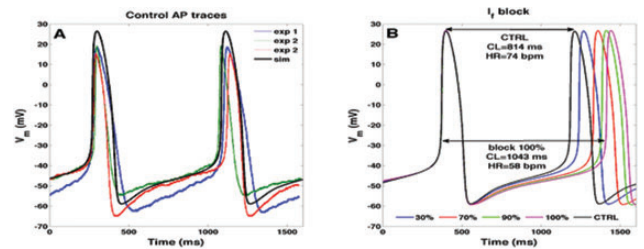
On the other hand, human SAN cell electrophysiology is still largely unexplored: only few studies provided experimental data from small tissue samples or isolated cells and a human SAN AP model is still lacking.

Purpose: This work aims to formulate an *in silico* human SAN AP model, able to reproduce the available experimental data and allowing to explore the effects on pacemaking of funny current (If) modulation.

Methods: The Severi-DiFrancesco rabbit SAN cell model is the starting point. Formulations for currents, pumps and exchangers were parameterized according to experimental data on electrophysiology and gene expression; an automatic parameter tuning was performed in order to reproduce AP morphology and intracellular calcium ([Ca²⁺]_i) transient, quantitatively assessed by computing AP features (action potential duration at 90% of repolarization (APD₉₀), diastolic depolarization rate for the first 100 ms (DDR100)) and [Ca²⁺]_i transient features (minimum and maximum Ca²⁺ concentration (Caimin, Caimax)). The effects of If modulation on cycle length (CL) were evaluated by simulating its progressive block (30,70,90,100%), and shifts of its activation voltage dependence (± 10 mV).

Results: Predicted AP and [Ca²⁺]_i transient features are in agreement with the experimental values (see Figure, panel A); CL=814ms (74bpm) vs. CL=828 \pm 15ms, APD₉₀=161.5ms vs. APD₉₀=143.5 \pm 34.9ms DDR100=48.1mV/s vs. DDR100=48.9 \pm 18mV/s, Caimin=84nM vs. Caimin=110nM, Caimax=189nM vs. Caimax=220nM. Full If block induces a CL increase of +28% (CL=1043ms, 58bpm), see Figure, panel B), in good accordance with the effect of the administration of 2 mM Cs⁺ (Δ CL=+26%). Shifts of If activation in the range of ± 10 mV show the capability to continuously regulate CL in the range -19+13% (91-65 bpm).

Conclusions: This model, strongly based on the few available data from human SAN, is a first step towards a reliable human SAN cell model. In spite of the lower amplitude of If, compared to other mammals, its modulation has significant effects on CL (and thus on pacing rate), suggesting funny current as an important actor in human pacemaking.



Control conditions and If modulation

135

iPSC-derived cardiomyocytes as a model to dissect ion current alterations of genetic atrial fibrillation

G. Campostrini¹; P. Benzioni¹; P. Dell' Era²; M. Serzanti²; MS. Olesen³; C. Muneretto⁴; G. Bisleri¹; D. DiFrancesco¹; M. Baruscotti¹; A. Bucchi¹; A. Barbuti¹
¹University of Milan, Department of Biosciences, Milan, Italy; ²University of Brescia, Department of Translational Medicine, Brescia, Italy; ³Rigshospitalet - Copenhagen University Hospital, Department of Biomedical sciences, Copenhagen, Denmark; ⁴University of Brescia, Division of Cardiac Surgery, Brescia, Italy

The molecular mechanisms of atrial fibrillation (AF) are still poorly understood, despite AF is the most common cardiac arrhythmia. The main impediments are: the paucity of human samples, the molecular

remodeling induced by AF and the fact that it is a complex, multigenic disorder. Here we used cardiomyocytes derived from patient's induced pluripotent stem cells (iPSC-CMs) as a human cellular model to study the molecular and functional basis of AF.

We generated iPSCs from two siblings with persistent AF, whose early onset suggests a genetic basis. Whole-exome screening revealed no mutations in AF-associated ion channels. iPSC-CMs were analyzed at two differentiation time points: days 15-18 and days 30-35. iPSC-CMs were mechanically and enzymatically isolated to perform gene expression and electrophysiological analyses. iPSCs derived from three unrelated healthy individuals (CTRL) were used for comparison.

We recorded action potentials from spontaneously beating iPSC-CMs and found that AF-derived iPSC-CMs have a significantly higher firing rate than controls without alterations of other parameters (maximum diastolic potential, amplitude and duration). We then characterized the expression and properties of If and L-type calcium (ICaL) currents. qPCR analysis showed that f-channel subunits (HCN) and the CaV1.2 calcium channel subunit are expressed at both time points tested; HCN4 subunit was the most expressed. Functional analysis at days 15-18 showed that If activates at more positive voltage in AF than in CTRL iPSC-CMs (shift of activation curve +7.5 mV) without changes in current density; ICaL had a larger density in AF than in CTRL iPSC-CMs (mean at 0 mV: CTRL = -3.9 pA/pF, AF = -8.8 pA/pF). At days 30-35 a larger shift of the If activation curve was observed (shift = +9 mV) with also an increase in current density (mean at -125 mV: CTRL = -3.0 pA/pF, AF = -6.9 pA/pF). Also ICaL density was still larger in AF (mean at 10 mV: CTRL = -2.9 pA/pF, AF = -8.2 pA/pF) than in CTRL iPSC-CMs.

In conclusions, we showed that CMs obtained from AF patient-derived iPSCs have significant alterations in two ion currents important for cell automaticity that may represent the substrate for triggering AF. Thus we demonstrated for the first time that iPSC-CMs represent a suitable in vitro model to study AF with complex genetic background.

136

Postextrasystolic potentiation in healthy and diseased hearts: effects of the site of origin and coupling interval of the preceding extrasystole

E. Jorge; G. Amoros-Figueras; S. Raga; B. Campos; C. Alonso-Martin; E. Rodriguez-Font; X. Vinolas; J. Cinca; JM. Guerra

Hospital de la Santa Creu i Sant Pau, cardiology, Barcelona, Spain

Background: Augmented contractility of the heartbeats following a premature ventricular contraction (PVC) has been reported and termed as postextrasystolic potentiation (PESP).

Purpose: The aim of this study was to characterize the postextrasystolic potentiation phenomenon in cardiac extrasystoles arising from different sites of origin and coupling intervals in healthy and diseased hearts.

Methods: We studied ten swines: 5 healthy controls and 5 with induced non-ischemic dilated cardiomyopathy (NIDCM) and left ventricular (LV) dysfunction. The aortic blood flow (ABF), LV and right ventricular (RV) pressures and the surface ECG were analyzed. Measurements were performed at baseline and after PVCs, which were induced from 16 LV sites (8 epicardial and 8 endocardial) and 3 RV sites, at decreasing coupling intervals (CI) from 500 ms to 350 ms. Each corresponding postextrasystolic beat was compared to the previous baseline beat and changes expressed as percentage. The compensatory pause (CP) post-PVC was also calculated and expressed in relation to the baseline cycle length.

Results: A total of 760 postextrasystolic beats were evaluated. PESP was higher in terms of ABF and LVP in NIDCM hearts compared to controls ($p < 0.001$, figure 1) with longer CP ($142 \pm 21\%$ vs $130 \pm 27\%$; $p < 0.001$). PESP increased with shorter CI in both groups ($p < 0.001$) with no impact on the CP, that did not change with the CI. Only NIDCM hearts showed differences in PESP and the CP in relation to the PVC site of origin (PEPS: $123 \pm 11\%$ RV vs $134 \pm 21\%$ LV; $p < 0.05$ for ABF; $133 \pm 10\%$ RV vs $143 \pm 21\%$ LV; $p < 0.05$ for the CP).

Conclusions: Hearts with LV dysfunction show higher degree of PESP than normal hearts. Extrasystole prematurity is the major determinant of the PESP phenomenon in healthy and diseased hearts. Regional differences in PESP were observed only in diseased hearts. Some but not all of these differences could be explained by the compensatory pause duration, that would theoretically allow an augmented filling.

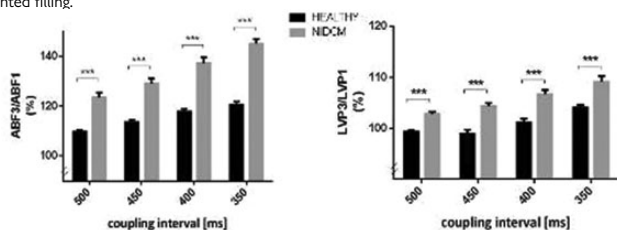


Fig1.PESP in healthy and diseased hearts

137

Absence of Nav1.8-based (late) sodium current in rabbit cardiomyocytes and human iPSC-CMs

S. Casini¹; I. Mengarelli¹; CA. Schumacher¹; MW. Veldkamp¹; AO. Verkerk²; CA. Remme¹

¹Academic Medical Center of Amsterdam, Experimental Cardiology, Amsterdam, Netherlands; ²Academic Medical Center of Amsterdam, Anatomy, Embryology and Physiology, Amsterdam, Netherlands

Background: Previous studies have suggested a role for the neuronal sodium channel Nav1.8 (encoded by SCN10A) in cardiac conduction and late sodium current magnitude. Nav1.8 is highly expressed in dorsal root ganglia and plays a role in pain perception, but its presence and functional relevance in cardiomyocytes is debated.

Purpose: In this study we investigated the functional presence of Nav1.8 in rabbit cardiomyocytes and human induced pluripotent stem cell derived cardiomyocytes (hiPSC-CMs).

Methods and Results: The effects of the Nav1.8 blocker A-803467 was investigated through patch clamp analysis in freshly isolated ventricular rabbit cardiomyocytes and hiPSC-CMs. In rabbit cardiomyocytes, A-803467 had no effect on resting membrane potential, action potential (AP) amplitude, or AP upstroke velocity. While A-803467 significantly reduced action potential duration (APD), late sodium current in rabbit cardiomyocytes was absent. In hiPSC-CMs, quantitative RT-PCR demonstrated very low expression levels of SCN10A compared to SCN5A. Similar to the results obtained in rabbit cardiomyocytes, A-803467 significantly reduced APD in hiPSC-CMs (in the absence of a significant late sodium current), but had no effect on peak sodium current density and kinetics.

Conclusions: These findings indicate that Nav1.8-based sodium channel activity is absent in isolated rabbit cardiomyocytes and hiPSC-CMs. The AP shortening effect of A-803467 observed in both species appears to be independent of (late) sodium current.

138

hiPSC-derived cardiomyocytes from Brugada Syndrome patients without identified mutations do not exhibit cellular electrophysiological abnormalities

I. Mengarelli¹; C. Veerman¹; K. Guan²; M. Stauske²; H. Tan¹; J. Barc²; A. Wilde¹; A. Verkerk¹; C. Bezzina¹

¹Academic Medical Center of Amsterdam, Experimental Cardiology, Amsterdam, Netherlands; ²University Medical Center Göttingen (UMG), Department of Cardiology and Pneumology, Heart Center, Göttingen, Germany; ³Research unit of l'Institut du thorax, Inserm UMR 1087/CNRS UMR 6291, Nantes, France

Background/Introduction: Brugada syndrome (BrS) is a rare cardiac rhythm disorder associated with sudden cardiac death. Mutations in the sodium channel gene SCN5A are found in ~20% of cases while mutations in other genes collectively account for <5%. In the remaining patients the genetic defect and the underlying pathogenic mechanism remain obscure.

Purpose: To provide insight into the mechanism of BrS in individuals without identified mutations, we here studied electrophysiological properties of cardiomyocytes (CMs) generated from human induced pluripotent stem cells (hiPSCs) from 3 BrS patients who tested negative for mutations in the known BrS-associated genes.

Methods: The hiPSC lines used were generated from skin fibroblasts of 3 BrS individuals, 2 unrelated controls and one SCN5A-1795insD carrier. The sodium current (INa) and action potential parameters were measured by patch clamp in cardiomyocytes derived from the hiPSC lines.

Results: Patch clamp studies revealed no differences in sodium current (INa) in hiPSC-CMs from the 3 BrS patients compared to 2 unrelated controls. Moreover, action potential upstroke velocity, reflecting INa, as well as other action potential parameters were not different between hiPSC-CMs from the BrS patients and the controls. hiPSC-CMs harboring the BrS-associated SCN5A-1795insD mutation exhibited a reduction in both INa and action potential upstroke velocity, demonstrating our ability to detect reduced sodium channel function.

Conclusion: Our findings indicate that ion channel dysfunction, in particular in the cardiac sodium channel, may not be a prerequisite for BrS.

Microcirculation

141

Atherogenic indices, collagen type IV turnover and the development of microvascular complications- study in diabetics with arterial hypertension

A. Nikolov¹; I. Tsinlikov²; I. Tsinlikova²; G. Nicoloff¹; A. Blazhev¹; A. Garea³

¹Medical University Pleven, Department of Biology, Plevna, Bulgaria; ²Medical University Plevna, Department of Propedeutics of Internal Diseases, Plevna, Bulgaria; ³City Clinic, Sofia, Bulgaria

Background and Aims: An important factor in the development of vascular wall lesions is degradation of the connective tissue major protein- collagen typeIV. Collagen type IV peptides (CIVDP) derived from this degradation are present in the circulation and are a stimulus for production of anti-collagen type IV antibodies (ACIVAbs) IgM, IgG and IgA. The aim of this study was to investigate for a possible association between ACIVAbs, lipid indices and development of microvascular complications.

Material and Methods: Sera of 93 patients with type 2 diabetes mellitus (T2DM) and arterial hypertension (AH) were investigated (mean age 61.4 ± 11.3 years, diabetes duration 9.88 ± 3.12 years; hypertension duration 9.28 ± 4.98). ELISA was used for determination of ACIVAbs. These values were compared to serum ACIVAbs in 42 age and sex matched controls. Diabetics were divided in two groups according to presence- Group 1 (n=67) or absence- Group 2 (n=26) of microangiopathy. Lipid profile and lipid indices (log TG/HDL, LDL/HDL, TC/HDL and TG/HDL) were examined too.

Results: Patients with T2DM and AH showed statistically significant higher levels of serum ACIVAbs IgG than healthy controls $0.298 (0.237 \div 0.381)$ vs. $0.210 (0.149 \div 0.262)$ (KW=14.01; $P < 0.0001$). Group 1 showed statistically significant higher levels of ACIVAbs IgG than patients without microangiopathy $0.323 (0.243 \div 0.391)$ vs. $0.241 (0.207 \div 0.291)$ (KW=7.66; $p=0.006$) and healthy controls $0.210 (0.149 \div 0.262)$ (KW=17.52; $P < 0.0001$). ACIVAbs IgG showed correlation with duration of diabetes ($r=0.49$); ($p=0.01$), retinopathy ($r=-0.20$); ($p=0.04$) and BMI ($r=-0.24$); ($p=0.05$), HbA1c ($r=0.21$); ($p=0.04$), SBP ($r=0.16$); ($p=0.05$). ACIVAbs IgG correlated with log TG/HDL ($r=0.21$); ($p=0.01$), LDL/HDL ($r=0.19$); ($p=0.02$) TC/HDL ($r=0.16$); ($p=0.05$) and with TG/HDL ($r=0.15$); ($p=0.05$).

Conclusion: Our study shows relationship between elevation of ACIVAbs IgG, high lipid indices and development of microvascular complications in patients with type 2 diabetes mellitus and arterial hypertension.

142

Changes in the microvasculature and blood viscosity in women with rheumatoid arthritis, hypercholesterolemia and hypertension

DS. Bublikov; AV. Andrienko; VG. Lychev; EN. Vorobova; DA. Anchugina

Altay State Medical University, Barnaul, Russian Federation

Rheumatoid artrit - chronic systemic inflammatory disease, that increases cardiovascular risk by increasing the rigidity of the vascular wall and changes in lipid profile. However, lack of awareness of

the association of microcirculation and blood viscosity in women with rheumatoid arthritis with hypertension and hypercholesterolemia.

Aim: Learn fssociation of peripheral microcirculation and blood viscosity in women with rheumatoid arthritis with arterial hypertension and hypercholesterolemia.

Materials and methods: Women (n = 33) at 48 ± 4.5 years prescription rheumatoid arthritis over 1 year, 2 radiographic stage ACCP positive and has rheumatoid factor in a blood, only receiving oral methotrexate at a dose of 20 ± 2.5 mg per week. Rheumatoid arthritis is exposed according to the criterion of the ACR (1987). Peripheral blood flow was studied by laser Doppler flowmetry on 2nd finger of his left hand, the end falage. All persons has 1st hypertension degree and well-controlled pressure - received amlodipin 5 ± 2.5 mg per day. Periferial blood flow was assessed by flux in perfusion ediitsah. Blood viscosity evaluated at the capillary viscometer, and measured in millipascal per second-1. Cholesterol-Enzyme Immunoassay "Cholesterol" Abbott Clinical Chemistry. Patients were divided into 3 groups: only having rheumatoid arthritis (n = 10) with rheumatoid arthritis and arterial hypertension (n = 13), with rheumatoid arthritis, arterial hypertension and hypercholesterolemia (n = 10).

Results are presented in the Table.

Conclusion: Arterial hypertension and hypercholesterolemia asociated with changes on peripheral circulation and blood viscosity in women with rheumatoid arthritis. A further impact of this fact on the clinic of rheumatoid arthritisand cardiovascular risks and ways of correction require further study.

Position	Rheumatoid arthritis (n = 10)	Rheumatoid arthritis and arterial hypertension (n = 13)	Rheumatoid arthritis, arterial hypertension and hypercholesterolemia (n = 10)	Statistically significant
Column	1	2	3	
Blood pressure, mm Hg	126 ± 2.1/ 80 ± 3.1	135 ± 2.6/ 81 ± 2.4	133 ± 3.1/84 ± 2.6	p (1-2)=0.0023 p (1-3)=0.0062 p (2-3)=0.0824
Cholesterol, mmol/l	4.1 ± 0.3	4.2 ± 0.2	6.4 ± 1.6	p (1-2)=0.0615 p (1-3)=0.0002 p (2-3)=0.0009
Flux, perfusion ediitsah	2.6 ± 0.4	2.1 ± 0.5	2.2 ± 0.7	p (1-2)=0.0053 p (1-3)=0.0009 p (2-3)=0.0312
Blood viscosity, millipascal per second ⁻¹	4.6 ± 2.1	5.2 ± 2.4	5.4 ± 2.9	p (1-2)=0.0030 p (1-3)=0.0061 p (2-3)=0.0311

Atherosclerosis

145

Shear stress regulates endothelial autophagy: consequences on endothelial senescence and atherogenesis

M. Kheloufi¹; AC. Vion¹; A. Hammoutene¹; J. Poisson¹; N. Dupont²; M. Souyri³; A. Tedgui¹; P. Codogno³; CM. Boulanger¹; PE. Rautou¹

¹Paris Cardiovascular Research Center (PARCC), Paris, France; ²University Paris-Descartes, Paris, France;

³University Pierre & Marie Curie Paris VI, Paris, France

Atherosclerotic plaques form preferentially in arterial areas exposed to low shear stress (LSS) where endothelial cells express senescence-associated phenotypes. We tested the hypothesis that endothelial autophagy is an anti-senescence and anti-atherogenic process regulated by shear stress.

Endothelial cells exposure to LSS (2 dyn/cm², 24h) decreased LC3II/I ratio compared to high shear stress (HSS, 20 dyn/cm²)(1.6 ± 0.2 vs. 2.0 ± 0.3, respectively p < 0.01). Bafilomycin A1 revealed that autophagic flux was elevated in HSS conditions. In mouse aorta, the surface of LC3 punctae/cell was lower in LSS than in HSS areas (9 ± 1 vs. 15 ± 1 mm²/cell, respectively p=0.01). Similar results were obtained in human carotid arteries. Both mTOR and AMPK pathways were involved in autophagy regulation by shear stress. Using culture endothelial cells, we observed more senescence-associated β-galactosidase activity under LSS than under HSS (48 ± 4 vs. 37 ± 3% positive cells, respectively p < 0.05). Autophagy inhibition using wortmannin under HSS increased endothelial senescence when compared to vehicle (71 ± 7% vs. 37 ± 4% positive cells, respectively p < 0.01), whereas autophagy activation using rapamycin under LSS prevented endothelial senescence (34 ± 1 vs. 48 ± 4% positive cells, respectively p < 0.05). In vivo, endothelial senescence in HSS areas was higher in mice with an endothelial-specific deletion of Atg5 than in control mice, as evaluated by SA-β-gal staining (3.8 ± 0.8 vs. 0.9 ± 0.1 positive cells/mm², respectively p < 0.01). No difference was observed in LSS areas. ApoE^{-/-} mice with an endothelial specific deletion of Atg5 developed larger atherosclerotic lesions in HSS areas than control mice (3.1 ± 0.5 vs. 1.4 ± 0.4% respectively p < 0.05), but no difference was observed in LSS areas.

In conclusion, endothelial autophagy is defective in endothelial cells in LSS areas and is associated with cellular senescence. This seems to contribute to the preferential development of atherosclerotic lesions in these areas.

146

Obstructive sleep apnea causes aortic remodeling in a chronic murine model

C. Rubies¹; AP. Dantas¹; M. Battle¹; E. Guasch²; M. Torres³; JM. Montserrat²; I. Almendros³; L. Mont²
¹Institute of Biomedical Research August Pi Sunyer (IDIBAPS), Barcelona, Spain; ²Hospital Clinic de Barcelona, Cardiology department, Barcelona, Spain; ³Hospital Clinic de Barcelona, Pneumology department, Barcelona, Spain

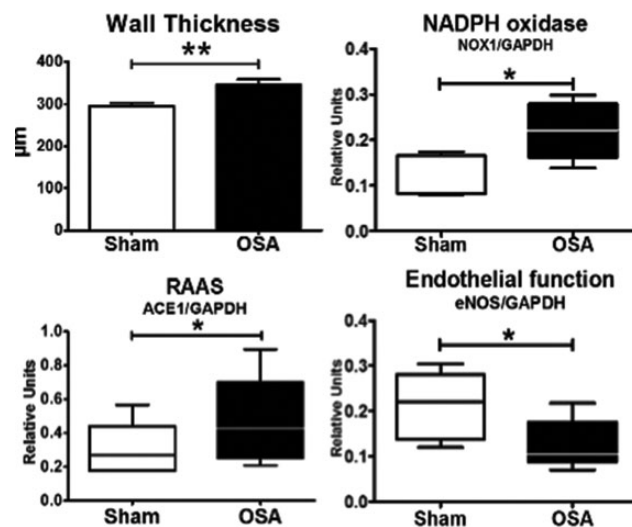
Background: Obstructive sleep apnea (OSA) syndrome is associated with hypertension, increased vascular stiffness and accelerated atherosclerosis progression. The mechanisms of deleterious vascular remodeling in OSA patients remain largely unknown.

Purpose: To investigate vascular remodeling in a clinically relevant chronic OSA rat model involving both thoracic pressure swings and intermittent hypoxia.

Methods: Thirty Sprague-Dawley male rats were randomized into 2 groups: OSA rats (n=16) were subjected to 15-second obstructions (60/hour, 6 hours/day, 21 days) in a custom-made setup resulting in intermittent increases in respiratory efforts and hypoxia. Sham rats (n=14) were placed in the setup without air obstructions. Descending thoracic aorta was dissected and fixed in OCT for morphometric measurements or frozen in liquid nitrogen for Western Blot analyses. Proteins involved in oxidative stress, the Renin Angiotensin Aldosterone System (RAAS) and the endothelial function were quantified.

Results: OSA increased descending aorta wall thickness but did not modify the lumen area (Figure). No changes in collagen deposition (Sirius red staining) of tunica media and protein levels of collagen 1-3 were triggered by OSA. Protein levels of NADPH oxidase subunits NOX1 and p47phox were increased in OSA compared to Sham rats (Figure). ACE1 protein levels and downstream effectors Erk1/2 and GTPase protein RhoA were upregulated in OSA rats (Figure). Endothelial dysfunction was suggested by decreased eNOS protein synthesis.

Conclusions: In this clinically relevant model, chronic OSA causes descending aorta hypertrophy and endothelial dysfunction that are at least partly mediated by increased oxidative stress and RAAS upregulation. Our results provide valuable insights into the role of OSA as an emerging independent risk factor for atherosclerosis. Confirmation in OSA patients is warranted.



147

Aortic perivascular adipose tissue displays an aged phenotype in early and late atherosclerosis in ApoE^{-/-} mice

R. E. Walker¹; C. A. Austin²; C. M. Holt¹

¹University of Manchester, Institute of Cardiovascular Sciences, Manchester, United Kingdom; ²Edge Hill, Faculty of Health and Social Care, Ormskirk, United Kingdom

Background: Perivascular adipose tissue (PVAT) surrounds the majority of blood vessels and is an important component of the vasculature. PVAT is an active endocrine organ and until recently has not been considered important in the pathogenesis of atherosclerosis. In healthy vessels, PVAT exerts an anti-contractile effect which is attenuated in states of metabolic disturbance.

Aim: The following experiments were conducted to determine the influence of PVAT, age and progression of atherosclerotic disease on isolated arterial contractility.

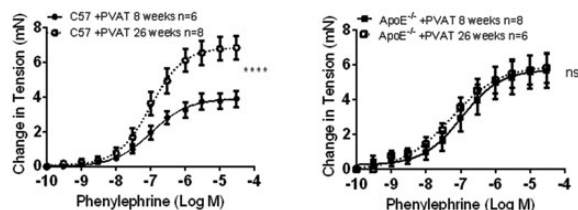
Methods: Upon weaning, male ApoE^{-/-} or C57BL6 (control) mice were fed a standard rodent chow diet for a period of eight or twenty-six weeks. Aortic atherosclerotic lesion area was analysed by en face quantification following Oil Red O staining. Contractile responses of the thoracic aortae to cumulative doses of phenylephrine (1x10⁻¹⁰ - 3x10⁻⁵ M) were measured in PVAT intact or PVAT denuded vessels using myography.

Results: Atherosclerotic lesions were present in the aortae of the ApoE^{-/-} mice but were not observed in C57BL6 mice. A significant increase in total lesion area occupying the aorta was observed in the aged ApoE^{-/-} mice compared to mice at the earlier time-point (0.11% versus 2.78% p < 0.006 n=6-7). As previously widely documented, PVAT significantly decreased vasoconstrictor responses to phenylephrine in young control (C57BL6) mice and the anti-contractile capacity of PVAT was abolished in aged control mice. The PVAT from young ApoE^{-/-} mice exhibited the characteristics of an

aged phenotype, exerting no anti-contractile effects on vessels; this was sustained during atherosclerotic disease progression and observed in the aged ApoE^{-/-}s. These findings were replicated in ApoE^{-/-} mice fed a 'Western'-type diet over identical time-courses.

Conclusions: PVAT from ApoE^{-/-} mice displayed an aged phenotype with no anti-contractile capacity. On-going studies are investigating the characteristics of PVAT from ApoE^{-/-} mice including release of adipokines in early and established atherosclerosis.

The contractility of thoracic aortae with intact perivascular adipose tissue in C57BL6 and ApoE^{-/-} mice



148

A systematic evaluation of the cellular innate immune response during the process of human atherosclerosis

RA. Van Dijk¹; K. Rijts¹; A. Wezel¹; J.F. Hamming¹; F.D. Kolodgie²; R. Virmani²; A.F. Schaapherder¹; J.H.N. Lindeman¹

¹Leiden University Medical Center, Vascula Surgery, Leiden, Netherlands; ²CVPath Institute, Gaithersburg, United States of America

Background: The concept of innate immunity is well recognized within the spectrum of atherosclerosis, which is primarily dictated by macrophages. Although current insights to this process are largely based on murine models, there are fundamental differences in the atherosclerotic microenvironment and associated inflammatory response relative to the humans. In this light, we characterized the cellular aspects of the innate immune response in normal, non-progressive, and progressive human atherosclerotic plaques.

Material and Methods: A systematic analysis of the innate immune response was performed on 110 well-characterized human peri-renal aortic plaques with immunostaining for specific macrophage subtypes (M1 and M2-lineage) and their activation markers neopterin and HLA-DR together with dendritic cells, NK cells, mast cells, neutrophils, and eosinophils.

Results: Normal aortae were devoid of LDL, macrophages, dendritic cells, NK cells, mast cells, eosinophils and neutrophils. Early, atherosclerotic lesions exhibited heterogeneous populations of (CD68+) macrophages whereby 25% were double positive "M1" (CD68+/iNOS-/CD163-), 13% "M2" double positive (CD68+/iNOS-/CD163+) and 17% triple-positive for (M1) iNOS (M2)/ CD163 and CD68 with the remaining (~40%) only stained for CD68. Progressive fibroatheromatous lesions, including vulnerable plaques showed increasing numbers of NK cells and fascin positive cells mainly localized to the media and adventitia while the M1/M2 ratio and level of macrophage activation (HLA-DR and neopterin) remain unchanged. On the contrary, stabilized (fibrotic) plaques showed a marked reduction in macrophages and cell activation with a concomitant decrease in NK cells, dendritic cells, and neutrophils

Conclusion: Macrophage "M1" and "M2" subsets together with fascin-positive dendritic cells are strongly associated with progressive and vulnerable atherosclerotic disease of human aorta. The observations here support a more complex theory of macrophage heterogeneity than the existing paradigm predicated on murine data and further indicate the involvement of (poorly-defined) macrophage subtypes or greater dynamic range of macrophage plasticity than previously considered.

149

Inhibition of Coagulation factor Xa increases plaque stability and attenuates the onset and progression of atherosclerotic plaque in apolipoprotein e-deficient mice

J.J. Posthuma; J.J.N. Posma; R. Van Oerle; H.M.H. Spronk; H. Ten Cate
Cardiovascular Research Institute Maastricht (CARIM), Biochemistry, Laboratory for Clinical Thrombosis and Haemostasis, Maastricht, Netherlands

Background/Introduction: Atherosclerosis is a progressive chronic inflammatory vascular disorder, which can result in atherosclerotic plaque rupture and subsequent thrombus formation. Numerous *in vitro* studies indicated that key clotting proteases such as thrombin and Xa (FXa) can promote a wide range of cellular actions related to cardiovascular function - e.g. vascular permeability, inflammation, and apoptosis, predominantly mediated through activation of protease activated receptors (PARs). However, exact mechanisms remain elusive.

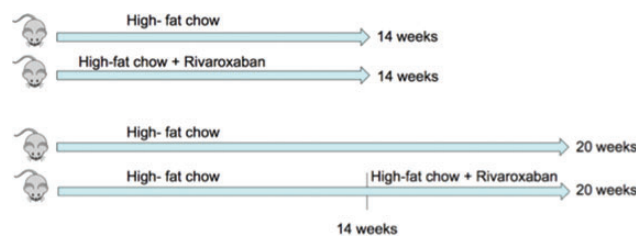
Purpose: To elucidate these mechanisms, we investigated the *in vivo* significance of pharmacological FXa inhibition by Rivaroxaban in a spontaneous atherosclerotic mice model for the development and vulnerability of atherosclerotic plaque.

Methods: In the first arm, female ApoE^{-/-} mice (age 8-9 weeks) received high-fat diet with or without Rivaroxaban (12mg/gram chow) 14 weeks (n=8/group). In the second arm, ApoE^{-/-} mice received high-fat chow for 14 weeks, followed by either continuation with standard high-fat diet or high-fat chow supplemented with Rivaroxaban (12mg/gram chow) for 6 weeks. (n=5/group). After sacrifice, aortic arches were collected and stained for haematoxylin & eosin to determine the extent of atherosclerotic plaque. Plaque vulnerability was examined by immunohistochemical (IHC) staining against collagen and matrix metalloproteinases (MMPs). In addition, PAR 1 and 2 expression in the plaque was determined by IHC.

Results: Rivaroxaban treated mice showed less atherosclerotic lesions after 14 weeks compared to control (-36,92%, p<0,01 and -46,47% p<0,01). In addition, Rivaroxaban mice showed less atherosclerotic lesions after 20 weeks compared to control (-30,93%, p<0,05). These results were accompanied by reduced necrotic core size in all Rivaroxaban treated mice compared to control.

Additionally, inhibition of FXa resulted in a more stable atherosclerotic phenotype reflected by altered collagen and mean fibrotic cap thickness in all groups. These findings were accompanied by reduced expression of MMPs and PARs.

Conclusion: Inhibition of FXa by Rivaroxaban reduces the onset and progression of atherosclerotic plaque in ApoE^{-/-} mice at different time points in the disease. Accompanied by reduced plaque vulnerability possibly mediated through reduced PAR expression, this argues in favor of direct inhibition of coagulation to reduce the incidence of atherothrombotic events in the future.



Study design

150

Regulatory CD4+ T cells from patients with atherosclerosis display pro-inflammatory skewing and enhanced suppression function

I.E. Dumitriu; S. Dinkla; J.C. Kaski
St. George's University of London, London, United Kingdom

Background/Introduction: Regulatory T (Treg) cells have been implicated in atherosclerosis pathogenesis but the mechanisms involved remain poorly defined. Potent suppressive capacity constitutes the most important and defining Treg feature. Data on Treg frequency in atherosclerosis patients is contradictory: some studies found reduced frequencies; others suggested that Treg frequency does not correlate with atherosclerosis severity; and other studies suggested that Treg reduction increases myocardial infarction (MI) risk. Information on Treg suppressive function in atherosclerosis patients is even scarcer.

Purpose: We aimed to characterise Treg frequency, phenotype and function in atherosclerosis patients.

Methods: CD4+CD25highCD127lowFOXP3+ Treg were quantified in atherosclerosis patients (myocardial infarction (MI), n=60; stable angina, SA, n=40), and in healthy subjects (n=30) by flow cytometry. Sorted Treg from atherosclerosis patients and controls were used for direct and cross-suppression assays.

Results: Treg number was significantly lower in MI and SA patients compared to healthy subjects. This was due to reduction of naive Foxp3lowCD45RAhigh Treg (p<0.0001), while effector Foxp3highCD45RALow Treg were not affected. Moreover, we found a significant increase in cytokine-producing Foxp3lowCD45RALow Treg (p<0.0001). Strikingly, suppression assays demonstrated that Treg from MI patients display enhanced suppressive function compared to Treg from healthy individuals, in line with increased effector/resting Treg ratio in MI. In depth phenotypic and functional characterisation of Treg subsets to identify mechanisms responsible for altered frequency and suppressive activity is ongoing.

Conclusions: Our data indicate that Treg from atherosclerosis patients are potent suppressors and have pro-inflammatory phenotype and functions. These results contrast previous findings that suggested decreased Treg suppressive function in MI. Our results reveal a complex role for Treg in human atherosclerosis beyond generic suppression of inflammation into dynamic cells that exhibit pathogenic traits.

151

Hypoxia-inducible factor (HIF)-1alpha regulates macrophage energy metabolism by mediating miRNAs

E. Karshovska; A. Schober
Institute for Cardiovascular Prevention (IPEK), Munich, Germany

Background: Macrophage profound plasticity enables these cells to regulate different stages of inflammation. The transcription factor hypoxia-inducible transcription factor (HIF)-1alpha induces an inflammatory M1 macrophage phenotype by shifting the energy metabolism from oxidative phosphorylation to aerobic glycolysis. However, the underlying mechanism of this metabolic shift and macrophage function are currently unknown.

Purpose: Our aim is to investigate the molecular mechanisms that regulate the macrophage metabolic shift and macrophage survival during chronic inflammatory diseases.

Methods: We used ApoE^{-/-} mice expressing HIF-1a flox/flox and LysM Cre-recombinase. As a control we used non-floxed mice. Macrophages we differentiated from bone marrow using M-CSF. Lesional macrophages we collected from plaques using laser microdissection system. To assess gene expression and miRNAs profile we performed qRT-PCR, for the metabolic profiles-flux analyzer, and to measure reactive oxygen species (ROS) production or cell death we used flow cytometry. For the intracellular ATP depletion we used ATP bioluminescent assay. To determine the effect of microRNAs we performed gain- and loss functions experiments using miRNA mimics and inhibitors, respectively.

Results: HIF-1alpha deficiency in M1 type macrophages increased oxidative respiration and key enzymes of oxidative energy metabolism. Furthermore, HIF-1alpha increased necroptosis, ATP depletion in inflammatory macrophages, and promoted the plaque size by increasing necrosis in lesional macrophages, without affecting apoptosis. This effect was associated with increased miR-210 and reduced miR-383 expression. Inhibition of miR-210 increased the expression of key enzymes of oxidative energy metabolism and decreased mitochondrial ROS generation in M1 type macrophages. Suppression of miR-383 by HIF-1alpha increased necroptosis, ROS generation, and ATP level by depressing its putative target poly (ADP-ribose) glycohydrolase. These results suggest the synergistic effects of miR-210-mediated suppression of oxidative energy metabolism and ATP depletion due to

inefficient repair of oxidative DNA damage in the absence of miR-383 may play a key role in HIF-1 α -induced macrophage necroptosis.

Conclusion: Characterizing the role of the HIF-1 α /mir-210 and HIF-1 α /miR-383 axes will provide new insights into the regulation of macrophage energy metabolism and survival in chronic inflammatory diseases. Thus, we aim to develop novel therapeutic strategies to modulate macrophage function by miRNA-mediated metabolic reprogramming.

152

Extracellular S100A4 is a key player of smooth muscle cell phenotypic transition: implications in atherosclerosis

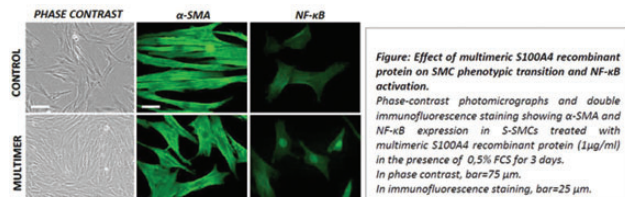
A. Sakic¹; C. Chaabane¹; N. Ambartsumian²; M. Grigorian²; ML. Bochaton-Piallat¹

¹University of Geneva, Pathology and Immunology, Geneva, Switzerland; ²Institute of Cancer Biology, Department of Molecular Cancer Biology, Copenhagen, Denmark

During atherosclerosis and restenosis, smooth muscle cells (SMCs) are known to accumulate into the intima and to switch from a contractile to a synthetic phenotype. In our previous studies, two distinct SMC populations were isolated from the porcine coronary artery, spindle-shaped (S) and rhomboid (R) SMCs. R-SMCs display the features of synthetic SMCs. S100A4, a calcium-binding protein, was identified as being a marker of the R-SMC population in vitro and of intimal SMCs, in both pig and man. Recently we have shown that the extracellular form of S100A4 is essential for the establishment of the R-phenotype and acts, to some extent, through the receptor for advanced glycation end products (RAGE). Remarkably, S-SMCs treated with S100A4-rich conditioned medium (collected from S100A4-transfected SMCs) acquire pro-inflammatory properties.

To further study the pivotal role and exclusive responsibility of extracellular S100A4 on SMC phenotypic transition, S-SMCs were treated with dimeric and multimeric form of recombinant S100A4. The multimeric form, and not the dimeric form, of S100A4 produced in bacterial expression system was active in other experimental models (Novitskaya et al. *J Biol Chem* 2000; 275:41278-41286). We have shown that the multimeric recombinant S100A4 is responsible for a transition from S- to R-phenotype, which was associated with increased proliferative activity, NF κ B translocation to the nucleus, increased expression of S100A4 and decreased expression of α smooth muscle actin (α -SMA), a well-known SMC differentiation marker (Figure).

Our results suggest that the multimeric form of extracellular S100A4 is responsible for the S- to R-phenotypic transition. The transition is associated with increased cell proliferation and disorganization of α -SMA-positive stress fibers. It is necessary to investigate whether the R-phenotype observed after treatment with multimeric form of extracellular S100A4 recapitulates the proinflammatory-like profile observed in the R-phenotype arising after the treatment with S100A4-rich conditioned medium. A better understanding of S100A4 expression, release and regulation in SMCs will help to shed light on the mechanisms of SMC accumulation in the intima.



Figure

153

Microparticles of healthy origins improve atherosclerosis-associated endothelial progenitor cell dysfunction via microRNA transfer

N. Alexandru; E. Dragan; E. Andrei; L. Niculescu; A. Georgescu

Institute of Cellular Biology and Pathology 'Nicolae Simionescu' of Romanian Academy, Bucharest, Romania

Background: Endothelial progenitor cells (EPCs) are a type of stem cells present in the peripheral blood with role in the maintenance of vascular endothelium integrity. Normal EPC function can be preserved by certain microRNAs (miRNAs), but little is known about EPC dysfunctionality in atherosclerosis.

Purpose: In this study we aimed: (1) to obtain and functionally characterize the late EPC cultures from the animal blood; (2) to investigate the potential beneficial effects of circulating microparticles (MPs) of healthy origins on EPC dysfunctionality in atherosclerosis as well as the involved mechanisms.

Methods: The late EPCs were obtained and expanded in culture from the peripheral blood mononuclear cells isolated from two animal groups: hypertensive-hyperlipidemic hamsters (HH), and control hamsters (C). The late EPCs after 4 weeks in culture were compared using immunophenotyping and multiple in vitro functional assays. In parallel experiments, the late EPC cultures from HH were incubated with MPs isolated from control group, for 48 hours, to follow the EPC function recovery.

Results: The results showed that late EPCs presented endothelial cell phenotype: (1) have the ability to uptake Dil-ac-LDL and UEA-1; (2) express CD34, CD133, KDR, CD144, vWF, Tie-2 specific markers. Also, late EPCs from HH exhibited different morphological and functional characteristics compared to late EPC from control: (1) are smaller and irregular in shape; (2) present decreased expression of cell surface markers specific to endothelial cells; (3) display reduced proliferative, migratory and adhesive capacity; (4) lose the ability to organize themselves into tubular structures and integrate into vascular network; (5) have diminished function of inward rectifier potassium channels. In addition, the incubation of late EPC with MPs improved the EPC functionality by transfer of miR-10a, miR-21, miR-126, miR-146a; the kinetic study of MP (labeled with PKH26 dye or transfected with siRNA-FITC) incorporation into EPCs demonstrated the miRNA transfer and MP uptake by EPCs.

Conclusions: To our knowledge, this is the first study that examines late EPC cultures from atherosclerotic animal model. The data reveal that late EPCs from HH exhibit distinctive features and are dysfunctional, and their recovery can be supported by MP ability to transfer miRNAs. These findings bring a new light on the MP role in the cell-cell communication and EPC-mediated endothelial vascular repair.

154

Arterial remodeling and metabolism impairment in early atherosclerosis

M. Martin-Lorenzo¹; L. Gonzalez-Calero¹; AS. Maroto¹; P.J. Martinez¹; A. Heredero²;

G. Aldamiz-Echevarria²; F. Vivanco¹; G. Alvarez-Llamas¹

¹IS-Fundacion Jimenez Diaz, Immunology, Madrid, Spain; ²Foundation Jimenez Diaz, Cardiac Surgery, Madrid, Spain

Introduction: Atherosclerosis develops asymptomatic and silently. Main risk factors are known and current efforts are dedicated to improve prevention. However, a prompt intervention should be guaranteed and, for that, novel key players in the course of disease have to be identified and evaluated in individualized cardiovascular risk prediction.

Purpose: Investigate those changes taking place at early stages of atherosclerosis development in intact aortic tissue, and further evaluate their potential reflection in a fingerprint measurable in plasma.

Methods: A double approach was applied to study molecular changes (proteins and metabolites) in an early atherosclerosis rabbit model. A novel intact-tissue-approach based on nuclear magnetic resonance (NMR) was applied in the study of metabolites and differential gel electrophoresis analysis (DIGE) was used to elucidate protein alterations. Confirmation and highly selective quantitation of molecular targets of interest was carried out by liquid chromatography coupled to mass spectrometry (LC-MS/MS). The reflection of those alterations observed in rabbit aortic tissue was first investigated in rabbit plasma and then a translational study was performed in human plasma from 62 individuals (35 healthy subjects and 27 patients undergoing coronary artery bypass surgery (CABG)).

Results: Data link the structural remodeling taking place in atherosclerotic arteries in terms of loss of contractile properties and favored cellular migration, with an up-regulation of integrin linked kinase, tropomyosin isoform 2 and capping protein gelsolin-like, and a down-regulation of vinculin. A molecular response to oxidative stress is also evidenced, involving changes in the glucose metabolism enzymes pyruvate kinase (PKM) and phosphoglycerate kinase (PGK), and pyruvate. Up-regulation of aspartate connects different changes observed in amino acids metabolism and, additionally, alterations in the phosphatidylcholine route of the glycerophospholipid metabolism were found. Conclusions: A specific molecular marker panel composed by PKM, valine and pyruvate is shown here linked to cardiovascular risk in humans.

155

Role of pannexin1 in atherosclerotic plaque formation

F. Malica¹; M.J. Meens¹; G. Pelli¹; B. Foglia¹; E. Scemes²; BR. Kwak¹

¹University of Geneva, Pathology and Immunology, Geneva, Switzerland; ²Albert Einstein College of Medicine, Neuroscience, New York, United States of America

Background: Atherosclerosis is a chronic inflammatory disease in the vascular wall characterized by endothelial dysfunction, leukocyte recruitment, lipid accumulation and cell death. Pannexin1 (Panx1) forms ATP-release channels that are known to play a role in endothelium-dependent regulation of arterial tone, neutrophil migration, T lymphocyte activation and macrophage apoptosis.

Aim: Our study aims to clarify the contribution of Panx1 to atherosclerosis.

Methods: We investigated plaque development in atherosclerosis-prone mice with ubiquitous (Panx1-/-Apoe-/-) or endothelial (Panx1ECdelApoe-/-) deletion of Panx1 after 5 or 10 weeks of high-cholesterol diet (HCD). Expression of Panx1 in atherosclerotic plaques was assessed by immunofluorescence. Total cholesterol and triglyceride (TG) levels in the serum of the mice were measured using a Cobas C111 analyser. Lipid deposition and the extent of atheroma formation in the thoracoabdominal aortas and aortic roots were determined after Sudan IV staining. The size of atherosclerotic lesions as well as the CD68+ macrophage content was analysed on cryosections from aortic roots.

Results: Panx1-/-Apoe-/- (n=10) mice displayed reduced bodyweight before (21.5 \pm 0.5 vs 25.9 \pm 0.7g; P<0.01) and after (24.8 \pm 0.5 vs 29.2 \pm 0.6g; P<0.01) 5 weeks HCD compared to Apoe-/- mice, but the bodyweight gain during HCD was similar for both groups. Moreover, lower serum cholesterol (727 \pm 36 vs 922 \pm 67mg/dL; P<0.05) and TG (133 \pm 16 vs 284 \pm 48mg/dL; P<0.01) concentrations were found in Panx1-/-Apoe-/- mice after HCD, suggesting a difference in lipid uptake or metabolism between the 2 groups of mice. Surprisingly, atherosclerotic plaque development did not differ between Panx1-/-Apoe-/- and Apoe-/- mice after 5 and 10 weeks HCD. However, atherosclerotic lesions of Panx1-/-Apoe-/- contained more CD68+ macrophages (35.6 \pm 2.3 vs 27.2 \pm 2.4%; P<0.05). Increased macrophage content in plaques may be due to enhanced recruitment, enhanced proliferation or decreased apoptosis. In contrast to mice with ubiquitous Panx1 deletion, plaque formation was enhanced in the thoracoabdominal aortas of Panx1ECdelApoe-/- mice (n=10) compared to their controls (14.2 \pm 3.6 vs 6.9 \pm 0.9%; P<0.05), pointing to a protective role for endothelial Panx1 during atherogenesis. No differences were observed in bodyweight, serum cholesterol or TG as well as in CD68+ macrophage content in atherosclerotic plaques between Panx1ECdelApoe-/- and control mice.

Conclusions: Panx1 in endothelial cells plays a protective role during atherogenesis. This protection seems masked by simultaneous effects of Panx1 deletion on lipid uptake or metabolism in mice with ubiquitous Panx1 deficiency.

Calcium fluxes and excitation-contraction coupling

158

Amphiphysin II induces tubule formation in cardiac cells

RF. Taylor; JL. Caldwell; DA. Eisner; KM. Dibb; AW. Trafford

University of Manchester, Institute of Cardiovascular Sciences, Manchester, United Kingdom

Amphiphysin II (amplII) is a BAR domain protein thought to be crucial for the biogenesis of transverse (t)-tubules in skeletal muscle. T-tubules are essential for efficient excitation-contraction coupling in both skeletal and cardiac muscle; however, little is known of the role of amplII in the heart. In humans, some amplII mutations result in centronuclear myopathy (CNM), a neuromuscular disease where loss of t-tubules is thought to contribute to skeletal muscle weakness; despite this, there are few reports of

cardiac symptoms in these patients. The aim of this project is to investigate the role of WT and CNM ampl mutants in cardiac t-tubule biogenesis.

Using PCR and DNA sequencing, isoforms 5 and 8 were identified as the major variants of ampl expressed in both ovine and human ventricle. Isoforms 5 and 8 of ampl were tagged with mKate2 fluorescent protein and transiently over-expressed in neonatal rat ventricular myocytes (NRVMs) and an atrial cell line, HL-1. Expression of mKate2 alone was used as a control. Under control conditions, neither NRVMs nor HL-1 cells have t-tubules; however, expression of isoform 5 or 8 of ampl induced tubule formation in both cell types.

D151N, R154Q and K35N are ampl mutations that cause autosomal-recessive CNM. Expression of isoform 8 ampl in C2C12 myoblasts resulted in tubule formation; however, no tubules were formed in these cells upon expression of any of the three ampl mutants. Similar results were found in HL-1 cells. In contrast, there was no significant difference in tubule density between NRVMs transfected with WT, D151N or R154Q ampl; a small, but a significant reduction ($39.7 \pm 0.14\%$, $p < 0.005$) in tubule density was observed upon expression of the K35N variant.

Together these data suggest that fundamental differences in tubule biogenesis exist between C2C12 myoblasts, HL-1s and NRVMs, and these disparities may provide key insight into how t-tubules are formed and maintained. Further work will attempt to elucidate any differences in binding partners between WT and ampl mutants in all three cell types, and if tubules formed by these ampl mutants in NRVMs, are functional.

159

Interleukin 1 beta regulation of connexin 43 in cardiac fibroblasts and the effects of adult cardiac myocyte: fibroblast co-culture on myocyte contraction

L. Mearthur¹; L. Chilton²; G. L. Smith¹; S. A. Nicklin¹

¹University of Glasgow, Institute of Cardiovascular and Medical Sciences, Glasgow, United Kingdom; ²James Cook University, College of Public Health, Medical and Veterinary Sciences, Townsville, Australia

Background: In the cardiac myocyte, gap junctions [composed of connexin (Cx) proteins] are mainly present at the intercalated discs between neighbouring myocytes, and assist in rapid electrical conduction through the myocardium. Fibroblasts, another major cardiac cell type, provide the structural skeleton of the heart. However in heart disease the numbers of fibroblasts are significantly increased. Interestingly, cardiac fibroblasts have been demonstrated to increase Cx43 expression in experimental models of myocardial infarction (MI) which may augment myocyte: fibroblast coupling in the heart. We are investigating the mechanisms of fibroblast Cx43 up-regulation in disease and effects of heterocellular coupling.

Methods: Adult rat cardiac fibroblasts were stimulated with a range of proinflammatory mediators including: angiotensin II, TGF β 1, TNF α and IL1 β . In a subset of experiments fibroblasts were pre-treated with the NF κ B inhibitor, SC-514, 1 hr prior to IL1 β stimulation. Cx43 mRNA and protein expression were detected by qRT-PCR and immunoblotting respectively. Next we established an adult cardiac myocyte: fibroblast co-culture model, whereby freshly isolated rat adult myocytes were added to fibroblast cultures that had been pre-treated with or without IL1 β . Cells were co-cultured for 24hrs before contraction parameters were measured while myocytes were paced at 1Hz.

Results: Cx43 mRNA expression was significantly up-regulated by TGF β 1 (fold increase from control \pm SEM: 2.6 ± 0.6 ; $P < 0.05$) and IL1 β (12.5 ± 3.5 ; $P < 0.001$). IL1 β also augmented the expression of Cx43 protein. Inhibition of NF κ B by SC-514 reduced IL1 β mediated increase of both Cx43 mRNA (10.1 ± 1.8 vs. 4.6 ± 1.8 ; IL1 β vs. IL1 β + SC-514; $P < 0.01$) and protein. In contraction experiments, co-cultured myocytes relaxed more quickly than mono-cultured myocytes irrespective of IL1 β treatment (contraction transient duration at 25% relaxation: 23.4 ± 0.5 ms vs. 30.4 ± 0.7 ms; co-culture vs. mono-culture; $P < 0.001$; 26.3 ± 0.7 ms vs. 30.4 ± 0.7 ms; IL1 β co-culture vs. mono-culture; $P < 0.001$). However, myocytes in culture with IL1 β treated fibroblasts had a slower relaxation to untreated fibroblast cultures ($P < 0.05$).

Conclusions: IL1 β , acting via NF κ B, may mediate increased Cx43 expression observed in fibroblasts in an experimental model of MI. The presence of fibroblasts shortened the myocyte contraction duration which may suggest that Cx43 expression in unstimulated fibroblasts is sufficient to influence contraction parameters of coupled myocytes. Further studies will examine mechanisms for these effects and the role of Cx43 in heterocellular coupling.

160

T-tubule electrical defects contribute to blunted beta-adrenergic response in heart failure

C. Crocini¹; R. Coppini²; C. Ferrantini²; P. Yan³; LM. Loew³; C. Poggesi²; E. Cerbai¹; F. S. Pavone¹; L. Sacconi¹

¹University of Florence, LENS - Laboratory for Non Linear Spectroscopy, Sesto Fiorentino, Italy; ²University of Florence, Firenze, Italy; ³University of Connecticut, Center for Cell Analysis & Modeling, Farmington, United States of America

Introduction: Beta-adrenoceptors start the most powerful signalling pathway for the control of the cardiac function. Human and animal models of heart failure (HF) show alterations of the beta-adrenergic signalling. Number and function of beta-adrenoceptors, namely the beta-1 subtype, are impaired in HF, representing a major (mal)adaptive feature of myocardial remodelling. Moreover, HF is characterized by structural and functional remodelling of T-tubules (TT). We previously observed failure of action potential conduction in about 6% of HF TTs accompanied by profound alterations of local Ca²⁺ transient.

Purpose: Here, we assess the effect of beta-adrenoceptor activation on local Ca²⁺ release in electrically coupled and uncoupled tubular elements.

Methods: We employ an ultrafast random access multi-photon (RAMP) microscope to simultaneously record action potentials (AP) and Ca²⁺ transients from multiple TT sites in isolated HF cardiomyocytes. The beta-adrenergic agonist isoproterenol (10⁻⁷ M) is acutely used in the cell suspension.

Results: We find that beta-adrenergic stimulation increases the frequency of Ca²⁺ sparks in diastole while it reduces Ca²⁺ sparks in systole, both in HF and in controls cells. This likely reflects the effects of beta-adrenergic stimulation on the open probability of ryanodine receptors (RyR2) and it is not dependent on the electrical activity of the correspondent TT. Conversely, we observe an accelerated Ca²⁺ rise exclusively in the proximity of TT that regularly conduct the action potential (AP+), while Ca²⁺ rise close to AP-failing T-tubular elements (AP-) is unchanged in beta-adrenergic stimulated cells.

Conclusion: Taken together, these findings indicate that HF cells globally respond to beta-adrenergic stimulation, except at T-tubules that fail to conduct APs, where the blunted effect of the beta-adrenergic signalling may be directly caused by the lack of electrical activity.

161

Beat-to-beat variability of intracellular Ca²⁺ dynamics of Purkinje cells in the infarct border zone of the mouse heart revealed by rapid-scanning confocal microscopy

T-A. Matsuyama¹; H. Tanaka¹; H. Ishibashi-Ueda²; T. Takamatsu¹

¹Kyoto Prefectural University of Medical Graduate School of Medical Science, Kyoto, Japan; ²National Cerebral and Cardiovascular Center Hospital, Department of Pathology, Suita, Osaka, Japan

Background: Cardiac Purkinje cells, which are widely distributed on the endocardial surface to form reticulated networks, play pivotal roles in impulse conduction throughout the ventricles. During the course of myocardial infarction (MI), certain layers of the subendocardial myocardium including Purkinje cells are commonly spared from ischemic necrosis, and the surviving Purkinje cells are believed to be an important substrate for arrhythmias. However, functional demonstration of the surviving Purkinje cells in the infarcted heart is lacking.

Purpose: We sought to demonstrate how the intracellular Ca²⁺ ([Ca²⁺]_i) dynamics are altered in the surviving Purkinje cells in the ischemic border zone of the MI.

Methods: C57BL/6N adult male mice weighing 20-30 g were used. The MI model was created by ligation of the left coronary artery. We used 3-day-old (n=5) and 7-day-old (n=5) infarcted hearts and non-infarcted hearts (n=5) for experiments. The fluo-4-loaded heart under Langendorff perfusion was totally exposed by a longitudinal incision at the posterolateral wall. Under 2-Hz atrial pacing with mechanical arrest by cytochalasin D, the fluo-4-fluorescence images (361 x 241 μ m, 384 x 256 pixels) were visualized on the subendocardial surface of the LV by a spinning disc-based rapid scanning confocal microscope at a frame rate of 100/s.

Results: In contrast to the spatiotemporally uniform Ca²⁺ transients in and among individual Purkinje cells in the non-infarcted hearts, beat-to-beat alternans of the amplitudes of Ca²⁺ transients were evident in both the 3-day-old and 7-day-old infarcted hearts. The beat-to-beat variability of the Ca²⁺ transient amplitudes was more evident in the infarcted border zone (middle LV regions) than in the remote, non-infarcted region (basal LV regions) ($P < 0.01$). Subsequent immunohistochemistry of the endocardial surface enabled definitive discrimination of Purkinje cells from the sub-jacent infarcted myocardium or granulation tissue by expression of connexin40.

Conclusions: Our present study indicates an unstable [Ca²⁺]_i dynamics of Purkinje cells in the vicinity of the infarct lesions at days 3 and 7 after MI. Such functional inhomogeneity of surviving Purkinje cells might indicate arrhythmic potentials of infarcted hearts.

162

The efficacy of late sodium current blockers in hypertrophic cardiomyopathy is dependent on genotype: a study on transgenic mouse models with different mutations

L. Mazzoni¹; R. Coppini¹; C. Ferrantini²; F. Gentile²; JM. Pioner²; L. Santini¹; L. Sartiani¹; V. Bargelli¹; C. Poggesi²; A. Mugelli¹; E. Cerbai¹

¹University of Florence, NeuroFarBa, Florence, Italy; ²University of Florence, Clinical and Experimental Medicine, Florence, Italy

Introduction: The late-Na⁺ current (I_{NaL}) blocker ranolazine reduced the rate of arrhythmic events and improved diastolic function in the myocardium of patients with hypertrophic cardiomyopathy (HCM), via shortening of action potentials and reduction of intracellular Na⁺ and Ca²⁺ concentration (Coppini et al. Circulation 2013). However, it is unclear whether the different causing mutations determine a variable efficacy of I_{NaL}-blockers in this disease.

Methods: Here we characterize the electro-mechanical abnormalities occurring in cardiomyocytes and intact trabeculae from the hearts of two transgenic HCM mouse models carrying mutations in the troponin-T gene (R92Q and E163R) and test how the two different lines respond to I_{NaL}-blockers. Cells and trabeculae were exposed to ranolazine (10 μ M) or the novel selective I_{NaL}-blocker GS-967 (0.5 μ M).

Results: Trabeculae from both R92Q and E163R mice showed slower twitch kinetics, increased diastolic tension and an increased rate of spontaneous activity, as compared with age-matched WT littermates. However, at single cell level, the degree of EC-coupling remodeling was much more pronounced in R92Q: cardiomyocytes from R92Q hearts showed lower Ca²⁺ transient amplitude with slower rate of rise and decay and markedly elevated diastolic [Ca²⁺]_i, while Ca²⁺ transients recorded in E163R cells were comparable to WT. Both R92Q and E163R cells showed frequent spontaneous Ca²⁺ waves and premature Ca²⁺ transients.

In R92Q cardiomyocytes and trabeculae, ranolazine and GS-967: (i) shortened action potentials, (ii) hastened Ca²⁺ transient kinetics and reduced diastolic Ca²⁺, (iii) accelerated contraction kinetics and (iv) reduced the rate of spontaneous beats and Ca²⁺ waves.

In E163R preparations, instead, I_{NaL}-blockers: (i) did not affect action potentials nor the kinetics or amplitude of Ca²⁺ transients, (ii) did not hasten twitch kinetics. Nevertheless, ranolazine and GS-967 reduced diastolic [Ca²⁺]_i at high pacing rate and lowered the occurrence of spontaneous beats and Ca²⁺ waves.

Discussion: Different HCM-related mutations, even though located in the same gene, lead to different degrees of EC-coupling remodeling. I_{NaL}-blockers exert their full efficacy only in the presence of severe Ca²⁺ handling abnormalities, as in R92Q mice. However, as shown in E163R mice, I_{NaL}-blockers may exert an antiarrhythmic effect even in the absence of complex EC-coupling abnormalities. Our data suggest that the efficacy of I_{NaL}-blockers in HCM patients is dependent on genotype.

163

Synthesis of cADPR and NAADP by intracellular CD38 in heart: role in inotropic and arrhythmic effects of beta-adrenoceptor signaling

W. K. Lin; M. Maciejewska; E. L. Bolton; Y. Wang; F. O'Brien; M. Ruas; M. Lei; R. Sitsapesan; A. Galione; D. A. Terrar

University of Oxford, Department of Pharmacology, Oxford, United Kingdom

Background: Nicotinic acid adenine dinucleotide phosphate (NAADP) and cyclic ADP-ribose (cADPR) are calcium mobilising messengers that are upregulated during the activation of

beta-adrenoceptors. They are positive inotropic agents that have roles in modulating excitation-contraction coupling and disease development of the heart. The enzyme responsible for producing these molecules is a potential therapeutic target, but its identity remains unclear. CD38 is an ADP-ribosyl cyclase that catalyses synthesis of both NAADP and cADPR in various tissues, although this is frequently found on the extracellular surface of the plasmalemma.

Methods: Synthesis of NAADP was detected and quantified using sea urchin egg homogenates, and synthesis of cADPR from NAD was gauged from the conversion of its analogue (NGD) to a fluorescent product (cGDPR). Calcium transients were measured using Fluo-5F and spinning disk confocal microscope and sarcomere shortening was measured using an IonOptix system. A whole heart arrhythmia study was carried out with programmed electrical stimulation and monophasic action potential measurement.

Results: Membrane preparations as well as single cells from CD38^{-/-} mouse hearts failed to synthesise NAADP and cADPR. Isolated superfused ventricular myocytes from CD38^{-/-} mice showed smaller peak calcium transients and contractions than myocytes from WT mice, both under basal conditions (F/F₀: WT, 3.73 ± 0.45 vs KO, 2.65 ± 0.57 ; contractions (μm): WT, 0.07 ± 0.01 vs KO, 0.04 ± 0.02) and when stimulated by the 5 nM isoproterenol (F/F₀: WT, 8.11 ± 1.55 vs KO, 5.23 ± 0.35 ; contractions (μm): WT, 0.17 ± 0.02 vs KO, 0.14 ± 0.05). In isolated WT cardiac myocytes, membrane permeabilisation with Triton X-100 increased NAADP synthesis, suggesting there might be additional intracellular CD38. This is further supported by the observation that permeabilised WT myocytes showed a striated immunostaining pattern (consistent with location of CD38 on sarcoplasmic reticulum) for CD38 while CD38^{-/-} myocytes and non-permeabilised WT myocytes showed little or no staining.

Our experiments showed that sarcoplasmic reticulum enriched membrane preparations from sheep hearts showed ability to synthesise NAADP and cADPR, with enzyme properties consistent with a CD38 identity. This synthesis of NAADP and cADPR was blocked by a novel drug, SAN4825. Blind docking experiments showed that SAN4825 binds to the active site of CD38 with possible pi-pi interactions with the Trp 125 and Trp 189. Whole hearts isolated from CD38^{-/-} mice as well as hearts perfused with SAN4825, a CD38 inhibitor, showed a reduced tendency to arrhythmias in the presence of isoproterenol (300 nM).

Conclusion: The above observations support the hypothesis that intracellular CD38 generates NAADP and cADPR, thereby enhancing excitation-contraction coupling under basal conditions and contributing towards effects of β -adrenoceptor stimulation (positive inotropy and arrhythmogenicity).

Contractile apparatus

166

Towards an engineered heart tissue model of HCM using hiPSC expressing the ACTC E99K mutation

T.J. Owen¹; J.G. Smith²; D. Garcia³; R. Barria-Villa³; L. Monserrat³; S.E. Harding¹; C. Denning²; S.B. Marston¹

¹Imperial College London, National Heart and Lung Institute, London, United Kingdom; ²Nottingham University Hospitals NHS Trust, Nottingham, United Kingdom; ³University Hospital Complex A Coruña, A Coruña, Spain

Background: The ACTC E99K mutation is associated with hypertrophic cardiomyopathy (HCM-predominantly apical) and left ventricular non-compaction in a large group of patients from North-west Spain. We have previously characterized this mutation in patient heart muscle samples, and in a transgenic mouse model. We report on investigation of this mutation in hiPSC.

Purpose: Engineered heart tissue with the ACTC E99K mutation will be used to investigate the relation between mutation and contractile phenotype of HCM.

Methods: Punch biopsies were taken from 18 patients (14 mutation carriers and 4 related non-carriers); fibroblasts were expanded and 6 samples (2 mutation carriers and one healthy relative each from two different families) were taken forward for Sendai virus reprogramming. CrispR/Cas9 was used for knocking the E99K mutation into the Hues7 cell line and used to make isogenic controls. Engineered Heart Tissue (EHT) was generated using E99K and control cells.

Results: 5 fibroblast lines were successfully reprogrammed, confirmed by staining for pluripotency markers; moreover, after differentiation into cardiomyocytes, the presence of the mutation in the myofibrils was confirmed with an antibody specific to the ACTC E99K mutation. In addition, the ACTC E99K mutation was knocked into the embryonic stem cell line Hues7 and isogenic controls were generated by CrispR/Cas9 gene editing technology. Expression of the ACTC E99K mutation was confirmed by PCRs, Nar1 digestion, and by sequencing. Moreover, pluripotency was confirmed after targeting, and differentiation into cardiomyocytes was achieved. WT and ACTC E99K hiPSC function was investigated by incorporating the cells into EHT that allows for measurement of contractility and force production. In our initial experiments Hues7 cells were taken and EHT was generated for comparison against controls. ACTC E99K constructs were generated and the diameter of the constructs decreased rapidly overnight, so that mutant constructs were significantly narrower than controls ($n=4$ $p<0.001$). qPCR was carried out which suggested a low level of cardiomyocyte markers in E99K cells compared to controls.

Conclusions: We will report on optimizing differentiation strategies for ACTC E99K in Hues7 and hiPSC cell lines. EHTs will be generated and the comparative contractile behavior of ACTC E99K and WT constructs will be assessed. These results will elucidate the mechanism of the disease causing mutation ACTC E99K, and assess its usefulness in investigating treatments for HCM.

167

Diastolic mechanical load delays structural and functional deterioration of ultrathin adult heart slices in culture

M. Scigliano¹; S. Watson²; S. Tkach²; G. Faggiani¹; C.M. Terracciano²; F. Perbellini²

¹University of Verona, Dipartimento di Scienze Chirurgiche Odontostomatologiche e Materno-Infantili, Verona, Italy; ²Imperial College London, Myocardial function, National Heart and Lung Institute, London, United Kingdom

Introduction: Ultrathin myocardial slices arise as an innovative, simple, widely-accessible, model to study cardiac properties, pathophysiology and novel treatments in vitro. Compared to cell cultures, cells within the

slices are exposed to local environmental conditions that are more representative of the native state. Moreover, cell-cell mechanical and electrical interactions as well as the 3-dimensional structure are preserved. Despite their structural integrity, slices in culture undergo a progressive de-differentiation process that significantly affects contractile properties and ultrastructure.

Hypothesis: We hypothesised that the reason for the de-differentiation of cultured slices is the lack of physiological mechanical load. The native structure and function can be preserved by application of mechanical load.

Methods: Multiple 300 μm thick, vibratome-cut myocardial slices were prepared from the left ventricular free wall of adult healthy rat and canine hearts and from explanted failing human hearts at transplantation. Once isolated, slices were cultured either in unloaded condition at liquid-air interface or in loaded condition using A-shaped plastic stretchers. Some slices were continuously paced (1 Hz) during culture. Viability, contractile properties and morphology of slices were assessed using immunohistochemistry, electrophysiology and histology.

Results: For all the different species evaluated, a degree of functional deterioration with time while cultured in unloaded condition was detected, in particular within the first 24 hours in culture (contractility reduction: rat $42.5 \pm 6\%$, dog $48.9 \pm 7\%$ and human $90.5 \pm 0.5\%$).

Conversely, loaded slices showed a better maintained contractility, even after several days in culture (contractility reduction after 24 hours: rat $25 \pm 6\%$, dog $18.9 \pm 6\%$, human $22.5 \pm 11\%$). Data obtained from paced and loaded slices showed not significantly different trend compared to non paced group indicating that diastolic, rather than systolic load may be the responsible factor for the maintenance of contractile functionality.

Structurally, unloaded slices showed a progressive degeneration in the myocytes sarcomere organization, a decrease in sarcomere length (dog slices: from $1.84 \pm 0.06 \mu\text{m}$ on day 0 to $1.57 \pm 0.03 \mu\text{m}$ and $1.3 \pm 0.02 \mu\text{m}$ respectively on day 3 and 7) and a loss of T-tubule organization. The sarcomere length was better preserved in the loaded group (dog slices: $1.70 \pm 0.03 \mu\text{m}$, $1.54 \pm 0.02 \mu\text{m}$ and $1.38 \pm 0.09 \mu\text{m}$ respectively on day 1, 3 and 7) as well as the sarcomere organization.

Conclusions: The application of mechanical load delays functional and structural deterioration of 300 μm -thick adult cardiac slices in culture. Culturing methods need further improvements and the molecular mechanisms that account for this behaviour need to be elucidated to better understand the potential and the applications of these preparations in studies of cardiac pathophysiology and treatments.

168

Structural investigation of the cardiac troponin complex by molecular dynamics

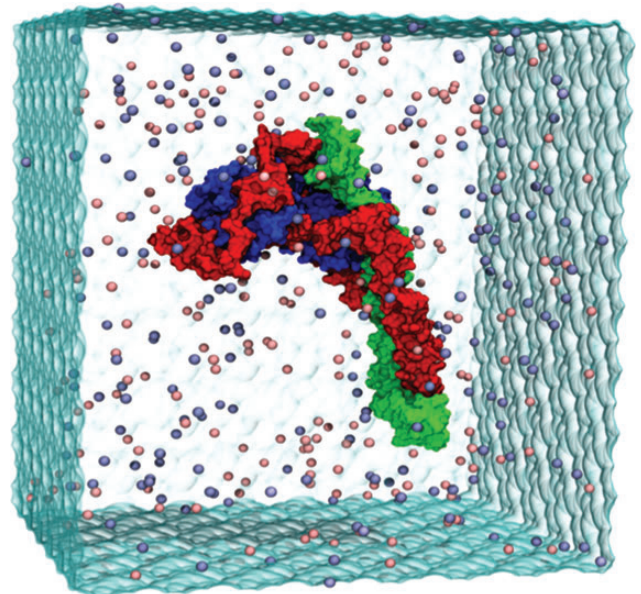
A. Sheehan¹; J. Eiros Zamora²; M. Papadaki¹; A. Messer¹; S. Marston¹; I. Gould²

¹Imperial College London, National Heart and Lung Institute, London, United Kingdom; ²Imperial College London, Department of Chemistry, London, United Kingdom

Troponin is the Ca²⁺ switch of heart muscle and it is physiologically modulated by PKA-dependent phosphorylation at Ser22 and 23. The modulation of Ca²⁺ sensitivity by phosphorylation of the cardiac specific N-terminal segment of TnI (1-30) is subtle and has proven hard to investigate. The crystal structure of cardiac Troponin describes only the relatively stable core of the molecule and the crucial mobile parts of the molecule are missing including TnI 1-30, TnI 134-149 ('switch' peptide) and the C-terminal 28 amino acids of TnT that are intrinsically disordered.

Molecular dynamics simulations facilitate the description of protein structure at the atomic level and its dynamics on the ns- μs time scale. We modelled unphosphorylated and phosphorylated troponin dynamics over 10 μs . Starting with the crystal structure of Takeda et al. Missing residues were modelled using UCSF Chimera. HCM and DCM mutations were introduced using Chimera under the "swapa" rotamer syntax command. The phosphorylated and unphosphorylated Troponin complex was simulated using AMBER MD under the AMBER force field ff99SB.

The emerging model confirms the stable core structure of troponin and the mobile structure of the intrinsically disordered segments. We define these segments in terms of dynamic transitions between a small number of states with the probability distributions being altered by phosphorylation and by HCM or DCM-related mutations that can explain how Ca²⁺-sensitivity is modulated by phosphorylation and the effects of mutations.



Single MD simulation Frame of Troponin

169

Exercise training restores myocardial and oxidative skeletal muscle function from myocardial infarction heart failure rats

A R. Bezerra Gurgel¹; A. Johnston²; M. Dunne¹; G. Smith¹; OJ. Kemi¹¹University of Glasgow, Institute of Cardiovascular and Medical Sciences, Glasgow, United Kingdom; ²British Heart Foundation, The Rayne Institute, King's College, London, United Kingdom

Background: Energetic collapse in cardiac and skeletal muscles is a hallmark in heart failure (HF). In this condition, the skeletal musculature undergoes impairments as muscle atrophy, fibre type shifting, contractile dysfunction, and energetic metabolic myopathy with reduction in lipolytic and oxidative enzymes, all of which leads to muscle weakness and early onset of exertional fatigue. This therefore contributes to exercise intolerance and muscle disuse and deconditioning, with concomitant worsening of health and well-being. Exercise training improves physical capacity and skeletal muscle contractile performance, but less is known about metabolic effects, including the potential benefit of exercise training after the onset of heart failure.

Purpose: Explore the underlying causes of improvement following exercise training after onset of myocardial infarction-induced heart failure.

Methods: Controlled chronic high-intensity aerobic treadmill running or untrained control was administered 4 weeks after induction of coronary artery ligation resulting in myocardial infarction and subsequent heart failure in Wistar rats. Results: Heart failure was confirmed by echocardiography and reduced exercise capacity (15-20%), presence of ~35% left ventricular scar tissue, pathologic hypertrophy of cardiomyocyte (20-30%), and reduced cardiomyocyte contraction and Ca²⁺ transient amplitude (both 30-40%). Exercise training improved global heart function, normalized exercise capacity, and partly reversed cardiomyocyte remodeling and dysfunction. In particular, amplitude and rates of contraction and relaxation and intracellular Ca²⁺ handling improved at high twitch-stimulation frequencies. Thus, exercise training has a clear and demonstrable beneficial effect on myocardium. Next, we hypothesized that skeletal muscle also experiences loss-of-function by myocardial infarction heart failure and gain-of-function by exercise training. We investigated metabolic enzymes and found that oxidative type-I muscle (m. soleus) adapts to heart failure and exercise training in line with injury and exercise training, especially with respect to citrate cyclase expression, whereas glycolytic type-II muscle (m. extensor digitorum longus) experiences paradoxical effect.

Conclusions: Heart failure reduces contractile and metabolic capacity in myocardium and skeletal muscle, whereas exercise training restores myocardial and oxidative skeletal muscle function.

Oxygen sensing, ischaemia and reperfusion

172

A novel antibody specific to full-length stromal derived factor-1 alpha reveals that remote conditioning induces its cleavage by endothelial dipeptidyl peptidase 4

DI. Bromage; M. Pillai; SM. Davidson; DM. Yellon

University College London, Hatter Cardiovascular Institute, London, United Kingdom

Background/Introduction: Stromal derived factor-1 α (SDF-1 α /CXCL12) is a chemokine that has been implicated in both acute and chronic cardioprotection. Remote ischaemic conditioning (RIC), a technique of cyclical, non-injurious ischaemia applied to an organ or tissue remote from the heart, has been shown to increase circulating SDF-1 α . Subsequent activation of its receptor, CXCR4, has been proposed as the mechanism by which RIC facilitates acute cardioprotection. However, the mechanism of SDF-1 α regulation is poorly understood.

Purpose: We hypothesized that dipeptidyl peptidase 4 (DPP4/CD26), a protease that cleaves and inactivates SDF-1 α , may be centrally involved in the mechanism of acute cardioprotection conferred by RIC.

Methods: To elucidate the role of SDF-1 α cleavage after RIC we established an ELISA to full-length SDF-1 α using a novel recombinant human antibody we developed called HCL.SDF1 α . RIC was achieved by 3 cycles of 5 min cuff inflation and 5 min deflation on the hind limb of Sprague-Dawley rats or on the arms of healthy human volunteers, and samples were taken for SDF-1 α measurement either immediately or 1 h after the protocol.

The role of membrane-bound DPP4 was investigated using cultured human umbilical vein endothelial cells (HUVECs) subjected to oxidative stress with 5 min x 1 mM H₂O₂ to mimic RIC.

In a separate experiment, rats were randomly allocated to receive a sham procedure, RIC or RIC + AMD3100, a specific inhibitor of CXCR4, prior to 30 min reversible occlusion of the left anterior descending artery and 120 min reperfusion.

Results: In vivo infarction experiments confirmed that AMD3100 eliminated protection by RIC (56.2 \pm 4.2% vs. 31.3 \pm 3.3%, P<0.01). We demonstrate for the first time that HCL.SDF1 α can be used to specifically quantify full-length SDF-1 α in blood. Unexpectedly, despite an increase in total SDF-1 α as previously reported, levels of intact SDF-1 α declined after RIC in both rats (670 \pm 130 pg/ml vs. 1150 \pm 160 pg/ml, P<0.05) and humans (329.8 \pm 148.7 pg/ml vs. 380.0 \pm 154.9 pg/ml, P<0.05). Furthermore, oxidative stress significantly increased DPP4 activity (150 \pm 20 vs. 90 \pm 20, P<0.05).

Conclusion(s): We report for the first time the application of a novel antibody for full-length, active SDF-1 α , which demonstrated a significant decrease in intact SDF-1 α in response to RIC. This may be mediated by the activation of membrane-bound DPP4 in response to oxidative stress. These results suggest that RIC is not mediated by an increase in full length SDF-1 α , as previously thought. We speculate that altered CXCR4 trafficking or an alternative ligand for CXCR4 may mediate RIC. Further studies will investigate the relation between SDF-1 α , acute cardioprotection and the dynamics of bone marrow progenitor cell mobilization.

173

Attenuation of myocardial and vascular arginase activity by vagal nerve stimulation via a mechanism involving alpha-7 nicotinic receptor during cardiac ischemia and reperfusion

A. Kiss¹; Y. Tratsiakovich²; J. Jang²; AT. Gonor²; J. Pernow²¹Medical University of Vienna, Biomedical Research, Vienna, Austria; ²Department of Medicine, Division of Cardiology, Karolinska Institutet, Stockholm, Sweden

Background: Electrical vagal nerve stimulation (VNS) protects from myocardial and vascular injury following cardiac ischemia/reperfusion (IR) via a mechanism involving activation of alpha-7 nicotinic

acetylcholine receptors ($\alpha 7$ nAChRs) and reduced inflammation. Arginase has been proposed to be involved in development of IR injury and endothelial dysfunction after induction by pro-inflammatory mediators.

Purpose: The present study aimed to clarify (1) whether VNS attenuates IR-induced arginase upregulation in the myocardium as well as aorta and (2) whether this effect is mediated via a mechanism involving activation of the $\alpha 7$ nAChRs.

Methods: Anaesthetized Sprague-Dawley rats subjected to 30 min left coronary artery (LCA) ligation followed by 2 h reperfusion were randomly allocated to: (1) sham operation (n=5); (2) control IR (n=10); (3) VNS (n=13, IR and intact right VNS 0.1-1 mA, 15 Hz throughout IR) and (4) methyllycconitine (n=7, MLA; 10 mg/kg ip, an $\alpha 7$ nAChRs blocker)+VNS group. The stimulation was optimized to obtain a 10-20% reduction in heart rate (HR) from baseline values. Infarct size was determined by triphenyltetrazolium chloride staining and expressed as % of the area at risk. Arginase activity was determined in the myocardium and aorta.

Results: VNS reduced infarct size compared to control IR (41 \pm 3% vs. 66 \pm 3%, P<0.001). Myocardial IR increased arginase activity 1.6-fold (P<0.05 vs. sham) in the myocardium at risk and 3.1-fold (P<0.001 vs. sham) in aorta. VNS attenuated the increase in arginase activity compared to control IR both in the myocardium (1.2-fold vs. 1.6-fold of sham, P<0.05) and in aorta (1.3 \pm 0.2 fold vs. 3.1 \pm 0.3 fold of sham, P<0.001). The administration of MLA partially abolished the infarct size limiting effect of VNS (55 \pm 3% vs. 66 \pm 3% in control, P<0.05) and completely abrogated the effect of VNS on arginase activity (1.6-fold increase of sham in the myocardium and 2.5-fold increases in aorta), without affecting HR.

Conclusion: VNS reversed the upregulation of arginase not only in the affected organ, but also in the remote vasculature via a mechanism mediated through $\alpha 7$ nAChRs activation. This finding may represent a novel cardiovascular protective effect of VNS mediated via attenuated arginase activity

174

Novel nanoparticle-mediated medicine for myocardial ischemia-reperfusion injury simultaneously targeting mitochondrial injury and myocardial inflammation

G. Ikeda; T. Matoba; J. Koga; K. Egashira

Kyushu University, Cardiovascular Research, Fukuoka, Japan

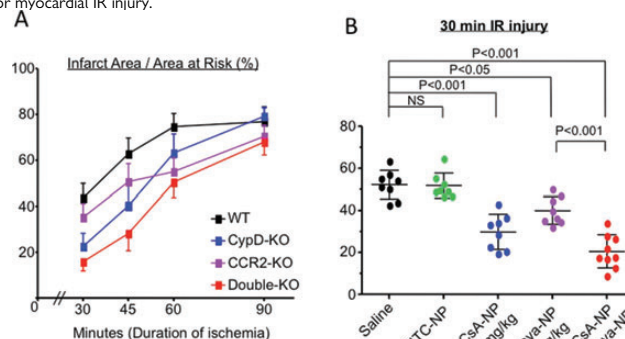
Introduction: The opening of mitochondrial permeability transition pore (mPTP) and myocardial inflammation may cooperatively progress myocardial ischemia-reperfusion (IR) injury, which hampers therapeutic effects of primary reperfusion therapy for acute myocardial infarction.

Hypothesis: Novel nanoparticle-mediated medicine that simultaneously targets mPTP and myocardial inflammation may settle the un-met needs to suppress myocardial IR injury.

Methods and Results: We employed mice lacking cyclophilin D (CypD, a key molecule for mPTP opening) and CCR2 (a receptor for monocyte chemoattractant protein-1) and found that CypD contributed to progression of myocardial IR injury with shorter duration (30-45 min) of ischemia, whereas CCR2 contributed to IR injury with longer duration (60-90 min) of ischemia (Fig.A). Double deficiency of CypD and CCR2 showed superior cardioprotection over single deficiency regardless of the duration of ischemia (Fig.A). CCR2 deficiency markedly reduced IL-1 β protein levels and the number of Ly6Chigh activated monocytes in IR-injured myocardium, whereas CypD deficiency reduced infarct size without affecting inflammation in the IR heart.

Then we engineered poly (lactic-co-glycolic acid) nanoparticle containing cyclosporine A (CsA-NP) that inhibits mPTP opening and pitavastatin (Pit-NP) that reduces monocyte-mediated inflammation. In CypD-KO mice, Pit-NP reduced the recruitment of Ly6Chigh inflammatory monocytes and infarct size, whereas CsA-NP reduced infarct size in CCR2-KO mice. Simultaneous treatment with CsA-NP and Pit-NP at the time of reperfusion presented a remarkable reduction in infarct size after IR injury with 30 or 60 min of ischemia (Fig.B).

Conclusion: Nanoparticle-mediated simultaneous targeting to mitochondria and inflammatory monocytes can be developed as a novel nanoparticle-mediated medicine that provides a solution for myocardial IR injury.



Figure

175

Acetylcholine plays a key role in myocardial ischaemic preconditioning via recruitment of intrinsic cardiac ganglia

J M J. Pickard; N. Burke; SM. Davidson; DM. Yellon
Hatter Cardiovascular Institute, London, United Kingdom

Background: Myocardial ischaemic preconditioning (IPC) is a receptor-mediator phenomenon, dependent on release and subsequent action of adenosine, opioids and bradykinin. This study adds to the IPC paradigm by proposing a crucial role of acetylcholine and intrinsic cardiac ganglia in the mechanism.

Methods: Isolated Langendorff perfused rat hearts were subjected to either IPC (3x5min global ischaemia-reperfusion) or sham. Effluent was collected and perfused through a naïve-isolated heart for 10-min prior to a 35-min regional ischaemia and 60-min reperfusion. The ganglionic antagonist hexamethonium (50 μ M) and nitric oxide synthase (NOS) blocker L-NAME (100 μ M) were used to investigate the mechanism of effluent-mediated cardioprotection. Finally, the concentration of acetylcholine in effluent from isolated rat hearts was measured before and immediately after the IPC protocol.

In a separate experiment, isolated Langendorff perfused rat hearts were subjected to the following conditions: (1) Sham IPC; (2) IPC (as above); (3) Sham+Hexamethonium (50 μ M); (4) IPC+Hexamethonium (50 μ M); (5) Sham+Atropine (100nM); (6) IPC+Atropine (100nM). Hearts were subjected to ischaemia-reperfusion injury as described above and were analysed for infarct size using triphenyl-tetrazolium chloride staining. Data are presented as mean \pm SEM.

Results: A tenfold increase in acetylcholine concentration was observed in effluent following IPC (Control=0.036 \pm 0.03 μ M vs IPC=0.36 \pm 0.03 μ M, $p > 0.001$). IPC effluent significantly reduced infarct size in naïve isolated hearts (I/AAR%=19.5 \pm 2.0 vs control=46.1 \pm 5.6, $p < 0.01$). This protection was abrogated by hexamethonium (I/AAR%=35.8 \pm 4.9) and L-NAME (45.8 \pm 4.8). Direct ischaemic preconditioning was also abrogated by both hexamethonium (I/AAR%=33.7 \pm 5.7 vs IPC=14.2 \pm 1.9, $p < 0.05$) and atropine (I/AAR%=39.9 \pm 2.8, $p < 0.05$ vs IPC).

Conclusion: IPC induces release of acetylcholine, which acts to recruit intrinsic cardiac ganglia and NOS to stimulate cardioprotection. The isolated heart is generally thought of as a denervated tissue, however this study suggests intrinsic cardiac neural pathways remain intact and form a novel aspect to the mechanism of IPC-mediated cardioprotection.

176 The role of nitric oxide and VEGFR-2 signaling in post ischemic revascularization and muscle recovery in aged hypercholesterolemic mice

G. Wirth; P. Korpisalo; H. Hakkarainen; S. Laidinen; S. Yla-Herttuala
University of Eastern Finland, A.I. Virtanen Institute for Molecular Sciences, Dpt of Biotechnology and Molecular Medicine, Kuopio, Finland

Introduction: Vascular endothelial growth factor (VEGF) via angiogenic signaling through its receptor 2 (VEGFR-2) is generally considered to have a major role in ischemic tissue recovery. Still, despite numerous clinical and preclinical studies, angiogenic therapies do not have an established role in the treatment of ischemic cardiovascular diseases. While misleading preclinical modelling has been suggested a possible cause for the discrepancies between theory and translation (Dragneva G et al 2013 Dis Model Mech) we wanted to explore how crucial VEGFR-2 signaling is in subacute ischemic recovery in aged, genetically hypercholesterolemic mice.

Methods: Hypercholesterolemic LDLR-/-ApoB100/100 mice (age 6-21 months) underwent unilateral hindlimb ischemia operation. The mice then received either L-NAME (nitric oxide synthase inhibitor; 50mg/kg) or NaCl control i.p. starting four days after ischemia induction, or adenoviral (Ad) soluble VEGFR-2 or AdLacZ control (10e11vp) i.m. gene transfer three days post-operatively. Contrast enhanced ultrasound imaging, photoacoustic imaging and histological studies were carried out to evaluate perfusion recovery, oxygen saturation and tissue responses, respectively. All animal experiments were licensed according to the Finnish legislation.

Results: When administrated after the initial opening of collateral vessels, the treatment with either systemic L-NAME or intramuscular AdsVEGFR-2 reduced capillary size and delayed perfusion recovery in the LDLR-/-ApoB100/100 mice. Interestingly, the vasoconstrictive treatments did not result in worsened muscle morphology as compared to the controls. In fact, the oldest L-NAME treated animals (13-15 months of age) seemed to even benefit from the vasoconstrictive treatment with more normal muscle (28% vs 5% in the controls) and less necrosis (9% vs 27% in the controls) in the histological analysis 11 days post operation.

Conclusions: VEGFR-2 signaling or endothelial nitric oxide production does not seem indispensable for post ischemic muscle recovery after the initial opening of the collateral vessels in aged hypercholesterolemic mice. Moreover, some level of vasoconstriction may even be helpful to support muscle regeneration after ischemia.

177 Efficacy of ischemic preconditioning to protect the human myocardium: the role of clinical conditions and treatments

K. Casos¹; G. Ferrer-Curriu¹; M. Perez¹; E. Permyaner¹; A. Blasco-Lucas¹; JM. Gracia¹; MA. Castro¹; J. Barquiner²; M. Galianes¹
¹University Hospital Vall d'Hebron, Department of Reparative Therapy of the Heart/Cardiac Surgery Department, Vall d'Hebron Research Inst, Barcelona, Spain; ²University Hospital Vall d'Hebron, Department of Cell and Gene Therapy, Vall d'Hebron Research Inst, Barcelona, Spain

Background: Ischemic preconditioning (IPreC) is a powerful intervention to reduce myocardial ischemic injury in all species studied including human beings. The aim of this study was to investigate whether the protection afforded by IPreC of the human myocardium: (i) is a common phenomenon, and (ii) is influenced by cardiac and systemic clinical conditions and medical treatments.

Material and Methods: Right atrial appendages (n=300) were obtained from patients undergoing elective cardiac surgery prior to cardiopulmonary bypass without exclusion criteria. The muscles were sectioned and stabilized in oxygenated Krebs-Henseleit buffered media for 30min. Samples were then allocated to one of the following groups: Aerobic control (AC); I/R alone, 90min of simulated ischemia followed by 120min of reoxygenation; and IPreC, induced by 5min ischemia/5min reoxygenation prior to the 90min ischemia. LDH leakage was measured in the media to assess cell damage and tetrazolium bromide (MTT) was measured in the muscle to determine viability. LDH and MTT were expressed in AU/g wet tissue.

Results: IPreC significantly decreased LDH and increased the MTT mean values ($p < 0.05$) as compared to I/R alone (e.g. protection) in 52% of all cases. However, IPreC did not influence LDH and

MTT mean values in 26% of cases (e.g. no protection) and induced more damage than I/R alone ($p < 0.05$) in 22% of cases. The myocardium from patients with atrial fibrillation and from those treated with coumadin was less responsive to IPreC than other heart conditions and medical treatments.

Conclusion: These results shows that IPreC induces protection in only half of cardiac surgical cases and the other half could not be protected or even exhibited more damage. The efficacy of IPreC was reduced in the presence of atrial fibrillation and with coumadin treatment, results that may have important clinical implications.

Cardiomyopathies and fibrosis

180 Plakophilin-2 haploinsufficiency leads to impaired canonical Wnt signaling in ARVC patient

A. Khudiakov; D. Kostina; A. Kostareva; A. Malashicheva
Federal Almazov North-West Medical Research Centre, St. Petersburg, Russian Federation

Background: Arrhythmogenic right ventricular cardiomyopathy (ARVC) is a severe inherited disease characterized by adipose and fibrotic substitution of heart muscle. Lack of cardiomyocytes impairs both contractility and conductivity. Mutations of PKP2 gene coding desmosomal protein plakophilin-2 are most common genetic abnormalities associated with ARVC. Molecular pathogenesis of this disease is not completely understood. Abnormal regulation of signalling pathways underlying cellular differentiation is one of the most likely cause for ARVC development.

Purpose: The aim of this study was to investigate whether the canonical Wnt signaling activity is impaired during ARVC patient-derived iPSC cardiac differentiation.

Methods: During genetic screening of ARVC patients the carrier of two mutations in PKP2 gene (frameshift deletion and missense mutation) was identified. iPSC lines were generated from adipose stem cells of ARVC patient and healthy control. Cardiac differentiation of iPSC was initiated by its coculture with END-2 cell line. Levels of desmosomal proteins were measured using immunocytochemistry and western blot analysis. Wnt activity was evaluated during different steps of differentiation using luciferase reporter introduced into iPSC and by accession of Wnt target genes (AXIN2, SOX2, SOX9) expression levels.

Results: Expression of PKP2 and intracellular level of plakophilin-2 during cardiac differentiation of iPSC from ARVC patient was decreased in comparison with control iPSC indicating that PKP2 frameshift deletion leads to haploinsufficiency. In contrast intracellular level of the other desmosomal protein plakoglobin was not affected. Measurements of canonical Wnt activity revealed that Wnt level was significantly reduced during differentiation of iPSC lines from ARVC patient in comparison with control iPSC lines. Intriguingly no plakoglobin nuclear translocation known for ARVC development was observed.

Conclusions: Taken together obtained data indicate that PKP2 haploinsufficiency leads to impaired canonical Wnt signaling activity during iPSC differentiation. In addition we have demonstrated that mechanisms underlying regulation of Wnt activity could be independent on plakoglobin nuclear translocation denote the diverse ways of desmosomal regulation.

181 Improved technique for customized, easier, safer and more reliable transverse aortic arch banding and debanding in mice as a model of pressure overload hypertrophy

JF. Nistal¹; D. Merino²; L. Ruiz¹; J. Gomez¹; C. Juarez¹; A. Gil¹; R. Garcia³; MA. Hurlé³
¹University Hospital Marques de Valdecilla, Santander, Spain; ²Instituto de Investigación Sanitaria Valdecilla IDIVAL, Santander, Spain; ³University of Cantabria, Physiology and Pharmacology, Santander, Spain

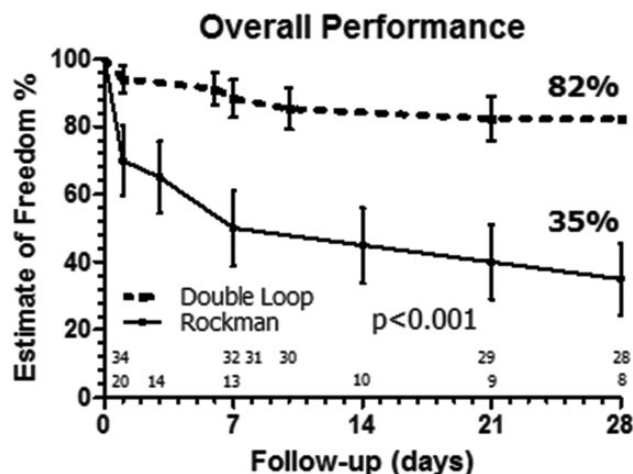
Purpose: Pressure overload LV hypertrophy and its reversion are complex biological phenomena that appear in the natural and treated histories of very prevalent cardiovascular diseases. Several animal models mimic the clinical scenario and most popular is the constriction of the aortic arch in mice according to Rockmañs technique (RT). RT is highly operator-dependent, technically demanding, poorly reproducible, and traumatic for the aorta. We devised a novel technique that provides individualized, fully controlled, reproducible and technically easier constriction of the mid aortic arch with no need for even transient aortic occlusion.

Methods: The banding suture is individually prepared with 2 knots spanned a controlled distance according to echo diameter of arch and desired degree of constriction. These parameters are entered in an algorithm that calculates the inter-knot distance to obtain aimed constriction. Suture is passed twice around the aorta, forming a double loop, and a vascular microclip is applied under both knots to close the banding with the predefined circumference. Basal and weekly echocardiograms (Visual-Sonics Vevo-770) monitor cardiac geometry and function.

Results: We performed aortic constriction with RT (n=20) and the double loop-clip (DLC) (n=34) techniques in C57BL/6 mice. Actuarial analysis proved superiority of DLC technique at 4 wk post-banding follow-up in survival (RT: 65 \pm 11%; DLC: 85 \pm 6%; $p < 0.05$), freedom from aortic gradient < 30 mm Hg in the absence of LV dysfunction (RT: 54 \pm 14%; DLC: 96 \pm 4%; $p < 0.001$), and global efficiency defined as absence of either of the two previous complications (RT: 35 \pm 11%; DLC: 82 \pm 7%; $p < 0.001$, Figure). Debanding 4 wks after constriction (n=30) reduced survival to 84 \pm 4% unchanged for 4 more wks. At debanding, DLC facilitated the procedure thus reducing mortality. Echo data showed post-banding increases of LVM: 31 \pm 4 and 45 \pm 5 % at 1 and 2 wks. LV gene analysis showed overexpression of extracellular matrix and sarcomeric elements.

Conclusions: Our technique provides a consistent, customized aortic constriction with excellent global efficiency. The double loop feature facilitates the surgery, disturbs minimally the aorta and

prevents suture internalization. DLC allows a precise, fully controlled constriction that can be performed by laboratory personnel with basic surgical training.



182

Late sodium current inhibitors for the treatment of inducible obstruction and diastolic dysfunction in hypertrophic cardiomyopathy: a study on human myocardium

C. Ferrantini¹; R. Coppini¹; JM. Pioner¹; F. Gentile¹; L. Mazzoni¹; A. Rossi¹; C. Tesi¹; L. Belardinelli²; I. Olivetto³; E. Cerbai¹; A. Mugelli¹; C. Poggesi¹

¹University of Florence, Interuniversity Center of Molecular Medicine and Applied Biophysics (CIMMBA), Florence, Italy; ²Careggi University Hospital (AOUC), Florence, Italy; ³Gilead Sciences Inc, Foster City, CA, United States of America

Background: Disopyramide, ranolazine and the novel compound GS-967 are late Na⁺-current (INaL) inhibitors with progressively increasing selectivity. Disopyramide is largely employed in hypertrophic cardiomyopathy (HCM) patients as a negative inotropic agent to relieve obstruction. We previously showed that ranolazine reduces electro-mechanical dysfunction in human HCM myocardium. Here, we aim to study the mechanical and electrophysiological properties of INaL-inhibitors in HCM and dissect their potential beneficial effects on diastolic dysfunction, obstruction and arrhythmias.

Methods and Results: Intact trabeculae were dissected from myectomy samples of obstructive HCM patients and used for mechanical measurements; patch-clamp studies and intracellular Ca²⁺ recordings were performed in single myocytes. Disopyramide reduced twitch tension in a dose-dependent manner (EC50: 5.29 ± 1.55 μM) and accelerated contraction kinetics in HCM trabeculae. In myocytes, disopyramide (5 μM) shortened action potential duration (APD), accelerated Ca²⁺ transients and reduced diastolic [Ca²⁺].

GS-967 (1 μM) hastened twitch kinetics and decreased diastolic tension. In single cardiomyocytes, GS-967 shortened APD, reduced arrhythmogenic early after-depolarizations and decreased diastolic [Ca²⁺].

GS-967 (1 μM) and ranolazine (10 μM) lowered isometric twitch tension of HCM trabeculae in the presence of β-adrenergic stimulation (isoproterenol 10-7M), despite the absence of negative inotropic effects at baseline.

Conclusions: (1) Disopyramide, through INaL inhibition, may improve diastolic function and protect against arrhythmias in HCM patients, besides reducing obstruction. (2) The novel selective INaL-inhibitor GS-967 improves the electro-mechanical function of HCM myocardium at 1 μM concentration, matching the effects of 10 μM ranolazine. (3) Selective INaL-inhibitors may reduce septal contractility only at peak exercise, representing a safer option to treat dynamic obstruction compared to disopyramide.

183

Angiotensin II receptor antagonist fimasartan has protective role of left ventricular fibrosis and remodeling in the rat ischemic heart

S-J. Park¹; E. Eun-Ji²; B-K. Lim³; D-J. Choi²

¹Samsung Medical Center, Seoul, Korea Republic of; ²Seoul National University Bundang Hospital, Seongnam, Korea Republic of; ³Kangwon National University Hospital, Chuncheon, Korea Republic of

Backgrounds: The progressive cardiac dysfunction after myocardial infarction (MI) related with left ventricular fibrosis and remodeling.

Objectives: This study investigated whether new angiotensin II receptor antagonist 'Fimasartan' is able to protect in the post-MI progression of left ventricular dysfunction and unknown under lining mechanism.

Methods: MI was induced in SD rats by permanent ligation of the left anterior descending artery (LAD). Treatment with the new angiotensin II receptor antagonist compound 'Fimasartan' (10mg/kg) was initiated 24 hours post-MI and continued for 7 weeks through oral administration. All animals performed baseline echocardiography and then randomly assigned into 3 groups; surgery control (Sham group, n=8), MI without fimasartan treatment (MI group, n=11), and MI with fimasartan treatment (MI+Fima group, n=14), respectively. Results: In histologic finding, infarct size and fibrosis were significantly decreased, and remodeling was attenuated in MI+Fima. Echocardiography was performed in 1 week and 7 weeks post-MI with fimasartan (MI+Fima) or without fimasartan (MI). LV end-systolic and diastolic dimension were significantly increased in MI. Left ventricular function was dramatically preserved in MI+Fima after 7 weeks fimasartan treatment compare with MI (FS, 71.65 ± 1.49% VS 51.77 ± 5.14%, P=0.02). Hemodynamic measurement was performed 3 days after

final echocardiography using Millar catheter system. Hemodynamic study showed higher positive (4526 ± 240 mmHg/sec) and negative dP/dt (-4187 ± 303) in MI+Fima compare with MI (3670 ± 239, -3301 ± 280 mmHg/sec, p<0.05 respectively).

Conclusion: A new ARB, fimasartan, could prevent LV remodeling and development cardiac dysfunction in myocardial infarction rat model. It shows possibility of fimasartan as a clinical treatment option to prevent progression of cardiac dysfunction after MI.

	MI+Fimasartan	MI	P-value
LVEDD, mm	78.4 ± 0.78	82.2 ± 1.26	0.03
LVEDS, mm	53.1 ± 1.10	55.3 ± 1.75	0.04
Fractional shortening, %	71.65 ± 1.49	51.77 ± 5.14	0.02
Ejection fraction, %	69.10 ± 6.99	56.57 ± 6.67	0.01
Positive dP/dt, mmHg/sec	4526 ± 240	-4187 ± 303	0.02
Negative dP/dt, mmHg/sec	3670 ± 239	-3301 ± 280	0.02

184

Role of High-Mobility Group Box 1 (HMGB1) redox state on cardiac fibroblasts activities and heart function after myocardial infarction

S. Di Maggio¹; G. Milano²; M. Bertolotti¹; F. De Marchis³; F. Zollo¹; E. Sommariva²; M. C. Capogrossi⁴; G. Pompilio²; M. E. Bianchi²; A. Raucci¹

¹Cardiology Center Monzino IRCCS, Experimental Cardio-Oncology and Cardiovascular Aging Unit, Milan, Italy; ²Cardiology Center Monzino IRCCS, Vascular Biology and Regenerative Medicine Unit, Milan, Italy; ³San Raffaele Scientific Institute, Division of Genetics and Cell Biology, Milan, Italy; ⁴Dermatologic Institute of the Immacolata (IRCCS), Laboratory of Vascular Pathology, Rome, Italy

Background: HMGB1 is a nuclear factor that when secreted, is able to signal tissue damage. HMGB1 is also implicated in cardiac regeneration and remodeling after myocardial infarction (MI). The extracellular HMGB1 activity depends on its redox state: the fully-reduced-HMGB1 has chemotactic effect while the disulfide-HMGB1 induces cytokines expression.

Purpose: To examine the role of HMGB1 redox isoforms and the non-oxidizable mutant 3S-HMGB1 on human cardiac fibroblasts (hCFBs) functions in vitro and evaluate their effects on cardiac remodeling in vivo.

Methods: The responses to fully-reduced-HMGB1 or 3S-HMGB1 in different conditions were evaluated through Boyden chamber migration. The expression of HMGB1 receptors was evaluated by FACS. Pro-inflammatory cytokines expression was assessed by qRT-PCR. C57BL/6 mice were infarcted using left anterior descending artery ligation and 4 hours after infarction were injected in the peri-infarcted area with vehicle, fully-reduced-HMGB1 or 3S-HMGB1 and euthanized after 4 weeks.

Results: Fully-reduced-HMGB1 and 3S-HMGB1, but not disulfide-HMGB1, were able to induce hCFBs migration and both proteins inhibited hCFBs cell adhesion. Only the 3S-HMGB1 was resistant to oxidation and, indeed, its chemotactic effect was maintained in presence of H₂O₂. hCFBs express CXCR4 but not TLR4 and RAGE. Treatment of cells with AMD3100 abolished migration induced by fully-reduced-HMGB1 but not in response to 3S-HMGB1 suggesting an higher affinity of the 3S mutant for CXCR4. In addition, CXCR4-/- mouse embryonic fibroblasts did not migrate in response to fully-reduced-HMGB1 or 3S-HMGB1. Furthermore, disulfide-HMGB1 or 3S-HMGB1 did not modulate pro-inflammatory cytokines levels. In vivo experiments showed that infarcted mice receiving fully-reduced-HMGB1 exhibited a significant recovery of cardiac function while treatment with 3S-HMGB1 determined an increase in LV dilation and infarct size and a worsening in LV function, compared to the vehicle. Finally, only fully-reduced-HMGB1-treated mice presented a thicker wall of the infarcted area and no sign of cardiomyocytes hypertrophy.

Conclusions: HMGB1-induced migration of hCFBs is CXCR4 dependent, and both fully-reduced and 3S-HMGB1 influence hCFBs activities in vitro. However, the 3S-HMGB1 is also active in oxidizing conditions that may occur soon after MI. Whether this is the reason for the 3S-HMGB1-dependent worsening of the infarcted heart function and adverse remodeling observed in vivo has to be determined.

185

Atrial remodeling in hypertrophic cardiomyopathy: insights from mouse models carrying different mutations in cTnT

F. Gentile¹; JM. Pioner¹; R. Coppini²; B. Scellini¹; J. Tardiff³; C. Tesi¹; C. Poggesi¹; C. Ferrantini¹

¹University of Florence, experimental and clinical medicine, Florence, Italy; ²University of Florence, Department of Neurofarba, Florence, Italy; ³University of Arizona, College of Medicine, Tucson, United States of America

Background: We recently showed that in hypertrophic cardiomyopathy (HCM), genotype is not predictive of onset or severity of atrial myopathy, which rather appears to be driven by hemodynamic determinants, such as diastolic dysfunction and outflow obstruction (Bongini et al. Am J Cardiol 2016). In human and murine HCM ventricular myocardium, primary changes in myofibrillar function, related to the presence of disease-causing mutations in sarcomeric proteins, are often associated with secondary abnormalities due to adverse remodeling of cardiomyocyte EC-coupling (Coppini et al. Circulation 2013).

Methods and Results: Here we characterize the changes in sarcomere function and EC-coupling that occur in the atria of two HCM mouse models carrying different mutations in cTnT, R92Q and E163R. Echocardiography showed LV hypertrophy, diastolic dysfunction and enlarged left atria in both HCM models; atrial dilatation was more pronounced in the R92Q mice. Left atrial trabeculae were dissected and mounted isometrically to record twitch tension. We studied the steady-state force-frequency relationship and the response to positive inotropic stimuli such as Isoproterenol 10-7 mM (ISO) and 8 mM extracellular [Ca²⁺]. Compared to WT, R92Q atrial trabeculae showed: (i) slower kinetics of both force development and relaxation, (ii) impaired twitch amplitude at high pacing rates, (iii) depressed rested-state contractions and (iv) blunted increase of twitch tension in

ISO and high $[Ca^{2+}]_i$. None of these changes were observed in intact E163R atrial trabeculae. Last, we studied the mechanical properties of E163R myofibrils and found that in spite of a significant increase in the rate of the initial isometric slow phase of relaxation, overall relaxation from maximal activation was impaired and prolonged vs WT. The kinetics of force development and maximal tension at saturating Ca^{2+} were instead similar in E163R and WT. Preliminary isometric force and ATPase measurements performed on skinned E163R trabeculae are in line with the results obtained from single myofibrils.

Conclusions: Atrial remodeling in R92Q is more pronounced compared to E163R, and related to E-C coupling alterations. In E163 mice, the mild atrial dilatation detected in vivo is associated with impaired myofibrillar function. These findings suggest that atrial myopathy in HCM can be produced via different pathophysiological mechanisms, depending on the underlying mutation involved.

186

Electrophysiological abnormalities in ventricular cardiomyocytes from a Maine Coon cat with hypertrophic cardiomyopathy: effects of ranolazine

L. Dini¹; L. Mazzoni¹; L. Sartiani¹; R. Coppini¹; L. Diolaiuti¹; P. Ferrari²; E. Cerbai¹; A. Mugelli¹
¹University of Florence, NeuroFarBa, Florence, Italy; ²University of Perugia, Perugia, Italy

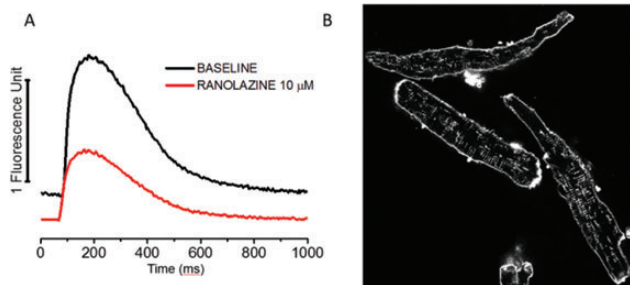
Introduction: Hypertrophic cardiomyopathy (HCM) occurs spontaneously in a number of cat breeds including Maine Coon, with a relatively high prevalence (up to 10% in Maine Coon—Mary et al. J Vet Cardiol. 2010). The typical disease-phenotype of cats with HCM is very similar to that of human patients, and include diastolic dysfunction, atrial dilatation, left-ventricular (LV) outflow obstruction and a high risk of progression towards terminal heart failure -HF- (Maron et al. J Vet Cardiol. 2015). In cats with severe obstruction and HF symptoms, current treatment with β -blockers and diuretics is palliative.

Purpose: We sought to characterize the electrophysiological and EC-coupling changes in cardiomyocytes from a cat with HCM and to test the efficacy of ranolazine as a potential candidate for treatment.

Methods: A Maine Coon cat with HCM and terminal HF symptoms related to severe LV outflow obstruction was euthanized, the heart used to isolate single viable LV cardiomyocytes. Cells were used for patch-clamp measurements, studies of intracellular Ca^{2+} , and confocal imaging of t-tubules.

Results: As compared with previous reports on healthy cat cardiomyocytes (Villa-Abrille et al., J Physiol 2007; Wang et al., Am J Physiol H.C.Ph. 2008), LV cardiomyocytes from the HCM cat showed prolonged action potentials (APs) and Ca-transients (Fig. A). Moreover, they showed a marked disorganization and a reduced density of t-tubules (Fig. B). Ranolazine shortened the duration of APs and Ca-transients, reduced Ca-transient amplitude and diastolic Ca^{2+} (Fig. A).

Conclusions: Abnormalities at cardiomyocyte level are similar to those observed in LV cells from human patients with HCM (Coppini et al., Circulation 2013). Ranolazine is a valid candidate for treatment of cats with symptomatic HCM.



187

ZBTB17 is a novel cardiomyopathy candidate gene and regulates autophagy in the heart

B. Buyandelger¹; C. Mansfield²; P. Luther²; R. Knoell¹

¹Karolinska Institute, Integrated Cardio Metabolic Center, Stockholm, Sweden; ²Imperial College London, National Heart and Lung Institute, London, United Kingdom

Introduction: Mutations mainly in sarcomeric and Z-disc proteins including cysteine and glycine-rich protein 3 (CSR3) have been shown to cause hypertrophic (HCM) and dilated cardiomyopathies (DCM). However, the underlying molecular mechanisms remain not well understood.

Purpose: Here we aim to analyze, in vitro and in vivo, the mechanisms underlying various heart failure phenotypes.

Methods and Results: We used cysteine and glycine-rich protein 3 (CSR3), a known cardiomyopathy gene, in a yeast two-hybrid screen and identified zinc finger and BTB domain containing protein 17 (ZBTB17) as a novel interacting partner. Interestingly, ZBTB17 is a transcription factor that contains the peak association signal (rs10927875) at the replicated 1p36 cardiomyopathy locus. The interaction between CSR3 and ZBTB17 was confirmed by forced yeast two hybrid, co-immunoprecipitations, cross linking and co-localization studies. ZBTB17 expression protected cardiac myocytes from apoptosis in vitro (n=4, p<0.05) and in a mouse model with cardiac myocyte-specific deletion of Zbtb17 (n=6/group, p<0.001), which develops cardiomyopathy and fibrosis after biomechanical stress. ZBTB17 activates various calcineurin and NFAT genes and regulates cardiac myocyte hypertrophy in vitro and in vivo in a calcineurin-dependent manner. In addition, adenoviral overexpression of human ZBTB17 in neonatal rat cardiomyocytes increases expression of autophagic genes and the formation of autophagic vacuoles in vitro. In vivo, transverse aortic constriction (TAC) causes an increase in autophagic gene expression which is attenuated in Zbtb17 deficient animals. Electron microscopy of papillary muscles showed that cKO animals develop less autophagy which points to the necessity of autophagy during biomechanical stress.

Conclusions: ZBTB17 regulates cardiac hypertrophy and cell survival, a recognized dual-property of genes of central importance for cardiac myocyte biology. In addition, ZBTB17 regulates cardiac autophagy and may underlie the locus at 1p36.13.

188

Inhibition of SRSF4 in cardiomyocytes induces left ventricular hypertrophy

J. Larrasa-Alonso¹; M. Villalba¹; F. Sanchez-Cabo¹; MM. Lopez-Olaneta¹; P. Ortiz-Sanchez²; P. Garcia-Pavia²; E. Lara-Pezzi¹

¹National Centre for Cardiovascular Research (CNIC), Madrid, Spain; ²University Hospital Puerta de Hierro Majadahonda, Madrid, Spain

Introduction and Aim: Cardiovascular diseases are the first cause of death worldwide. Incomplete knowledge about their molecular mechanisms precludes the development of effective therapies. Particularly, little is known about Alternative Splicing (AS) regulation in heart disease. Our preliminary data show a decrease in serine/arginine-rich splicing factor 4 (SRSF4) expression in heart failure (HF) patients. The function and targets of this splicing regulator in the heart are completely unknown. For these reasons we investigated the role of SRSF4 in the heart.

Methods and Results: To study the role of SRSF4 in the heart we performed loss of function studies. We crossed SRSF4 conditional knockout mice with Nkx2.5-Cre transgenic mice in order to generate mice that do not express SRSF4 neither in the myocardium nor the endocardium (cKO). Echocardiographic analysis of control and KO mice at different ages from 2 to 14 months showed that cKO mice develop asymmetrical cardiac hypertrophy which is due to an increase in cardiomyocytes area. cKO mice also showed increased expression of the HF markers BNP and β MHC. Histological analysis indicated that cKO hearts do not present fibrosis. To study the molecular mechanism of action of SRSF4 we carried out an RNA-Seq analysis comparing the splicing and gene expression pattern between control and KO mouse hearts. The result showed general changes in genes related with metabolic pathways, transport and cytoskeleton organization.

Conclusion: Our results suggest that the downregulation of SRSF4 is implicated in left ventricular hypertrophy. Increasing our understanding of its molecular mechanism of action could allow the development of new therapeutic approaches against this cardiac pathology.

189

Molecular characterization of a novel cardiomyopathy related desmin frame shift mutation

I. Schirmer; B. Klauke; D. Gerdes; U. Schulz; J. Gummert; H. Milting

Heart and Diabetescenter NRW, University Clinic of the Ruhr-University Bochum, Erich and Hanna Klessmann-Institute for Cardiovascular Research and Development, Bad Oeynhausen, Germany

Introduction: The majority of mutations in the gene DES coding for the intermediate filament (IF) protein desmin causes myopathies and different forms of cardiomyopathies. At present, it is not known why certain DES-mutations cause preferentially cardiomyopathies or skeletal muscle disease, respectively. The minority of desminopathies present as a combined cardiomyopathy with skeletal muscle involvement. Desmin is a highly conserved class III IF protein. Up to now 68 missense and 30 nonsense mutations in DES are listed in the HGMD-database. We recently found a novel frame shift mutation in a patient suffering from a combined skeletal muscle myopathy and cardiomyopathy with right ventricular dilation and AV-block III who was evaluated for heart transplantation (HTx) and had a pedigree with reported sudden cardiac deaths. Currently, the cellular and molecular pathomechanisms of this DES mutation are not known.

Methods: DNA from a patient waiting for HTx was analysed by Illumina panel sequencing. Sequence variants were verified by Sanger sequencing. DES-PCR fragments from the patient's genomic DNA were cloned in pCR2.1-TOPO and transfected in E.coli for the analysis of the non-sense mutation. The cDNAs of wildtype (WT) and mutant desmin were cloned in pEm-GFP. Mutant and WT-desmin were analysed after transfection in HL-1, SW13, C2C12, H9C2 and HEK293 in parallel. Skeletal muscle biopsies were immunostained for desmin.

Results: We identified the novel mutation c.493_520del InsGCGT, p.Q165fs by Illumina-NGS and cloning of the PCR-fragment. The cDNA of this nonsense mutation forms in all cell types analysed so far a severe filament formation defect when compared to the WT. Desmin protein aggregates were also found in the skeletal muscle biopsy. As a consequence the analysis of the isolated recombinant protein is in progress.

Conclusion: In vitro analysis of the novel DES-mutation c.493_520del InsGCGT, p.Q165fs reveals a severe filament formation defect. These in vitro findings were supported by immunostaining of the skeletal muscle biopsy. Thus, this mutation is disease causing and leads to a late onset arrhythmogenic cardiomyopathy with right ventricular dilatation.

190

Autonomic characterisation of electro-mechanical remodeling in an in-vitro leporine model of heart failure

SH. Chin; E. Wake; G. Kocsis-Fodor; KE. Brack; GA. Ng

University of Leicester, Cardiovascular Sciences, Leicester, United Kingdom

Background: Sympathetic (SS) and vagus (VS) nerve stimulation exert positive and negative responses in heart rate (HR) respectively. They modulate ventricular fibrillation threshold (VFT), a marker of ventricular arrhythmia vulnerability. SS reduces VFT whilst VS raises VFT. Sympathetic overdrive, parasympathetic attenuation and left ventricular (LV) impairment are cardinal clinical features in heart failure (HF).

Purpose: To assess 1) the effect of SS and VS on HR and VFT; 2) LV size and function in a coronary ligation HF model.

Methods: Coronary ligation (HF; n=13) and sham (SHM; n=12) surgeries were performed on NZW rabbits. After 8 weeks of recovery, transthoracic echocardiography was performed to measure LV ejection fraction (EF), end-systolic (ESV) and end-diastolic (EDV) volumes. Hearts were procured for dual-innervated Langendorff perfusion, and for spinal cord stimulation at the stellate ganglia (SS) and the right cervical vagus nerve (VS). HR was examined from 0-20Hz. VFT, defined as the

minimum current inducing sustained VF by burst pacing, was assessed at nerve frequencies for equivalent HR responses (SS: INF-9Hz; SHM-8Hz / VS: INF-11Hz; SHM-8Hz). Data are mean \pm SEM, * P <0.05 taken as significant.

Results: In HF, vagal bradycardia (HF-VS) was attenuated whilst sympathetic tachycardia (HF-SS) was exaggerated at high frequencies (Fig 1A). VFT were lower in HF despite VS (Fig 1B). LV EF (28.8 ± 1.3 [HF] vs. 53.6 ± 2.4 [SHM]) was lower and ESV (546.7 ± 58.3 [HF] vs. 372.0 ± 47.6 μ L[SHM]) was greater in HF.

Conclusions: Infarct model of HF in rabbits leads to adverse electro-mechanical remodeling and abnormal autonomic phenotype characterized by exaggerated SS and attenuated VS responses at atrial and ventricular level, thereby providing arrhythmic substrates in HF.

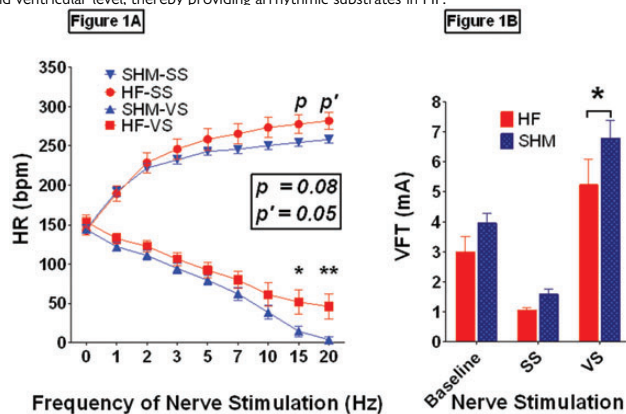


Fig 1

191

Modulation of Ca²⁺-regulatory function by three novel mutations in TNNI3 associated with severe infant restrictive cardiomyopathy

D. Cimiotti¹; A. Kostareva²; N. Smolina²; M. Majchrzak¹; D. Moehner³; A. Wies³; H. Milting⁴; R. Stehle³; G. Pfitzer³; A. Muegge¹; K. Jaquet¹

¹University Hospital St. Josef, Molecular Cardiology, Bochum, Germany; ²Karolinska Institute, Department of Women's and Children's Health, Stockholm, Sweden; ³University of Cologne, Institute of Vegetative Physiology, Cologne, Germany; ⁴Heart and Diabetes Center NRW, Erich & Hanna Klessmann Institute, Bad Oeynhausen, Germany

Restrictive cardiomyopathy (RCM) - a rare heart muscle disease defined by impaired relaxation and increased myocardial stiffness - is often caused by mutations in the gene encoding for cardiac troponin I (cTnI). The phenotype of these mutations is probably determined by altered Ca²⁺-regulation of contraction. Interfilament protein interactions are pivotal for the function of the sarcomere and the Ca²⁺-dependent regulation of contraction. Therefore this work focused on interactions between proteins of the thin filament including the N-terminal fragment of myosin binding protein C (MyBP-C C0-C2). Three novel mutations within cTnI (D127Y, R170G and R170W) were recently identified in infant patients with severe RCM. D127 is located near the inhibitory region within the IT arm of cTnI and R170 in the C-terminal domain that modulates the function of the inhibitory region and binds to actin in a Ca²⁺-dependent manner.

All three mutations resulted in altered interactions of thin filament proteins. In cosedimentation assays, binding of cTnI to reconstituted thin filaments was significantly decreased for R170W compared to wildtype (WT), and the interaction of R170W with actin was disturbed, as measured via SPR spectroscopy. In contrast, D127Y and R170G showed a stronger binding to actin compared to WT. Additionally, the affinity towards tropomyosin was highly increased for all three cTnI-mutants. While D127Y did not affect actin-myosin S1 ATPase activity, R170G and R170W caused a strong Ca²⁺-desensitization, a very new finding for RCM causing mutants. In presence of MyBP-C C0-C2, however, actin-myosin S1 ATPase activity of R170G/W was restored to WT levels. Interestingly, all three mutants showed a significant Ca²⁺-sensitization of force generation of skinned cardiac fibres from guinea pigs, which is again in good agreement with the RCM phenotype.

The fact that MyBP-C abolished the Ca²⁺-desensitizing effect of R170G/W demonstrates a direct impact of protein interactions beyond the thin filament for the pathogenesis of cTnI mutants. Other protein interactions within the sarcomere could as well be altered by these mutations, resulting in an overall Ca²⁺-sensitized phenotype. Thus, early childhood RCM could conceivably be defined rather by altered protein interactions and resulting structural perturbances within the sarcomere, than solely by cTnI-induced changes in Ca²⁺-sensitivity.

Our findings underline the relevance of protein interactions within the sarcomere for the development of RCM and deepen our understanding of the function of the cardiac contractile machinery.

Aging

194

The aging impact on cardiac mesenchymal like stromal cells (S+P+)

H. Martini; D. Maggiorani; L. Lefevre; M. Dutaour; J. Miallet-Perez; A. Parini; D. Cussac; V. Douin-Echinard

Institute of Cardiovascular and Metabolic Diseases, Toulouse, France

Ageing is associated with progressive modifications of heart structure and functions, and is a dominant risk factor for developing cardiovascular diseases. In general, the accumulation of senescent cells within a tissue is thought to drive age-related organ dysfunction. Concerning the heart, it has been recently

shown that cardiomyocytes biology and function are altered during ageing. In addition to cardiomyocytes, the heart contains mesenchymal-like stromal cells (S+P+) that participate in regulation of cardiac homeostasis through the differentiation into vascular cells and their paracrine activity. In the present study, we investigated the effects of ageing on the phenotype and function of cardiac mesenchymal-like stromal cells (S+P+). Cardiac mesenchymal-like stromal cells (S+P+) from young (3 months) and old (20 months) C57Bl/6 mice were isolated by enzymatic digestion of hearts and sorted by flow cytometry based on sca-1+ PDGFR α + co-expression and the lack of endothelial (CD31-) and hematopoietic (CD45-) markers. During physiological ageing, S+P+ cell population acquired a senescence associated secretory phenotype (SASP) characterized by increased gene expression of inflammatory mediators (Ccl2), growth factors (Igf1) and pro-angiogenic factors (Vegfa). In addition, we demonstrated, by immunofluorescence and gene expression analysis, that ageing modified the differentiation pathways of S+P+ cells with decreased endothelial and increased smooth muscle cell differentiation potentials. These modifications were associated with specific modulations of cell cycle-related senescence program (p15, p16, p18). To understand how oxidative damages could trigger a senescence program in S+P+ cells, we used a transgenic mice model with specific cardiomyocyte expression of the hydrogen peroxide producing enzyme MonoAmine Oxidase A. Gene expression and flow cytometry phenotype analyses showed that, in these mice, S+P+ cells underwent a senescent program and phenotype modifications similar to those observed in aged animals. These results suggest that oxidative stress may be one of the factors inducing senescence of S+P+ cardiac stromal cells. In conclusion, our results show that ageing induces significant changes in lineage and secretory properties of S+P+ cells that could play a role in age-associated cardiac dysfunction.

195

Reversal of premature aging markers after bariatric surgery

P.J. Hohensinner¹; B. Ebenbauer¹; C. Kaun¹; M. Prager²; J. Wojta¹; G. Rega-Kaun¹

¹Medical University of Vienna, Cardiology, Vienna, Austria; ²Hietzing Hospital, Vienna, Austria

Background: Obesity is considered to be a major risk factor in developing cardiac disease. In addition, obese patients suffer from a premature aging phenotype including increased secretion of senescence associated secretory proteins (SASP) and reduced telomere length compared to healthy controls.

Purpose: The aim of our study was to determine, if bariatric surgery and the resulting weight loss could reverse the previously observed premature aging phenotype.

Methods: We enrolled 76 patients undergoing bariatric surgery. Blood samples were taken before and 12 months after surgery. Markers of premature aging including the SASP IL6 and PAI-1 as well as telomere length and telomere oxidation were evaluated.

Results: Overall, patients showed a significant drop of body mass index (44.5 ± 4.2 before surgery versus 27.5 ± 3.6 after surgery, $p < 0.001$). In addition plasma levels for IL6 (3.1 ± 2.4 pg/ml before versus 1.7 ± 1.5 pg/ml after bariatric surgery, $p < 0.001$) and PAI-1 (98.4 ± 17.2 ng/ml before versus 83.8 ± 27.1 ng/ml after bariatric surgery, $p < 0.001$) were significantly reduced after surgery. Telomere length on average increased by 58% in the patient cohort (0.37 ± 0.28 a.u. before versus 0.59 ± 0.28 a.u. after bariatric surgery, $p < 0.001$). The telomere increase was accompanied by a reduction in the telomere oxidation index (2.86 ± 4.4 before versus 0.78 ± 0.56 after bariatric surgery, $p < 0.001$) indicating reduced oxidative stress for the telomeric region. This is further supported by an inverse correlation of telomere length with telomere oxidation at both time points ($r = -0.376$, $p < 0.001$ pre surgery and $r = -0.705$, $p < 0.001$ post surgery).

Conclusion: Our data indicate a significant reduction of the SASP IL6 and PAI-1 in plasma 12 months after bariatric surgery. In addition we observed an increase in telomere length in this setting. However, given the reduction in oxidative stress at telomeric regions we speculate that the increased telomere length is not due to active elongation but due to reduced breakage caused by telomere oxidation. Overall, bariatric surgery ameliorated the premature aging phenotype of previously morbidly obese patients.

196

Sex-associated differences in vascular remodeling during aging: role of renin-angiotensin system

M. Garabito¹; G. Costa¹; Y. Onetti²; F. Jimenez-Altayo²; E. Vila²; A. P. Dantas¹

¹Institute of Biomedical Research August Pi Sunyer (IDIBAPS), Cardiology, Barcelona, Spain; ²Autonomous University of Barcelona, Pharmacology, Barcelona, Spain

Background and Objectives: Aging is a cardiovascular risk factor associated to an increase of reactive oxygen species (ROS) and Renin-Angiotensin System (RAS) activation, which in turn contributes to vascular and remodeling. Both systems are known to be influenced by sex. Our study aims to determine whether sex-associated differences in ROS and RAS contribute to a differential regulation of vascular aging and associated dysfunction.

Methods: Male and female outbred CD-1 mouse were studied at 3, 7 and 12 months of age (M). To determine the contribution of RAS, mice were treated from 3 to 12 months with AT1 antagonist Losartan (0.6 mg/L in the drinking water). Morphometric analysis of aortas was performed by Haematoxylin-eosin staining. Oxidative stress was determined in aortic cross sections by dihydroethidium (DHE), treated with Apocynin (100 μ M), Losartan (10 μ M) and TNF α blocker, R-7050 (50 μ M). Signaling pathways involved in sex-associated differences in vascular remodeling was determined by quantitative PCR array.

Results: Aging triggers outward hypertrophy of aorta [Wall Thickness (μ m)]: 3M (Male: 54.5 ± 4.9 vs Female 47.0 ± 7.3); 12M (Male 101.4 ± 4.3 vs Female 100.3 ± 3.4); $P < 0.001$], which appears at earlier age (7M) in males (93.1 ± 2.5) than in females (78.6 ± 3.1), $P < 0.05$. Losartan treatment prevented hypertrophy in both males and females ($P < 0.001$). Aging-associated increase of ROS follows same chronology as vascular hypertrophy [DHE Fluorescence (%): 3mo (Male 35.3 ± 8.7 vs Female 30.5 ± 5.0); 7 M (Male 58.7 ± 3.3 vs Female 31.6 ± 5.5); 12M (Male 72.69 ± 2.6 vs Female 69.1 ± 4.3); $P < 0.001$]. Chronic treatment with losartan decreases ROS generation in 12M males, but not in 12M females. ROS generation in 12 M female ($P < 0.01$) and in 7 M and 12 M males ($P < 0.01$) was diminished by Apocynin. When TNF α was inhibited by R-7050, ROS generation was markedly decreased in aortas from 7M males. qPCR array revealed a contribution of PI3K/AKT/mTOR pathway to vascular remodeling, which are differentially regulate in male and females. Although Akt1 and Akt2 expression were markedly (> 10 -fold increase) increase in both aged male and females ($P < 0.001$), expression of PTEN (inhibitor of PI3K/Akt phosphorylation) was increased (> 6

fold-increase) only in females. Losartan treatment increases PTEN expression in 12M males, but does not modify the expression in females.

Conclusion: Aging induces outward hypertrophy in a different time-course in males and females. Although RAS plays a critical role in the aging-associated hypertrophy in both sexes, there is a sexual dimorphism in the signaling pathways activated by RAS during aging.

197

Role of the receptor for advanced glycation end-products (RAGE) in age dependent left ventricle dysfunctions

F. Zeni¹; G. Milano²; M. Bertolotti¹; A. Scopece²; L. Piacentini³; ME. Bianchi⁴; MC. Capogrossi⁵; G. Pompilio²; G. Colombo²; A. Raucci¹

¹Cardiology Center Monzino IRCCS, Experimental Cardio-Oncology and Cardiovascular Aging Unit, Milan, Italy; ²Cardiology Center Monzino IRCCS, Vascular Biology and Regenerative Medicine Unit, Milan, Italy; ³Cardiology Center Monzino IRCCS, Immunology and Functional Genomics Unit, Milan, Italy; ⁴San Raffaele Scientific Institute, Chromatin Dynamics Unit, Milan, Italy; ⁵Dermopatic Institute of the Immacolata (IRCCS), Laboratory of Vascular Pathology, Rome, Italy

Background: Aging is the major risk factor for cardiovascular (CV) diseases: on one hand, it prolongs exposure to other CV risks, on the other, intrinsic cardiac aging predisposes the heart to stress and increases mortality and morbidity in the elderly. The Receptor for Advanced Glycation End-Products (RAGE) is a multi-ligand receptor involved in many age-related disorders. Nevertheless, its role in intrinsic cardiac aging remains unexploited.

Purpose: To evaluate the role of RAGE in cardiac aging.

Methods: We compared 2 groups of female Rage-/- and C57BL/6 (wt) mice of different ages: 2.5- (Young) and 12-month (1 Year) old mice. Left ventricular (LV) parameters and function were evaluated by 2-D transthoracic echocardiography. Fibrosis was assessed by evaluating collagen I deposition on heart sections. Phosphorylation of AKT and GSK-3 β was determined on LV protein extracts. Microarray gene expression analysis was performed on RNAs from LV.

Results: Hearts of Rage-/- mice exhibited an increase in LV/tibia length ratio already at 2.5 months of age compared to age-matched wt mice, and this was accompanied with a slight but not significant increase of EDV and ESV (End-Diastolic and End-Systolic Volume) or EDD and ESD (End-Diastolic and End-Systolic Diameter). At 1 year of age, Rage-/- mice showed a further significant increase of EDV and ESV or EDD and ESD along with a reduction in the ejection fraction (EF) and fractional shortening (FS). In contrast, no significant differences were observed in the LV wall thickness between wt and Rage-/- mice at any age. Expression of heart failure marker genes (BNP, β -MHC and Ankrd1) did not differ between Young wt and Rage-/- mice, but was induced in the 1 Year Rage-/- group.

Compared with wt mice, 12-month old Rage-/- mice exhibited an increase in perivascular and interstitial fibrosis, and consistently a higher expression of TGF- β 2 and TGF- β 3 transcripts and activation of AKT, GSK-3 β phosphorylation, known to regulate cardiac fibrosis, increased with age in wt mice, but was already induced at high levels in Young Rage-/- mice.

Microarray functional annotation analysis based on the interaction between age-genotype revealed that the chronic lack of RAGE affected the expression of genes associated to heart development, contractile fiber function, antigen presenting process and adaptive immunity, insulin pathway, cell death and apoptosis.

Conclusions: Our results suggest that the absence of RAGE causes gene expression changes leading to age-dependent LV dilatation, fibrosis and heart failure.

Genetics and epigenetics

200

hsa-miR-21-5p as a key factor in aortic remodeling during aneurysm formation

S. Licholai; M. Blaz; B. Kapelak; M. Sanak
Jagiellonian University Medical College, Krakow, Poland

Introduction: Genetic background of TAA seems complex and has not been elucidated, which may suggest a role of epigenetic mechanisms in its pathogenesis. One of the most important epigenetic regulators of molecular pathways is microRNA. Unbiased molecular screening of microRNA expression revealed significant overexpression of hsa-miR-21-5p in human aneurysmal tissue. However, the precise mechanism of its contribution to TAA pathogenesis is unclear.

Aims: The aim of this study was to explain the mechanism in which has-miR-21-5p participate in pathogenesis of thoracic aortic aneurysms.

Materials and Methods: Screening phase of the study was based on RNA samples isolated from ascending aortic tissue (paired aneurysmal and healthy one) obtained from 15 patients during reparative surgery. We focused on hsa-miR-21 because this was the most upregulated one in the aneurysmal tissue. Using bioinformatic tools and literature search we selected endothelial nitric oxide synthase gene (NOS3 gene) as putatively regulated by this microRNA. Human endothelial cell cultures and transfection with miR-21-5p mimic and miR-21-5p inhibitor respectively was used to confirm the role of has-miR-21-5p and NOS3 in aortic aneurysm formation.

Results: hsa-miR-21-5p was overexpressed in aneurysmal tissue compared to the healthy one (RQ=2.6632, p=0.025). Average fold change for hsa-miR-21-5p in endothelial cells transfected with miR-21-5p mimic was 5.52 compared to the mock-transfected cells. Among cells transfected with miR-21-5p mimic RQ for NOS3 gene was 3.88, whereas in cells incubated with miR-21-5p inhibitor RQ was 0.28. In addition, there were statistically important correlations between hsa-miR-21-5p level and expression of NOS3 in endothelial cells transfected with miRNA mimic.

Conclusions: The role of NOS3 was studied in a mouse model of aortic aneurysm and increased expression of NOS3 was also documented in human TAA. hsa-miR-21-5p was up-regulated in aneurysmal tissue and it acts indirectly by phosphorylation of NOS3 augmenting nitric oxide (NO) production. NO is the major mediator causing relaxation of VSMC and delimited production of nitric oxide within the aneurysm may mechanically explain aneurysm progression. In our study, NOS3 transcripts paralleled miR-21 in TAA tissue. Thus, miR-21 could be a molecule perpetuating NOS3 overexpression within aneurysm and causing the progression of the disease. Specificity of this miR-21 effect we confirmed experimentally using miR-21 mimic or antagonist introduced to the endothelial cell line.

201

Co-inheritance of mutations associated with arrhythmogenic and hypertrophic cardiomyopathy in two Italian families

M. De Bortoli¹; B. Bauce²; C. Calore²; A. Lorenzon¹; M. Calore¹; G. Poloni¹; E. Mazzotti²; I. Rigato²; L. Daliento²; C. Basso²; G. Thiene²; P. Melacini²; D. Corrado²; A. Rampazzo¹

¹University of Padua, Department of Biology, Padua, Italy; ²University of Padova, Department of Cardiac, Thoracic and Vascular Sciences, Padua, Italy

Background: Arrhythmogenic cardiomyopathy (ACM) and hypertrophic cardiomyopathy (HCM) are genetically and phenotypically distinct diseases of the myocardium, showing an autosomal-dominant inheritance with incomplete penetrance and variable expressivity. These cardiomyopathies are the most common causes of sudden cardiac death in the young and athletes.

Purpose: To evaluate in 2 Italian families the effect of digenic inheritance of ACM and HCM mutations on the disease manifestation and the progressive clinical changes.

Methods: ACM probands of two families (A and B) were screened for mutations in 6 ACM genes (PKP2, DSP, DSG2, DSC2, JUP and CTNNA3) and 2 HCM patients, one for each family, were screened for mutations in the 2 major HCM genes (MYH7 and MYBPC3). Genetic analysis was carried out by denaturing high-performance liquid chromatography and direct sequencing. A comprehensive pedigree analysis, including both clinical evaluation and genotyping, was performed in all available family members.

Results: In family A, 5 patients resulted to be double heterozygotes for a missense mutation (p.Met1601Ile) in DSP gene and a frameshift mutation (p.F305Pfs*27) in MYBPC3 gene. In family B, the genetic analysis has identified 1 patient carrying an in frame deletion (p.del765L) in CTTNA3 gene and a missense mutation (p.Met877Ile) in MYH7 gene; in addition, 5 single ACM and 7 single HCM mutation carriers were found. Clinical evaluation of the 6 double heterozygotes has revealed a phenotypic heterogeneity with 1 asymptomatic case, 3 patients affected with ACM, 1 with HCM and 1 showing both phenotypes. In this latter subject the ECG was normal, whereas at the echocardiogram a LV asymmetric hypertrophy and a regional RV akinesia were found, with minor dysfunction and structural alterations of right ventricle, late potentials and a left ventricular wall thickness of 19 mm.

Conclusions: This is the first study reporting patients with co-inheritance of ACM and HCM mutations. The genotype-phenotype correlation in these rare patients indicates that such digenic inheritance is associated with heterogeneous phenotypes, probably due to the incomplete penetrance and variable expressivity of both mutations.

202

Lamin A/c hot spot codon 190: form various amino acid substitutions to clinical effects

L. Sivitskaya¹; NG. Danilenko¹; TG. Vaikhanskaya²; OG. Davydenko¹

¹Institute of Genetics and Cytology of NAS, Minsk, Belarus; ²Republican Scientific and Practical Centre of Cardiology, Minsk, Belarus

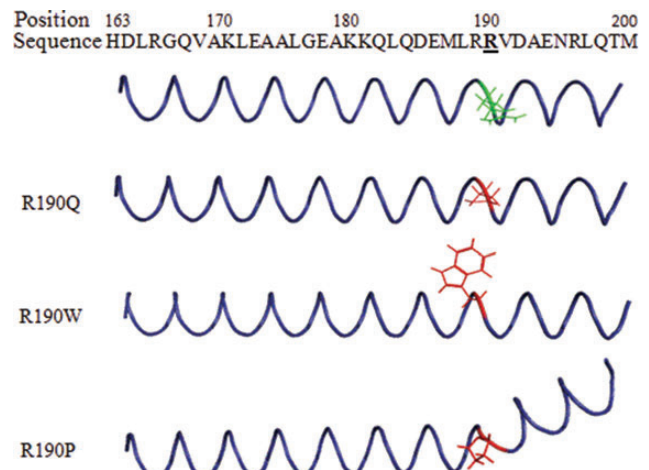
In 2014 we described novel missense mutation R190P (c.569G>C) in lamin A/C gene (LMNA) in patient with dilatation cardiomyopathy (DCM) and conduction diseases (CD). Codon 190 is the most prevalent LMNA mutation hot spot in DCM in Europe. Amino acid replacements R190Q and R190W were identified in patients from several European countries as well as from Korea and China.

We present a comparative analysis of R190Q, R190W and R190P mutations to evaluate the contribution to various amino acid substitutions in disease manifestation.

The codon 190 locates in the protein α -helical rod-domain that forms a simple dimeric coiled coil (CC). CC is one of the principal subunit oligomerization motives in protein. Proline intercalation in position 190 of lamin A/C would curve α -helix (Figure) and prevent the CC formation. The on-line predictor showed the lowest probability for R190P to form a regular CC. We propose it can reflect in earlier and sudden DCM-CD manifestation (Table). The R190P carrier showed subclinical skeletal muscle involvement: mild quadriceps muscles hypotrophy, calf muscles hypertrophy, high creatine phosphokinase (CPK) level. The highest ratings were given to R190P mutation as genetic factor associated with disease by on-line predictor.

The R190Q and R190W don't kink α -helical domain, but their side chains can disturb CC assembly. The carriers have later age of disease onset and no skeletal muscle involvement. Asymptomatic carriage of these mutations suggests additional factors of disease manifestation. The mutation effects might be modified by the general genetic background.

We conclude the R190P is the most critical for lamin A/C structure and leads to earlier and sudden DCM-CD phenotype.



Lamin A/C α -helical rod-domain fragment

Characteristics of LMNA mutations

Mutation	R190Q	R190W	R190P
No. of reports	2	6	1
Origin	Sporadic	Familial	Sporadic
Age at onset	42, 45	30-43, 58	24
Cardiac involvement	DCM-CD, AVB, AF/Br	DCM without CD or DCM-CD, AF	DCM-CD, AVB, AF, CHB
Skeletal muscle involvement	No	No	Yes
CPK, U/l	-	Normal (24-190)	High (276)
Asymptomatic carriers	Yes (under 35-40)	Yes	No
Disease predictor:	Disease associated	Disease associated	Disease associated
- Reliability index 0-10	4-9	7-9	8-10
- Probability, score 0-1	0.67-0.95	0.85-0.96	0.88-0.98
Coiled coil predictor	Probability 50-90%	Probability 50-90%	Probability less than 50%

AF-atrial fibrillation, Br-bradycardia, CHB-complete heart block

203

Treatment with aspirin and atorvastatin attenuate cardiac injury induced by rat chest irradiation: Implication of myocardial miR-1, miR-21, connexin-43 and PKC

C. Viczenczova¹; B. Szeifova Bacova¹; B. Kura¹; T. Egan Benova¹; CH. Yin²; R. Kukreja²; J. Slezak¹; N. Tribulova¹

¹Slovak Academy of Sciences, Institute for Heart Research, Bratislava, Slovak Republic; ²Virginia Commonwealth University, Richmond, United States of America

Background and Aim: Radiation therapy on the chest is associated with heart injury. Intercellular connexin-43 (Cx43) channels mediated communication and extracellular matrix homeostasis might be affected. We aimed to explore whether miRNA-1 which regulates GJA1 gene transcription for Cx43 and miR-21 that regulates expression of extracellular matrix proteins are altered in response to irradiation. Effect of anti-inflammatory treatment with aspirin and atorvastatin was examined as well.

Methods: Adult, male Wistar rats subjected to single dosage radiation on mediastinum at 25 Gy and non-irradiated were used. Both groups were treated during six weeks with aspirin (3 mg/day) or atorvastatin (0.25 mg/day) and compared to untreated rats. Left ventricular tissue was taken at the end of experiment for western blot and real-time PCR analysis. Expression of PKC-epsilon, which phosphorylates Cx43 and pro-hypertrophic/pro-apoptotic PKC-delta was also determined.

Key Results: Neither heart nor left ventricular weights were affected. Expression of miR-1 was decreased while miR-21 was increased due to irradiation. Aspirin prevented post-irradiation decline of myocardial miR-1 but did not affect an increase of miR-21. In contrast, atorvastatin did not affect decline of miR-1 but prevented post-irradiation elevation of myocardial miR-21. Interestingly, both aspirin and atorvastatin prevented irradiation-induced up-regulation of myocardial Cx43 protein. PKC-epsilon and PKC-delta expression was increased post-irradiated rat hearts and not affected by treatments.

Conclusion: Findings suggest implication of miR-1 and miR-21 in adaptive response to chest irradiation-induced cardiac injury and prophylactic effect of treatment.

Genomics, proteomics, metabolomics, lipidomics and glycomics

206

Differential phosphorylation of desmin at serines 27 and 31 drives the accumulation of preamyloid oligomers in heart failure

PP. Rainer¹; DI. Lee²; M. Sorge³; C. Glabe⁴; N. Paolucci²; C. Guarnieri³; GF. Tomaselli²; DA. Kass²; JE. Van Eyk²; G. Agnetti²

¹Medical University of Graz, Department of Cardiology, Graz, Austria; ²Johns Hopkins University School of Medicine, Johns Hopkins Hospital, Baltimore, United States of America; ³University of Bologna, DIBINEM, Bologna, Italy; ⁴University of California at Irvine, Irvine, United States of America; ⁵Cedars-Sinai Medical Center, Los Angeles, United States of America

Background: Heart Failure (HF) is one of the main causes of morbidity and mortality. The formation of preamyloid oligomers (PAOs), similar to those observed in Alzheimer's disease, has been reported in several models of HF. We first demonstrated that the induction of desmin phosphorylation at serines (S) 27 and 31 associate with increased cardiac PAO deposition in experimental, non-genetic HF. We now show that modified desmin is a likely candidate for the seed initiating the nucleation of toxic PAOs in the heart and isolated cardiac cells.

Methods: mice were subjected to transverse aortic constriction (TAC) for 4 weeks (FS%=29.3 ± 2.6, P=0.0001 vs. shams) and neonatal rat ventricular myocytes (NRVMs) transduced using lentiviral vectors carrying alanine (A) or phospho-mimetic aspartate (D) desmin double mutants at S27 and S31, fused to GFP. We analyzed the formation of PAOs in cardiac protein extracts by western blot analysis combined with infrared detection, which enables the contemporary measurement of PAOs and desmin; in addition, we monitored the effects of phospho-mimetic desmin expression in NRVMs by live imaging.

Results: Co-staining for PAOs and desmin in TAC mice and NRVMs confirmed the co-migration of PAOs with modified (by molecular weight) desmin along with an increased expression in

experimental HF (≈3-fold, P=0.023 and ≈2-fold, P=0.038, respectively). Cells expressing the double phospho-mimetic mutant, which we hypothesize is the physiological form, displayed a "healthier" phenotype as documented by the number of contracting cells (P=0.041) and localization of GFP-desmin at the Z-bands (P=0.003). On the contrary, the expression of mono-phospho-mimetic mutants (S27A, S31D) induced increased desmin aggregation (P=0.001).

Conclusions: These data suggest that modified desmins constitute the seed initiating the formation of cardiac PAOs, in non-genetic HF. The increased levels of toxic desmin PAOs in the heart could therefore represent a novel and universal mechanism of organ dysfunction in HF.

207

Potential role of kinase Akt2 in the reduced recovery of type 2 diabetic hearts subjected to ischemia / reperfusion injury

LE. Smith; SJ. Cordwell; MY. White
University of Sydney, Sydney Medical School, Sydney, Australia

Despite improved recovery following cardiovascular events such as acute myocardial infarction (AMI) in the general population, those with comorbidities including Type 2 diabetes (T2D) continue to have poorer outcomes. The molecular mechanisms that underlie this reduced recovery are largely unknown. Large-scale investigation into vital phosphorylation mediated signaling cascades, as is undertaken in this study, may uncover key mediators of molecular recovery that are inefficient in T2D that contribute to the reduced function recovery observed following AMI.

Sprague Dawley rats were fed either CHOW (CH) (12% fat) or high fat (HF) (42% fat) diet for 4 weeks prior to a low dose of the pancreatic β-cell toxin, Streptozocin (STZ; 35mg/kg) to induce T2D in half the population for a further 4 weeks. Upon completion of the 8-week protocol, hearts were excised and subject to ex vivo retrograde perfusion to replicate global ischemia / reperfusion (I/R) injury (30I/30R). Myocardial peptides were isobarically labelled prior to phosphopeptide enrichment utilising titanium dioxide coupled with immobilised metal ion affinity chromatography followed by tandem mass spectrometry analysis.

Significantly impaired functional recovery post-I/R was observed in HF T2D hearts compared with CH control, 6.91 ± 2.42% and 32.68 ± 4.98% respectively as measured by rate pressure product. Following phosphoproteomic processing 11,803 unique phosphosites were identified, 6,432 of which were significantly regulated (z-score cutoff > +1 or < -1, where z-score is defined as the number of standard deviations from mean). Analysis of activated kinases revealed a role for Akt2 in the reduced recovery of HF T2D hearts following I/R. Reduced phosphorylation of Akt2 Ser474 when compared with CH control hearts was observed during I/R (log2ratio; -0.58, z-score; -2.00) implicating reduced activation of this vital survival kinase. Analysis of downstream targets revealed reduced phosphorylation of Tsc2 Ser939 (log2ratio; -0.36, z-score; -1.42), a site involved in mTORC inhibition, implicating a potential for increased flux through the mTOR signalling pathway. This is further supported by the reduced phosphorylation of Rheb Ser130 (log2ratio; -0.70, z-score; -2.29), this site is associated with the vital suppression of mTOR signaling during times of reduced energy, such as I/R. Together this data provides evidence for the reduced inhibition of the mTOR signalling pathway during I/R in HF T2D hearts via Akt2 regulation, providing one possible molecular mechanism behind the impaired functional recovery observed in T2D following AMI.

208

A proteomics comparison of extracellular matrix remodelling in porcine coronary arteries upon stent implantation

G. Suna¹; W. Wojakowski²; M. Lynch¹; J. Barallobre-Barreiro¹; X. Yin¹; U. Mayr¹; S. White³; M. Jahning⁴; J. Hill⁵; M. Mayr⁶

¹King's College London, London, United Kingdom; ²Medical University of Silesia, Third Division of Cardiology, Katowice, Poland; ³Bristol Heart Institute, Bristol, United Kingdom; ⁴St George's Healthcare NHS Trust, St. George's Vascular Institute, London, United Kingdom; ⁵King's College Hospital, King's Health Partners Academic Health Sciences, London, United Kingdom; ⁶King's College London, Cardiovascular Department, London, United Kingdom

Background: Extracellular matrix (ECM) remodelling related to arterial injury and healing after stenting contributes to both, in-stent restenosis and thrombosis. Despite its important clinical implications little is known about ECM changes post-stent implantation.

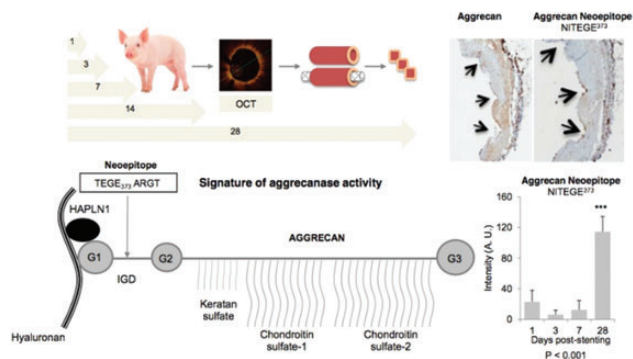
Objectives: To obtain temporal profiles of ECM changes following implantation of bare-metal (BMS) and drug-eluting stents (DES).

Methods: BMS and DES were implanted in pig coronary arteries with an overstretch under optical coherence tomography guidance. Stented segments were harvested 1, 3, 7, 14 and 28 days post-stenting for comparative proteomics analysis of the media and neointima.

Results: A total of 151 ECM and ECM-associated proteins were identified by mass spectrometry. The composition of the neointimal ECM was more diverse than of the media. Proteins involved in regulating calcification were upregulated in the neointima of DES. Within the first week after stent implantation the predominant changes in the media were proteins involved in inflammation and thrombosis. Thereafter, significant changes in regulatory ECM proteins such as small leucine rich proteins or matricellular proteins were observed. By day 28, basement membrane proteins as markers of cellularity were reduced in DES compared with BMS. In contrast, the large aggregating proteoglycan aggrecan was increased. Aggrecan belongs to the lectican protein family and acts as linker of ECM molecules. Aggrecan levels were markedly increased in human arteries compared to veins and aggrecan expression was induced upon grafting a vein into the arterial circulation. The presence of aggrecan and aggrecan cleavage products was confirmed by immunohistochemistry in stented human coronary arteries.

Conclusions: Significant differences were identified in ECM changes after BMS and DES implantation, most notably a reduction of basement membrane proteins and an upregulation of large aggregating proteoglycans, including aggrecan, a major ECM component of cartilaginous tissues that confers

resistance to compression.



Metabolism, diabetes mellitus and obesity

211

Targeting grk2 as therapeutic strategy for cancer associated to diabetes

J. Gambardella¹; D. Sorriento²; M. Ciccarelli¹; A. Fiordelisi¹; P. Campiglia¹; B. Trimarco³; G. Iaccarino¹
¹University of Salerno, Medicine and Surgery, Salerno, Italy; ²Institute of Genetics Biophysics CNR, Naples, Italy; ³Federico II University of Naples, Naples, Italy

Background: Diabetes is associated with an increased risk of cancer, and Hyperinsulinemia is likely responsible of this association given the mitogenic effects of insulin. GRK2 is a modulator of insulin response, and its inhibition improves insulin-sensibility both in vitro and in vivo.

Purpose: To evaluate the role of GRK2 in tumor progression, and its targeting as potential therapeutic strategy for Diabetes-associated cancer.

Methods: We evaluated GRK2 expression and subcellular localization in different cancer cell lines (TPC, BHT-101, KAT-4, TE-671, HT-1080) through western blot analysis; In TPC, we induced GRK2 over-expression by transient transfection and evaluated IRS-1 levels by immuno-precipitation and western blot analysis. We inhibited GRK2 activity, through a specific HJ-loop-derived inhibitor of GRK2, KRX-C9, in TPC and, at 24 and 48h, we evaluated phosphorylation of ERK and Rb, as proliferation markers, by western blot. Through a DNA-Dye binding assay, we evaluated cellular proliferation of TPC in response to GRK2 inhibition and/ or insulin treatment.

Results: GRK2 expression and subcellular localization were different among the various cell lines. In particular in TPC, which has the most high proliferation rate, GRK2 levels were reduced and it was mostly localized in mitochondria. This result suggests a role of the kinase in tumor progression. In this cells, the over-expression of GRK2 induced Insulin-receptor-substrate-1 (IRS1) degradation, indicating that also in cancer cells, the kinase can regulate insulin-signaling. In the same cells, KRX-C9 treatment, induced a significantly reduction of p-ERK and p-Rb, thus leading to a reduced cell survival and proliferation. These data were confirmed by proliferation assay; indeed KRX-C9 reduced the numbers of cells, both basally and in response to insulin.

Conclusion(s): Our data suggest that GRK2 is involved in tumor progression, and that also in cancer cells, is able to regulate insulin signaling. The selective inhibition of GRK2 activity, already known to be effective for the treatment of Diabetes, reduces cancer cell proliferation, also in response to insulin. Therefore, targeting GRK2 could represent an innovative therapeutic strategy for cancer in diabetic subjects.

212

Effects of salbutamol on large arterial stiffness in patients with metabolic syndrome

A. Cozma; AV. Sitar Taut; S. Schiau; O. Orasan; W. Halloumi; V. Negrean; D. Zdrenghea; D. Pop "Iuliu Hatieganu" University of Medicine and Pharmacy, Medicala IV, Cluj-Napoca, Romania

Background: Metabolic syndrome (MetS), defined as a cluster of features is highly prevalent all over the world, representing a critical risk factor for cardiovascular outcome. Endothelial dysfunction, characterized by a reduced bioavailability of endothelium-derived NO, is an important step in the progression of atherosclerosis. Changes in pulse wave velocity, brachial augmentation index (Aixb) and in the aortic augmentation index (AixAo), after b2-adrenoceptor agonist, can represent an useful tool in assessing the role of endothelium in vascular responsiveness. Purpose of the study was to evaluate the haemodynamic effects of inhaled salbutamol in patients with MetS vs without MetS (control group). Methods The study included 30 patients, (57% women), mean age of 56.63 ± 10.87 years. The classification of the metabolic syndrome was based on the IDF guidelines. Arterial parameters (augmentation index AixAo, brachial augmentation index Aixb, pulse wave velocity PWV) were determined using the TensioMedTMArteriograph.

Results: 67% patients presented MetS, 50% obesity, 60% diabetes, 57% hypertension. After salbutamol, aortic augmentation index (%) decreased in both groups (p=0.07 in MetS group, p=0.08 in control group). In neither one of groups, changes in brachial augmentation index were statistically significant. Pulse wave velocity (m/s) increased in MetS group (10.60 ± 2.89 vs 10.78 ± 2.51, p=NS) and decreased in patients without MetS (9.11 ± 2.48 vs 8.2 ± 1.96, p=NS). No significant differences were found between patients with vs without MetS regarding: aortic augmentation index before salbutamol (37.72 ± 14.04 vs 36.11 ± 15, p=NS), aortic augmentation index after salbutamol (35.22 ± 16.71 vs 34.51 ± 15.15, p=NS), brachial augmentation index before salbutamol (0.03 ± 27.5 vs -3.04 ± 29.64%, p=NS), brachial augmentation index after salbutamol (-2.69 ± 31.45 vs -6.13 ± 29.88, p=NS), pulse wave velocity (m/s) before salbutamol (10.60 ± 2.89 vs 9.11 ± 2.48, p=NS). But, pulse wave velocity after salbutamol significantly differed in patients with MetS vs without MetS (10.78 ± 2.51 vs 8.2 ± 1.96, p=0.008).

Conclusion: in metabolic syndrome patients, it is possible to spotlight the altered endothelial function using salbutamol test. The studied parameters had different capacity to identify endothelial dysfunction through salbutamol test, most probably due to different aspects of vascular changes quantified by them.

213

Circulating microRNA-1 and microRNA-133a: potential biomarkers of myocardial steatosis in type 2 diabetes mellitus

D. De Gonzalo Calvo¹; RW. Van Der Meer²; L.J. Rijzewijk³; JWA. Smit⁴; E. Revuelta-Lopez¹; L. Nasarre¹; JC. Escola-Gil⁵; H.J. Lamb²; V. Llorente-Cortes¹

¹Biomedical Research Institute Sant Pau (IIB Sant Pau), Cardiovascular Research Center (CSIC-ICCC), Barcelona, Spain;

²Leiden University Medical Center, Department of Radiology, Leiden, Netherlands;

³Cantonal Hospital of Baden, Department of Medicine, Baden, Switzerland;

⁴Radboud University Medical Centre, Department of Internal Medicine, Nijmegen, Netherlands;

⁵Biomedical Research Institute Sant Pau (IIB Sant Pau), Biochemistry, Barcelona, Spain

Background/Introduction: Effective tools to identify cardiac alterations during asymptomatic stages of type 2 diabetes mellitus (T2DM) are of clinical interest. Myocardial steatosis has been proposed as clinically useful for early identification and stratification of T2DM patients at high risk. However, the application of the gold standard for the evaluation of myocardial steatosis, proton magnetic resonance spectroscopy (1H-MRS), is currently impractical in large-scale population screening. Previous investigations have proposed blood microRNAs (miRNAs) as sensitive, specific and non-invasive biomarkers of cardiovascular disease.

Purpose: We explored the potential use of cardiomyocyte-enriched miRNAs as biomarkers of myocardial steatosis.

Methods: Cardiomyocyte-enriched miRNAs signature was analysed in serum from patients with well-controlled T2DM of short duration and with verified absence of cardiac ischemia and healthy volunteers in the same range of age and BMI, in serum from a high-fat diet-fed murine model of insulin resistance and in exosomes released into conditioned medium from lipid-loaded HL-1 cardiomyocytes. Myocardial neutral lipid content was analysed by 1H-MRS in patients and by thin layer chromatography after lipid extraction in both in vivo and in vitro models. miR-1, miR-133a/b, miR-208a/b and miR-499 were quantified using qRT-PCR.

Results: Multivariate regression analysis revealed that myocardial steatosis was directly associated with serum levels of miR-1 and miR-133a, independently of confounding factors. Patients in the highest quartile of serum miR-1 and miR-133a levels showed higher myocardial steatosis levels than those in the lowest miRNA quartiles. T2DM patients with serum levels of miR-133a below the limit of detection had lower myocardial neutral lipid content than subjects with detectable levels. Similar to myocardial steatosis, levels of miR-133a were higher in patients with uncomplicated T2DM compared to healthy subjects within the same range of age and BMI. Serum levels of miR-1 and miR-133a were significantly elevated in high-fat diet-fed mice compared to control diet-fed animals. Levels of miR-1 and miR-133a were higher in exosomes from lipid-loaded HL-1 cardiomyocytes.

Conclusions: Serum levels of the cardiomyocyte-enriched miR-1 and miR-133a are independent predictors of myocardial steatosis in T2DM patients with stable disease, and thus, are potential biomarkers for subclinical cardiac alterations in T2DM.

214

Anti-inflammatory nutrigenomic effects of hydroxytyrosol in human adipocytes - protective mechanisms of mediterranean diets in obesity-related inflammation

E. Scoditti¹; M. Pellegrino²; M. Massaro¹; MA. Carluccio¹; N. Calabro¹; M. Wabitsch³; C. Storelli²; R. De Caterina⁴

¹Institute of Clinical Physiology-CNR, Lecce, Italy;

²University of Salento, Department of Biological and Environmental Science and Technology (DiSTeBA), Lecce, Italy;

³University of Ulm, Division of Pediatric Endocrinology, Diabetes and Obesity, Dep of Pediatrics and Adolescent Medicine, Ulm, Germany;

⁴"G. d'Annunzio" University and Center of Excellence on Aging, Chieti, Italy

Background: Obesity is associated with increased risk of cardio-metabolic disorders. Excess adiposity results in oxidative stress and dysregulation of adipokine production, and is accompanied by macrophage infiltration in the adipose tissue, contributing to local and systemic inflammation. Purpose We investigated the effects of the Mediterranean diet olive oil polyphenolic antioxidant hydroxytyrosol (HT) on the expression of adipokines regulated by tumor necrosis factor (TNF)-α in human Simpson-Golabi-Behmel Syndrome (SGBS) adipocytes, exploring underlying mechanisms.

Methods: SGBS adipocytes were treated with 1-10 μmol/L HT for 1 h before 10 ng/mL TNF-α for 24 h. Adipokines mRNA expression and levels in the culture medium were measured by real time PCR and EIA, respectively. Effects on the activation of the transcription factor NF-κB p65 subunit were determined by ELISA and Western blotting. The production of reactive oxygen species (ROS) was detected by the fluorophore dichlorofluorescein diacetate.

Results: Under pro-inflammatory conditions induced by TNF-α, adipocytes increased expression and medium levels of monocyte chemoattractant protein(MCP)-1, chemokine (C-X-C Motif) Ligand 10, interleukin(IL)-1β, IL-6, vascular endothelial growth factor (VEGF), plasminogen activator inhibitor(PAI)-1, cyclooxygenase(COX)-2, macrophage colony-stimulating factor (M-CSF), metalloproteinase(MMP)-2, superoxide dismutase (SOD) and glutathione peroxidase (GPX), and the surface expression of intercellular adhesion molecule(ICAM)-1, and reduced the release of adiponectin (APN) and the expression of endothelial nitric oxide synthase (eNOS). Pretreatment with HT significantly inhibited TNF-α-induced expression and/or release of pro-inflammatory cytokines, and reverted TNFα-mediated inhibition of APN and eNOS. HT also prevented the TNF-α-induced binding activity and nuclear translocation of NF-κB and ROS production.

Conclusions: Our data suggest that HT, at concentrations achievable through Mediterranean diets, can modulate the expression and secretion of adipokines in adipocytes through a mechanism involving reduction in oxidative stress and NF-κB inhibition. By such mechanisms, HT may therefore blunt macrophage recruitment and improve adipose tissue inflammation, possibly preventing the activation of pathways involved in obesity-related diseases.

215

Alterations in the metal content of different cardiac regions within a rat model of diabetic cardiomyopathy

B. J. Clark¹; S. J. Church²; S. Callagy³; P. Begley²; N. Kureishy³; S. Mcharg³; P. N. Bishop²; R. D. Unwin²; G. J. S. Cooper²

¹University of Manchester, Institute of Cardiovascular Sciences, Manchester, United Kingdom; ²Central Manchester University Hospitals NHS Foundation Trust, Centre for Advanced Discovery and Experimental Therapeutics (CADET), Manchester, United Kingdom; ³University of Manchester, Centre for Endocrinology and Diabetes, Institute of Human Development, Manchester, United Kingdom

Background: Cardiovascular disease is the main cause of death among diabetic patients, in whom diabetic cardiomyopathy (DCM) is a leading, but poorly understood, pathology. It has been proposed that metal-catalysed oxidative stress contributes to the development of DCM.

Purpose: We sought to determine whether diabetes affects cardiac metal homeostasis and whether the Cu(II)-selective chelator, triethylenetetramine (TETA), could reverse diabetes-induced changes.

Methods: Absolute amounts of 12 essential metals (Na, Mg, K, Ca, Cr, Mn, Fe, Co, Cu, Zn, Se, Mo) were determined using inductively coupled plasma mass spectrometry on desiccated atrial, septal, right ventricular (RV) and left ventricular (LV) tissue samples from the hearts of control, diabetic and TETA-treated diabetic Sprague-Dawley rats (8 rats/arm). Hyperglycaemia was induced by intraperitoneal injection of streptozotocin (55 mg/kg bodyweight). TETA administration, commencing one day post-confirmation of hyperglycaemia, was achieved by supplementing drinking water with TETA disuccinate (30 mg/day) for 16 weeks. To protect against severe hyperglycaemia, diabetic and TETA-treated rats received low doses of insulin from week 11. Data were compared using Welch's t-tests.

Results & Conclusions: Compared with the atria, manganese, copper and zinc ($\mu\text{mol/kg}$ dry-weight) were significantly higher in the ventricles of control rat hearts (atria, RV, LV: Mn, 27.2, 34.9 ($P < 0.0001$), 36.6 ($P < 0.0001$); Cu, 281, 361 ($P < 0.0001$), 345 ($P = 0.001$); Zn, 940, 1058 ($P = 0.003$), 1013 ($P = 0.046$)), perhaps reflecting local elevations in the levels of protective antioxidant enzymes. In diabetes, dry-weight levels of iron (mmol/kg), manganese and molybdenum ($\mu\text{mol/kg}$) were significantly decreased within both the septum (control vs diabetic: Fe, 5.2 vs 4.2, $P < 0.0001$; Mn, 31.8 vs 27.5, $P = 0.01$; Mo, 2.0 vs 1.8, $P = 0.03$) and RV (control vs diabetic: Fe, 6.2 vs 4.7, $P = 0.0009$; Mn, 34.9 vs 28.8, $P = 0.0006$; Mo, 1.9 vs 1.7, $P = 0.041$), and also tended to be lower in the atria and LV, suggesting that diabetes impairs myocardial antioxidant defences. Thus, diabetes-mediated changes in cardiac metal homeostasis may promote DCM through increased oxidative stress. In contrast to previous findings, myocardial copper content was unchanged in diabetes, perhaps indicating that insulin represses copper homeostasis without fully restoring euglycaemia. TETA treatment did not affect the levels of any metal.

Tissue engineering

218

A novel conductive patch for application in cardiac tissue engineering

C. Mansfield¹; D. Mawad²; F. Perbellini¹; J. Tonkin¹; S. O. Bello¹; J. D. Simonotto¹; A. R. Lyon¹; M. M. Stevens²; C. M. Terracciano¹; S. E. Harding¹

¹Imperial College London, National Heart and Lung Institute, London, United Kingdom; ²Imperial College London, Department of Materials, London, United Kingdom

Introduction: Conductive cardiac patches offer a potential new therapeutic strategy for manipulating conduction across the infarcted heart thereby improving contractility and reducing arrhythmia generation. We have developed a novel conductive patch for application in cardiac tissue engineering.

Methods: The effects of applying the conductive patch on the conductivity of the heart were examined using whole heart epicardial voltage mapping of ex vivo Langendorff-perfused rat hearts. We studied both healthy hearts and those subjected to myocardial infarction (MI) by ligation of the Left Anterior Descending coronary artery 2 weeks prior to the experiment. Following explantation the hearts were perfused with a physiological solution containing the voltage-sensitive dye di-4-ANEPPS and blebbistatin. The heart was excited using 530nm LEDs and emitted light collected using a CMOS camera. Signals were recorded during pacing from the base of the left ventricular free wall (400 bpm; 1 mA). Action potentials were recorded with no patch on the heart and after suturing on of the conductive or non-conductive control patch.

Results: Conduction velocity (CV) was significantly lower in the infarcted hearts compared to the healthy hearts and this was most pronounced in the apex where the infarct is located ($26.9 \pm 2.7 \text{ cm/s}$ vs $59.8 \pm 4.7 \text{ cm/s}$, $p < 0.001$, $n = 10$). Apical CV dropped significantly when the conductive patch was sutured to healthy hearts ($66.3 \pm 4.2 \text{ cm/s}$ to $47.8 \pm 5.0 \text{ cm/s}$, $p < 0.02$, $n = 5$) while no significant effect on the CV was observed following the attachment of a non-conductive patch. For the MI group, the conductive patch increased the CV in the apical infarcted area ($24.3 \pm 4.9 \text{ cm/s}$ to $30.1 \pm 4.2 \text{ cm/s}$, $p < 0.05$, $n = 5$).

A significant increase in action potential duration (APD) was seen in the basal area of healthy hearts after application of the conductive patch ($n = 5$; $p < 0.05$), although no effect was seen on APD in the apical area. The APD in MI hearts was not significantly affected by the conductive patch.

Conclusion: Conductive polymer patches are able to modulate electrophysiological characteristics of the myocardium. The opposite changes in healthy and infarcted hearts is an exciting finding, but it remains to be established how this will affect arrhythmia generation in the damaged heart.

219

Establishment of a simplified and improved workflow from neonatal heart dissociation to cardiomyocyte purification and characterization

D. Eckardt; M. Kernbach; V. Czichowski; A. Bosio
Miltenyi Biotec GmbH, Research & Development, Bergisch Gladbach, Germany

Although isolation of functional cardiac cells from neonatal hearts is one of the most used experimental model in cardiac research, the manual dissociation of neonatal hearts is a laborious and difficult-to-standardize procedure. Therefore, we developed a fully automated dissociation process

allowing for simultaneous dissociation of up to 160 neonatal hearts within 1 h, resulting in high yields of single cells with excellent viability.

To purify CMs from dissociated neonatal hearts, we defined antibody cocktails enabling non-myocyte removal. Our depletion strategy allowed for the enrichment of CMs from whole hearts or preparations of individual heart chambers with purities of up to 98% within 20 min. Contractions of purified CMs were observed within 24 h after plating on a newly developed recombinant human fibronectin fragment as coating matrix. To enable simultaneous detection of CMs and subtypes, we developed recombinant antibodies against general CM markers such as alpha Actinin, Myosin Heavy Chain or Cardiac Troponin T as well as CM subtype-specific antibodies against MLC2a and MLC2v distinguishing between atrial and ventricular CMs, respectively. These antibodies were used for either flow cytometry analysis of single cell suspensions or immunofluorescence-based detection of CMs and subtypes in culture or in heart sections. A newly developed immunofluorescence protocol allowed for CM labeling within 45 min.

Besides, we developed magnetic enrichment strategies for the purification of cardiac fibroblasts (CF) and endothelial cells (EC). Since current purification strategies, solely based on antibodies against EC surface markers, do not result in sufficiently pure cardiac ECs, we established a new protocol completely removing contaminating fibroblasts. Similarly, our magnetic enrichment protocol for cardiac fibroblasts revealed virtually no contaminations with CMs or ECs.

In summary, we established an automated protocol for dissociation of neonatal hearts enabling subsequent purification, characterization and cultivation of CMs, CFs, and ECs which can readily be used for cell culture assays or to generate in vitro heart muscle models.

220

Effects of flexible substrate on cardiomyocytes cell culture

L. Gomez¹; L. Fuentes¹; I. Hernandez-Redondo¹; MS. Guillem²; ME. Fernandez¹; R. Sanz¹; F. Atienza¹; AM. Climent¹; F. Fernandez-Aviles¹

¹University Hospital Gregorio Marañon, Instituto de Investigación Sanitaria Gregorio Marañon, Cardiology Department, Madrid, Spain; ²Polytechnic University of Valencia, ITACA Institute, Valencia, Spain

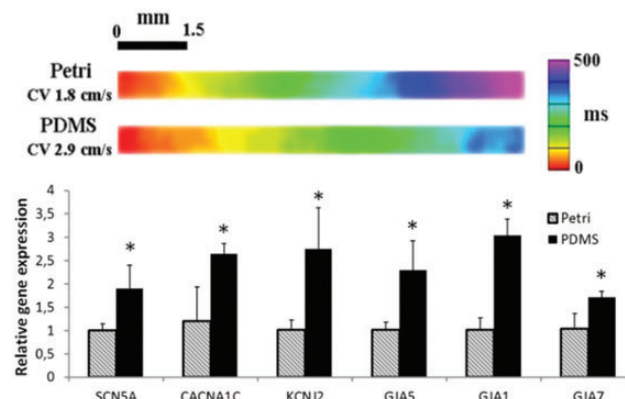
Background: Engineered cardiac patches are a promising tool to regenerate damaged cardiac tissue after ischemic and remodelling events. Major considerations in the design of engineered cardiac patches are the regenerative and electrophysiological properties of cardiac cells.

Purpose: The objective of this study is to compare key cardiomyocyte functional properties for cardiac repair (i.e. proliferation, migration and electrophysiological properties) and gene expression depending on the cell culture substrate.

Methods: Atrial murine cells (HL-1 myocytes) were cultured in two different substrates: (1) rigid Petri dishes and (2) flexible PDMS (polydimethylsiloxane) wells. The proliferation rate, migration and conduction velocity of the cardiac cells were analysed and compared in both substrates together with the expression of main genes involved in the action potential generation and propagation (i.e. SCN5A, CACNA1C, KNJ2, GJA5, GJA1, GJA7).

Results: Cell cultures grown on flexible membranes showed a significantly higher electrical conduction velocity than on Petri dishes (i.e. $2.4 \pm 0.6 \text{ cm/s}$ vs. $1.5 \pm 0.3 \text{ cm/s}$, $p < 0.01$). This increase in the conduction velocity was associated with an increase in the expression levels of certain genes associated with action potential generation and propagation (i.e. ion channels: sodium, calcium, potassium and connexins). (see Fig.). No significant differences were observed in terms of proliferation and migration rates (i.e. full confluence was achieved within 6 days on both substrates).

Conclusion: Flexible PDMS membranes not only maintain cell proliferation and migration rates, they have also shown to play an important role in the electrophysiological maturation of cardiac cells (i.e. characteristic gene expression and functional wavefront propagation). These results may help in the design of novel engineered cardiac tissue for regeneration therapies.



Isochrones maps and gene expression

221

Mechanical stretching on cardiac adipose progenitors upregulates sarcomere-related genes

A. Lucía-Valldeperas¹; C. Soler-Botija¹; C. Prat-Vidal¹; C. Galvez-Monton¹; S. Roura¹; I. Perea-Gil¹; R. Bragos²; A. Bayes-Genis³

¹Health Science Research Institute Germans Trias i Pujol, Badalona, Spain; ²University Polytechnic of Catalunya, Barcelona, Spain; ³Germans Trias i Pujol University Hospital, Badalona, Spain

Background: The cardiac tissue is an unfriendly environment for the implantation of therapeutic cells due to its unavoidable contractility. Cardiac cells respond to mechanical stimuli and adjust their

performance accordingly. It is also known that mechanical stimulation of tissue-engineered constructs improves their organization and contraction force.

Purpose: We hypothesize that mechanical conditioning of therapeutic cells could improve their retention and cardiovascular potential, to help in cardiac tissue restoration.

Methods: Cardiac adipose tissue-derived progenitor cells (ATDPCs) were mechanically stretched for 7 days at 1 Hz in 3 different surfaces (vertical, horizontal and smooth) (Figure 1). Gene and protein analysis were carried out for each cell type and condition. Secretome analysis after conditioning was also performed.

Results: A device was designed and validated to effectively apply a ~10% stretch. Mechanically stimulated cardiac ATDPCs increased the expression of cardiac transcription factors (GATA-4 and Tbx5) and structural genes (cTnI and α -actinin) after 7 days of mechanical stimulation. This gene modulation was different depending on the patterned surface, however the secretome analysis revealed that the vertical pattern was the most convenient for cardiac ATDPCs conditioning. Indeed, the secretome of cardiac ATDPCs stretched on vertical patterned surfaces was significantly associated to myocardial infarction, left ventricular extracellular matrix remodelling and the regulation of myoblast differentiation.

Conclusions: Mechanical conditioning of cardiac ATDPCs enhances the expression of early and late cardiac genes related with the cardiac sarcomere, and it is strongly dependent on the culture surface pattern.

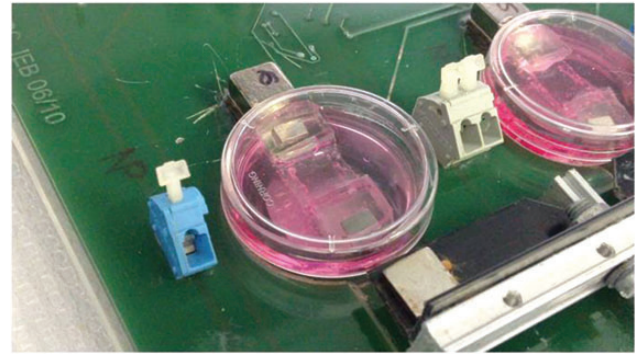


Figure 1. Mechanical stimulation device.